

DEPOSITIONAL ENVIRONMENT AND DIAGENETIC
HISTORY OF THE FRISCO AND HENRYHOUSE
FORMATIONS IN CENTRAL OKLAHOMA

By

PATRICK LEE MEDLOCK
Bachelor of Science
University of Kansas
Lawerence, Kansas

1982

Submitted to the Faculty of the
Graduate College of the
Oklahoma State University
in partial fulfillment of
the requirements for
The Degree of
MASTER OF SCIENCE
December, 1984

Thesis
1984
M491d
cop 2



DEPOSITIONAL ENVIRONMENT AND DIAGENETIC
HISTORY OF THE FRISCO AND HENRYHOUSE
FORMATIONS IN CENTRAL OKLAHOMA

Thesis Approved:

Zuhair al-shaich
Thesis Adviser

Blair Esteban

Gary F. Semmes

Norman D. Burkham
Dean of the Graduate College

ACKNOWLEDGMENTS

I would like to extend sincere appreciation to Dr. Zuhair Al-Shaieb for his support, guidance and motivation throughout the study. I would like to acknowledge the valuable suggestions of Dr. Gary Stewart and Dr. Mateau Esteban.

I wish to thank Dr. John Shelton and Rick Fritz of ERICO for providing financial support for research, as well as advice and information about the Hunton Group.

I wish to thank Dennis Prezbindowski of AMOCO for completing isotopic analyses on the Hunton Group.

I would like to thank the students and faculty of the Geology Department for their friendship, advice and criticism.

My parents deserve special appreciation for their encouragement and financial support. Finally, a special appreciation is extended to Tina Nelson for her encouragement and patience.

TABLE OF CONTENTS

Chapter	Page
I. INTRODUCTION.	1
Location	1
Objectives	1
Methods of Investigation	5
II. PREVIOUS WORK	8
Stratigraphy	8
Depositional Environment	9
Petrography.	10
Geochemistry	10
III. GEOLOGIC HISTORY.	12
IV. FRISCO FORMATION.	14
Introduction	14
Depositional Environment	15
Mound Facies.	20
Intermound Facies	20
Capping Facies.	26
Crestal Boundstone and Organic Veneers	26
Interfacies Relationship.	29
Summary	29
Crinoid Paleocology.	30
Sediment Production and Crinoids.	30
Crinoid Ecology	32
Crinoids as Sedimentary Particles	34
Petrology and Petrography.	36
Matrix/Cement	36
Sedimentary Features.	36
Frisco Fauna.	38
Diagenesis and Porosity.	45
Cements	45
Sparry Calcite	45
Micrite.	54
Porosity.	54
Fabric Selective Porosity.	57
Non-Fabric Selective Porosity.	60
Porosity Controls.	60
Paragenetic Sequence.	66

Chapter	Page
V. HENRYHOUSE FORMATION.	79
Introduction	79
Depositional Model	82
Lagoonal Facies	82
Oolitic Facies.	87
Subtidal Facies	87
Summary	92
Dolomitization of the Henryhouse	92
Introduction.	92
Hypersaline Dolomitization.	96
Freshwater/Marine Water Mixing Dolomitization.	100
Deep Burial Dolomitization.	104
Porosity Distribution and Its Relation- ship to Dolomite	108
Dolomitization of the Lagoonal Facies.	108
Dolomitization of the Oolitic Facies.	112
Dolomitization of the Subtidal Facies.	115
Summary.	115
VI. CONCLUSIONS	120
SELECTED BIBLIOGRAPHY.	122
APPENDIXES	130
APPENDIX I - STABLE OXYGEN AND CARBON ISOTOPES OF THE HENRYHOUSE.	130
APPENDIX II - STABLE OXYGEN AND CARBON ISOTOPES OF THE FRISCO.	131
APPENDIX III - CORE SUMMARIES	132
APPENDIX IV - SELECTED PETROLOGIC LOGS.	140

LIST OF TABLES

Table	Page
I. Samples and Data Taken.	6-7
II. Criteria for Facies Identification in the Frisco.	31

LIST OF FIGURES

Figure	Page
1. Location Map.	2
2. Geologic Provinces of Oklahoma.	3
3. Hunton Stratigraphy	4
4. Wilson's Mound Sequence	16
5. Depositional Model of the Frisco, Stage 1	17
6. Depositional Model of the Frisco, Stage 2	18
7. Depositional Model of the Frisco, Stage 3	19
8. Mound Facies.	21
9. Mound Facies.	21
10. Mound Facies.	22
11. Photomicrograph of Mound Facies	23
12. Photomicrograph of Mound Facies	23
13. Intermound Facies	24
14. Intermound Facies	24
15. Photomicrograph of Intermound Facies.	25
16. Photomicrograph of Intermound Facies.	25
17. Capping Facies.	27
18. Photomicrograph of Capping Facies	28
19. Density Increase in <u>Antedon bifida</u>	35
20. Graph of Sparite vs. Micrite.	37
21. Horizontal Grains	39

Figure	Page
22. Inclined Grains	39
23. Massive Bedding	40
24. Well Sorted Grainstone	41
25. Poorly Sorted Wackestone	41
26. Unfragmented Bryozoan	43
27. Fragmented Bryozoans	43
28. Diversity of Fauna	44
29. Drusy Sapra	44
30. Crinoid Overgrowth Patterns	47
31. Multiple Terminations	48
32. Multiple Zonations	49
33. Sharp Contacts and Enfacial Angle	50
34. Zonations of Cement in the Frisco	52
35. Nine Different Zones of Cement	53
36. Photomicrograph of Primary Micrite	55
37. Secondary Micrite	55
38. Secondary Micrite and Calcite	56
39. Enlarged Interparticle Porosity	58
40. Intraparticle Porosity	58
41. Enlarged Intraparticle Porosity	59
42. Enlarged Intraparticle Porosity	59
43. Vuggy Porosity	61
44. Vuggy Porosity	62
45. Material From Unconformity	63
46. Sand Filling a Vug	64
47. Fracture Filled with Calcite	65

Figure	Page
48. Paragenesis of the Frisco.	67
49. Corrosion of Cement.	69
50. Truncated Cements.	70
51. Cementation Before Compaction.	71
52. Compaction After Cementation	72
53. Fracture After Cementation	73
54. Fractures After Two Zones of Cement.	74
55. Two Stages of Dissolution.	75
56. Pyrite in Stylolite.	76
57. Pyrite Replacing Calcite	77
58. Stylolite Cross-Cutting Fractures.	78
59. Oolitic Facies in the Henryhouse	80
60. Isopach of Calcitic Oolite	81
61. Vertical Sequence of Henryhouse.	83
62. Depositional Model of the Henryhouse	84
63. Lagoonal Facies.	85
64. Photomicrograph of Lagoonal Facies	86
65. Photomicrograph of Lagoonal Facies	86
66. Calcitic Oolite.	88
67. Photomicrograph of Calcitic Oolite	88
68. Dolomitic Oolite	89
69. Photomicrograph of Dolomitic Oolite.	89
70. Upper Subtidal Facies.	90
71. Photomicrograph of Upper Subtidal Facies	90
72. Lower Subtidal Facies.	91
73. Photomicrograph of Lower Subtidal Facies	91

Figure	Page
74. Incipient Stylolite.	93
75. Stability Field of Dolomite and Calcite.	95
76. Subhedral Quartz in Dolomitic Oolite	98
77. Anhedral Dolomite.	99
78. Anhedral Dolomite.	99
79. Carbon 13 Values of Different Types of Dolomite.	101
80. Hypersaline Dolomitization Model	102
81. Mixed-Water Dolomitization Model	103
82. Limpid, Euhedral Dolomite.	105
83. Zoned Dolomite.	105
84. Zoning of Dolomite	106
85. Depletion of Oxygen 18 Isotope in Henryhouse Dolomite	107
86. Baroque Dolomite Healing Fracture.	109
87. Baroque Dolomite Replacing Fossil.	109
88. Graphs of Dolomite vs. Footage	110, 111
89. Zoned Dolomite in Ooliths.	113
90. Inter- and Intraoolitic Porosity	113
91. Inter- and Intraoolitic Porosity	114
92. Interoolitic Porosity.	114
93. Graph of Dolomite vs. Footage.	116
94. Photomicrograph of Zoned Dolomite in Northwest Subtidal Facies.	118
95. Meniscus Cement.	118
96. Dolomitization of Southeast Subtidal Facies. . .	119

CHAPTER ONE

INTRODUCTION

Location

The area of study (Figure 1) is located in portions of Blaine, Kingfisher, Logan, Canadian, Oklahoma, Cleveland, Grady, and McClain Counties in Oklahoma. Outcrops were examined in Pontotoc County, Oklahoma. The subsurface locations are northeast of the Anadarko Basin, west of the Nemaha Ridge, and northwest of the Arbuckle Mountains (Figure 2). The outcrops examined are located in the Lawrence uplift northeast of the Arbuckle Mountains and east of the Nemaha Ridge. The formations investigated are the Frisco Formation, Devonian System, Siegenian Stage and the Henryhouse Formation, Silurian System, Pridolian-Ludlovian Stages both formations are part of the Hunton Group (Figure 3).

Objectives

The objectives of the investigation for both formations were: (1) to determine a depositional model, and (2) to examine the diagenetic imprints.

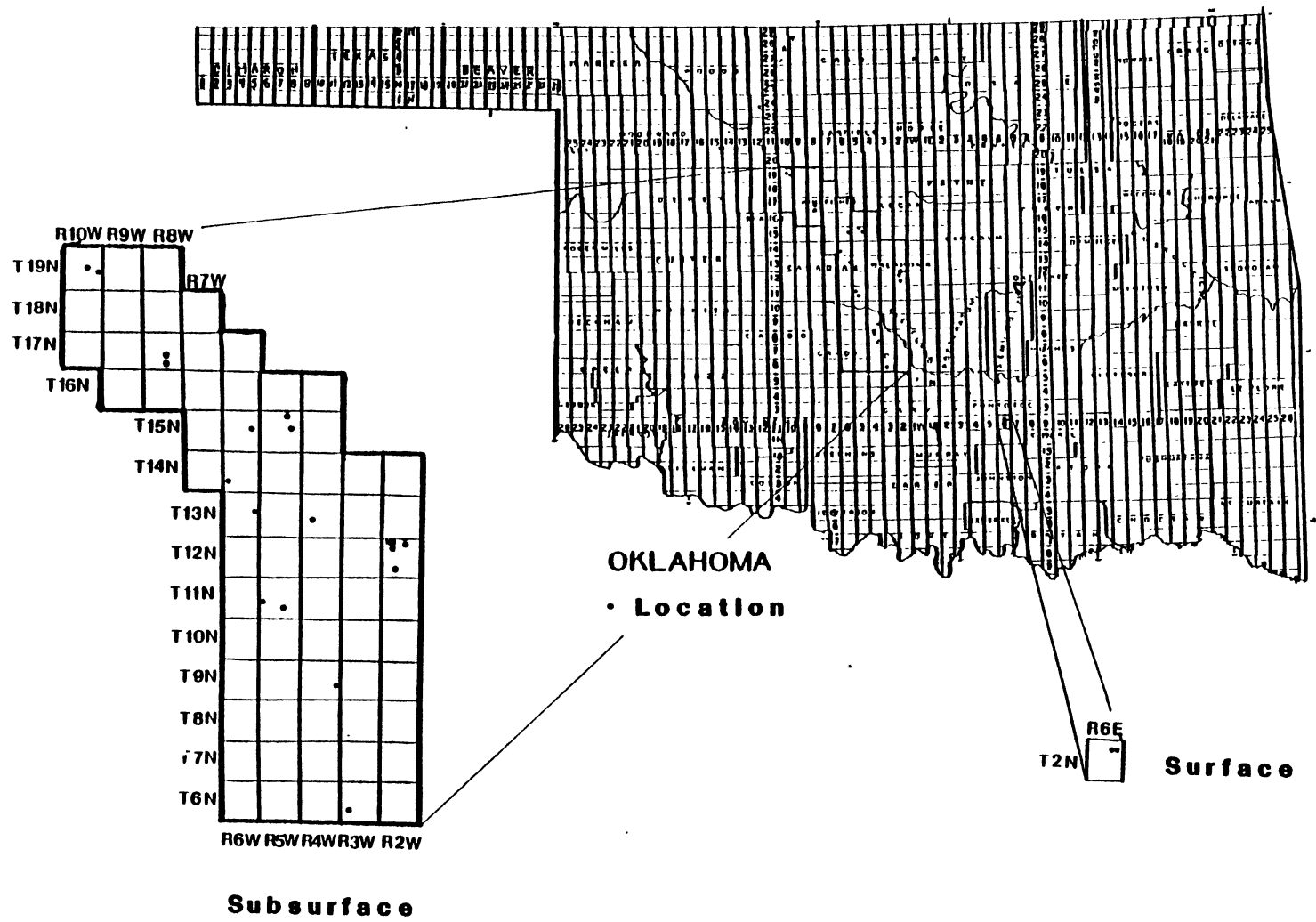


Figure 1. Location Map of Study Area

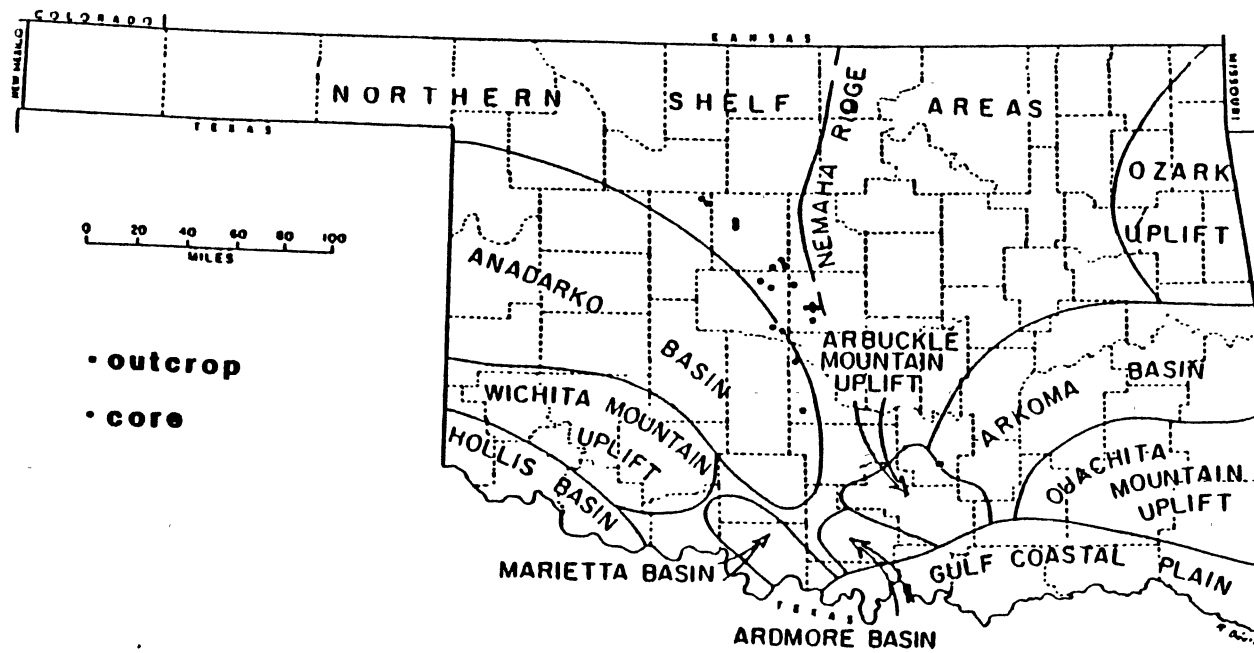


Figure 2. Area of Study in Relationship to the Geologic Provinces of Oklahoma (OGS).

Methods of Investigation

The methods (Table I) used investigate the sedimentology, petrology, petrography, and geochemistry of each formation.

1. Core analysis, which involved examination of the sedimentological features.

2. Petrographic examination of thin sections.

3. X-ray diffraction analysis to determine the mineralogy of various facies.

4. Scanning-electron microscopy to observe evidence of subtle diagenetic events and microporosity.

5. Cathodoluminescence to examine dolomite zonations in the Henryhouse Formation and the paragenetic sequence of the Frisco Formation.

6. Carbon and oxygen isotopic analysis to refine characterization of the carbonate genesis.

TABLE ONE
 SAMPLES AND DATA TAKEN

Name	Location	Footage	No. of Thin Sections	No. of X-ray Analysis	No. of Isotope Analysis
<u>Frisco</u>					
Pontotoc	11-2N-6E	39'	20	4	--
Phillips Brooks B#1	30-14N-6W	38'	7	16	--
Midwest McManus #1	13-13N-6W	40'	9	12	4
Gulf Streeter#1	20-13N-4W	89'	14	15	3
Jones & Pellow Boyd#1	28-12N-2W	52'	9	14	--
Gulf Holtzschue #1	8-12N-2W	34'	10	13	--
Gulf Wright Heirs B#1	5-12N-2W	46'	5	12	--
Gulf Wright Heirs#1	5-12N-2W	38'	5	7	--
Gulf Shroeder#1	3-12N-2W	41'	5	11	--
Apexco Curtis#2	27-11N-5W	70'	14	22	4
Sinclair Horlivy#1	19-11N-5W	51'	8	16	--
Jones & Pellow Leeper A#1	24-9N-4W	18'	5	7	3
Gulf Shaddix#1	29-6N-3W	45'	10	15	--
Total		620'	120	157	14

TABLE ONE, (CONTINUED)

Name	Location	Footage	No. of Thin Sections	No. of X-ray Analysis	No. of Isotope Analysis
<u>Henryhouse</u>					
Cleary Kramp					
Colob#1	24-19N-10W	37'	6	10	1
Shell Dill#1	15-19N-10W	62'	13	18	1
Texaco Theo					
Thompson#1	34-17N-8W	37'	9	12	1
Walter Duncan					
Garett#2	22-17N-8W	38'	8	12	1
Jones & Pellow					
Farrell#1	14-15N-6W	50'	10	13	1
Kirkpatrick					
Cronkite#1	14-15N-5W	38'	10	10	1
Eason Van					
Curen#1	3-15N-5W	56'	12	20	1
Gulf Streeter#1	20-13N-4W	105	8	10	1
Total		428'	76	105	8

CHAPTER TWO

PREVIOUS WORK

Stratigraphy

The Hunton Group was named after the Hunton townsite by Taft in 1902. Reeds (1911) differentiated the Hunton. In 1926 Reeds noted coquina-like limestone in the uppermost portion of the Hunton and called it the Frisco Formation. In an unpublished doctoral dissertation, Maxwell (1936) revised Reed's terminology. Amsden (1957, 1960, 1961, 1975, 1980) has studied the Hunton Group extensively, and has further divided the Hunton Group into distinct formations, members, and facies that are separated by numerous unconformities.

Several problems of nomenclature have arisen. Differentiation of the Henryhouse and Haragan is not practical on the basis of lithology; paleontological evidence is necessary to differentiate the two formations. Amsden (1975) described a subsurface biofacies consisting of the large pentamerid brachiopods Kirkidum pingue pingue and Kirkidium pingue latum. The Kirkidum biofacies is correlative to the Henryhouse Formation (Amsden, 1975).

Previous workers have commonly mislabelled porous

limestone near the top of the Hunton as the Bois D'Arc Formation. From biostratigraphic analyses (Amsden and Rowland, 1971; Morgan et al. 1982) it has been concluded that much of the production from the top of the Hunton is from the Frisco Formation. The major lithologic difference between the Frisco and Bois D'Arc is an increase in siliciclastic content in the Bois D'Arc. The siliciclastic increase may be seen as an increase in the gamma-ray log response (Morgan et al. 1982) but, of course, core analysis is the best method to ascertain which formation is present in the subsurface.

Depositional Environment

Amsden (1960) concluded that the Frisco was deposited in an outer sublittoral environment, in slightly agitated waters. Morgan et al. (1982) wrote "that the wide range in size of skeletal fragments suggests that grains were not transported long distances."

The Henryhouse commonly has been described as marlstone. Amsden (1975) observed no evidence diagnostic of shallow water, and he believed that the Henryhouse was deposited in quiet water in the outer neritic or outer sublittoral environments. Conversely, Beardall (1983) and Al-Shaieb (1983) observed features suggestive of shallow water and divided the Henryhouse into supratidal, intertidal, and subtidal facies. Harvey (1968) believed that dolomite in the Henryhouse was an indicator of shallow

water conditions.

Petrography

Amsden (1961) concluded that the Frisco is composed of three general lithofacies: coarse calcarenite or coquina, calcilutite or fine grained calcarenite, and pelmatozoan limestone; but no depositional environments were interpreted from the lithofacies. Amsden (1961) noted overgrowths on crinoids as the major cement. London (1973) considered the Frisco as a coarsely crystalline crinoidal limestone. Morgan et al. (1981) discussed destruction and generation of porosity. Swesnik (1948) observed six types of porosity in the Frisco and the Henryhouse: vuggy, inter-crystalline, oomoldic, interparticle, moldic, and fracture. Discussions on petrography of the Henryhouse have emphasized dolomitization (Harvey, 1968; Hollrah, 1978; Isom, 1973). The most extensive work was completed by Amsden (1975, 1980). Beardall (1983) discussed the petrography of the dolomite and its relationship with facies.

Geochemistry

Amsden (1975, 1980) has conducted various mineralogical and acid insoluble analyses on all formations of the Hunton Group. Morgan (1982, 1983) also conducted mineralogical analyses on various formations in the Hunton. Beardall (1983) examined the mineralogic and isotopic composition of the Henryhouse.

Amsden (1967) believed dolomitization of the Hunton took place by generation of a dolomite front. The Silurian dolomite exists in central, western and northeastern Oklahoma and limestone in southern Oklahoma. Amsden (1975) believed that dolomite formed by penecontemporaneous replacement at or slightly below the water-sediment contact. Harvey (1968) believed that dolomite was formed by penecontemporaneous replacement, direct precipitation or replacement by migrating connate water or ground water. Morgan (1983) believed that dolomite in the Henryhouse was not facies selective. Hollrah (1978), Isom (1973), and Harvey (1968) all believed that two stages of dolomitization took place in the Hunton; penecontemporaneous replacement and late-stage dolomitization. Beardall (1983) stated that dolomitization was a two-stage event beginning with penecontemporaneous, hypersaline dolomitization and concluding with eogenetic mixed water dolomitization; he used data from mineralogy, petrology, sedimentary structures, and isotopic analysis to support his conclusions.

CHAPTER THREE

GEOLOGIC HISTORY

Deposition of the Hunton Group was closely related to development of the Southern Oklahoman aulacogen. The Southern Oklahoman aulacogen underwent rifting, subsidence, and deformation stages. The Hunton Group was deposited during transition from the subsident stage to the deformational stage (Adler, 1971).

During Early Cambrian to Late Cambrian, the rifting stage included uplift and igneous activity. During the subsidence stage, a passive continental margin formed. Thicker stratigraphic sections are contained in the basins than on the more stable shelf areas around the aulacogen.

Hunton deposition marked the end of the subsidence stage (Adler, 1971). Slight deformation occurred during deposition of the Hunton; an angular unconformity is present between the Haragan (Devonian) and the underlying Silurian (Swesnik, 1948; Amsden, 1975). Many unconformities are present in the Hunton (Amsden, 1975).

During the deformation stage mostly siliclastic sediments were deposited. Uplift and erosion of the Hunton Group took place along the Nemaha Ridge area, in the

Wichita Mountains, and in northern Oklahoma. The structural basins were completely formed by this time.

CHAPTER FOUR

FRISCO FORMATION

Introduction

The Frisco (Devonian System, Siegenian Stage) was deposited upon an unconformity (Amsden, 1960) in relatively stable, subtidal conditions which allowed crinoidal mud mounds to develop. Mound deposits are common in many Paleozoic carbonate environments. Similarities between the Frisco and in other Paleozoic mounds are remarkable.

Carbonate mounds formed by the binding, baffling or trapping of sediment (lime mud) by a variety of different organisms. Textures and facies of Paleozoic mounds are similar, but the organism responsible for accumulation of sediments were of different types. Some fauna responsible for mound deposits are sponges and algae in the Cambrian and Ordovician, bryozoans in Ordovician, Silurian and Mississippian, tabular stromatoporoids in the Late Devonian, and platy algae in the Pennsylvannian (Wilson, 1975).

Mechanical accumulation of sediment is necessary to initiate mound growth (Wilson, 1975). Binding, baffling, or trapping of sediment by organisms was needed for continued growth. Subsequent generations of organisms grew

upon the baffled sediment (Wilson, 1975).

A stabilization mechanism was needed for the mound to withstand marine erosion. Encrusting organisms or root structures increased the angle of repose, allowing the mound to rise within the surrounding area. Stabilization was needed for growth and preservation.

Boundstones or a wall of organisms protected the mounds when they grew into active-wave depths. Corals or thickets of crinoids created adequate protection for the mound (Wilson, 1975).

The intermound area contained bioclastic debris that had fallen from the mound slopes. The bioclastic beds onlap the mound facies.

Wilson's generalized sequence (Figure 4) was not developed in all mounds. Carbonate mounds reported by Landon and Bowsher (1941), Harbaugh (1957), and Carozzi and Soderman (1962) do not have all the facies that are present in Wilson's generalized mound sequence, but micritic rich mounds and bioclastic intermound areas generally are represented in the stratigraphic record.

Depositional Environment

The Frisco Formation was deposited on an unconformity (Amsden, 1960). In the study area the presence of an unconformity is suggested by the Frisco overlying the Henryhouse Formation (Silurian) or the Bois D'Arc Formation (Devonian). The paleotopography was conducive to development of crinoidal mounds (Figure 5-7).

Idealized Mound Sequence

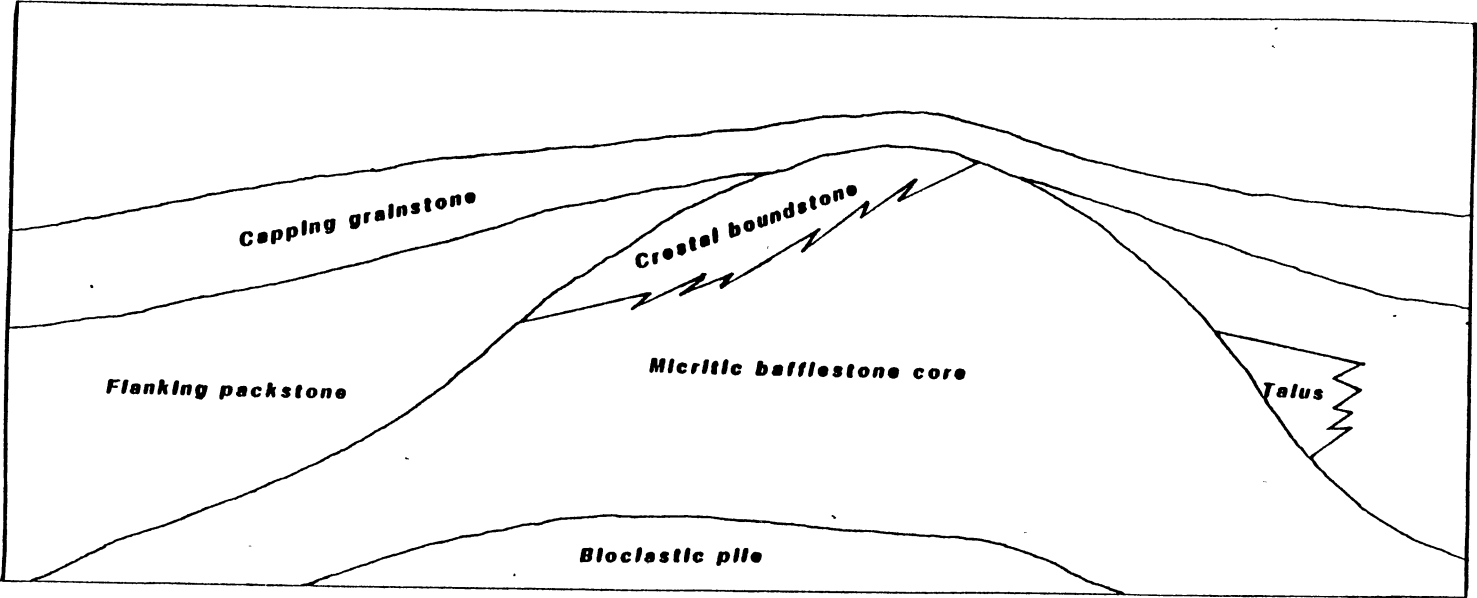


Figure 4. Wilson's Generalized Mound Sequence. (Wilson, 1975)

Mound Development in the Frisco

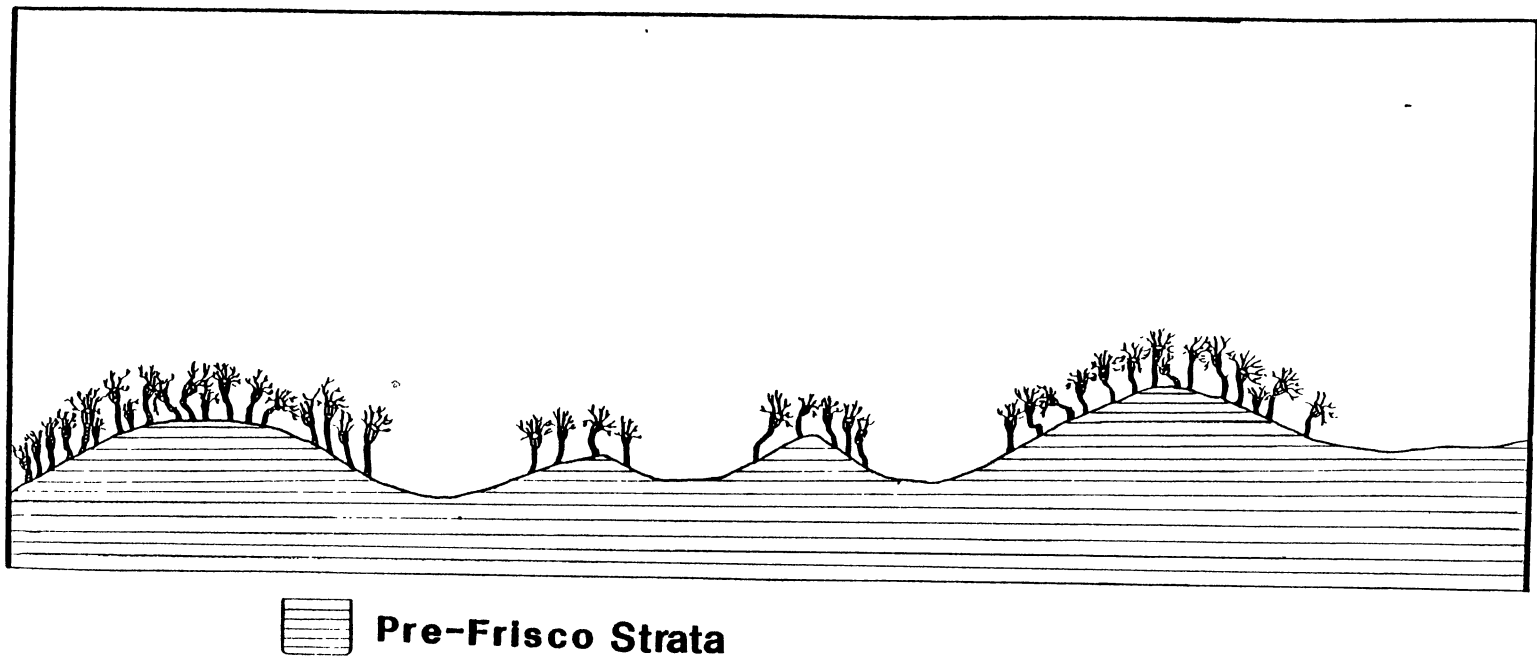
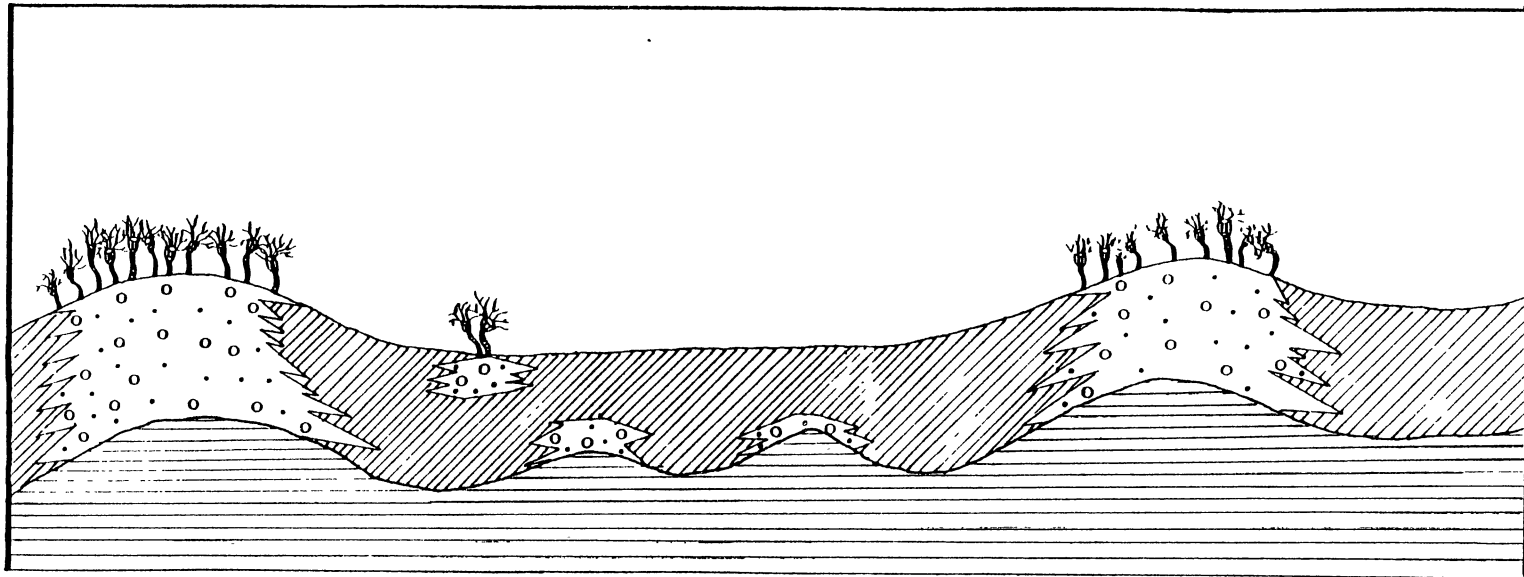


Figure 5. Depositional Model of the Frisco, Stage 1, Crinoids
Established on High Paleotopographic Positions.

Mound Development in the Frisco



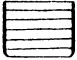
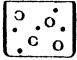

-  **Pre-Frisco Strata**
-  **Mound Facies**
-  **Intermound Facies**

Figure 6. Depositional Model of the Frisco, Stage 2, Development of Mound and Intermound Facies.

Mound Development in the Frisco

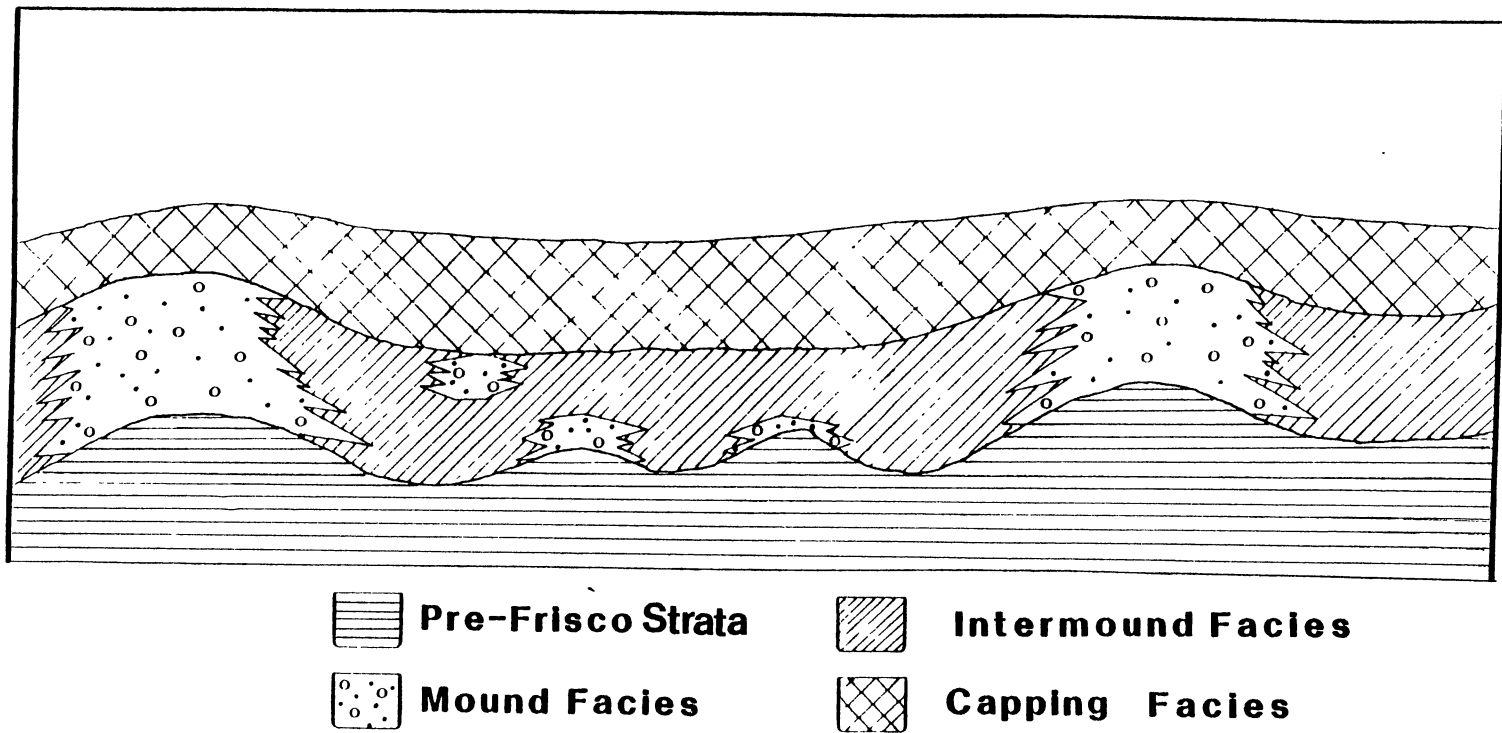


Figure 7. Depositional Model of the Frisco, Stage 3, Mound Growth Ceased and Capping Facies Developed.

Mound Facies

The mound facies is best developed where the Frisco overlies Bois D'Arc, but this facies is not limited by such stratigraphic position.

The mound facies is a poorly sorted wackestone-mudstone (Figure 8-12). The rock is dark and massive. The lime mud was baffled by crinoids on the mound's slope. The baffling reduced currents and sorting. Fewer and better preserved fossils are present in the mound facies than in other facies.

Intermound Facies

The most widespread facies in the Frisco Formation is the intermound facies. In the study area, the intermound facies has been observed overlying the Henry-house Formation and within the Frisco Formation, but it has not been recorded as overlying the Bois D'Arc Formation. Paleotopographically low areas formed by pre-Frisco erosion, probably were areas where the intermound facies was deposited.

The intermound facies is light-colored, moderately sorted packstone-grainstone (Figure 13-16). Current-formed structures commonly are present. Currents winnowed the sediment and removed mud. Apparently, crinoids were not dense enough to baffle mud. Currents also sorted grains, to some degree. Sorting in the intermound facies is

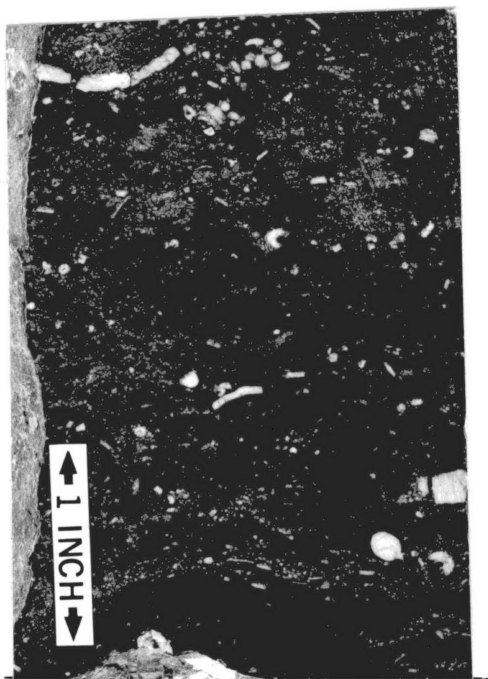


Figure 8. Mound Facies, Poorly
Sorted Wackestone
(Apexco Curtis 2,
8546)

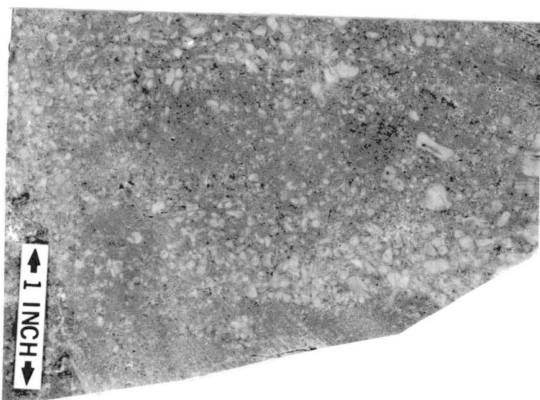


Figure 9. Mound Facies, Wacke-
stone with Intra-
particle Porosity
(Gulf Shaddix,
9246)

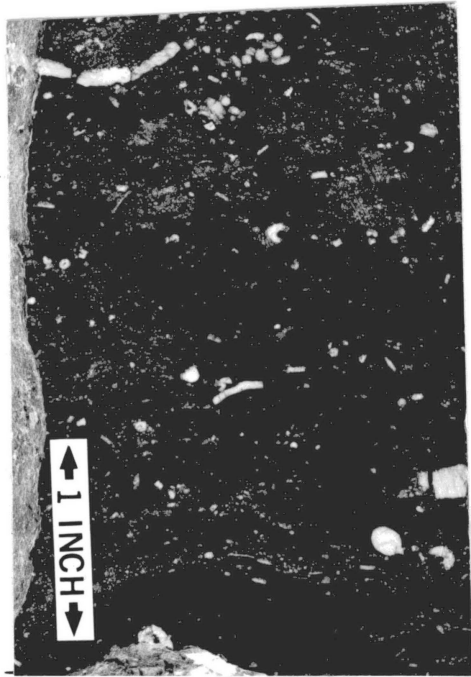


Figure 8. Mound Facies, Poorly Sorted Wackestone (Apexco Curtis 2, 8546)



Figure 9. Mound Facies, Wackestone with Intraparticle Porosity (Gulf Shaddix, 9246)



Figure 10. Mound Facies with Massive Bedding. (Outcrop on Bois D'Arc Creek)

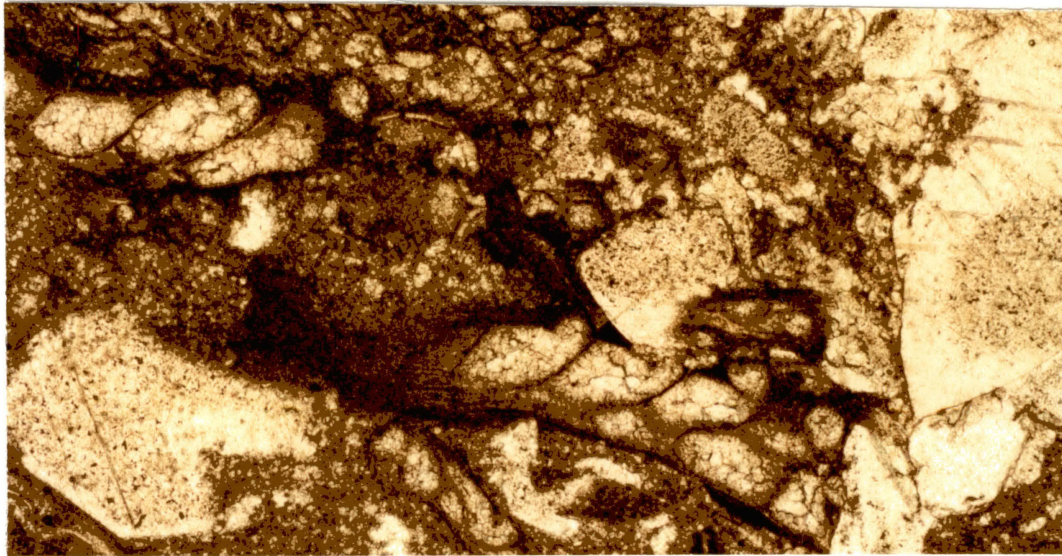


Figure 11. . Photomicrograph of Mound Facies, Note Micrite in Sparry Calcite-neomorphic indicator, (Apexco Curtis 2, 8542, x 40 ppl)

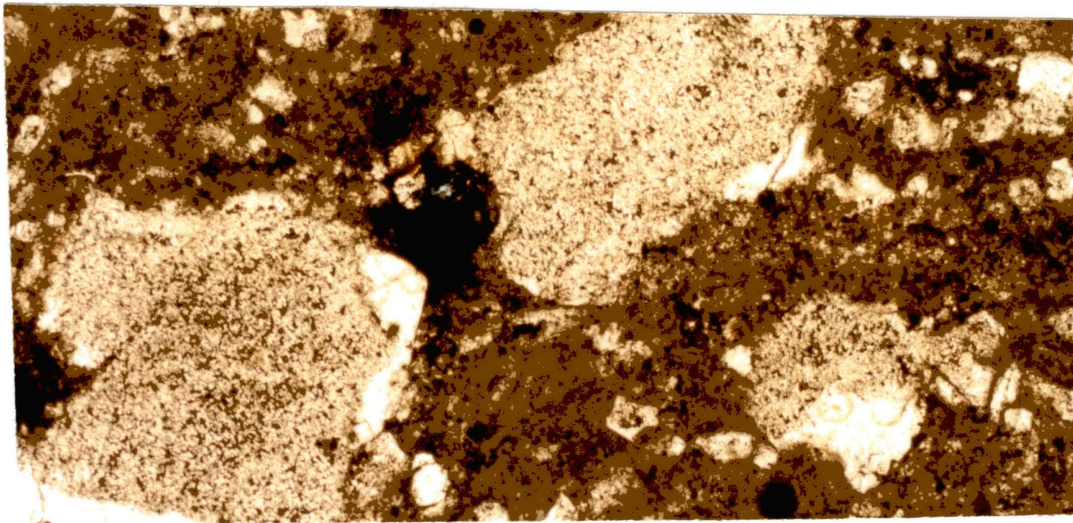


Figure 12. Photomicrograph of Mound Facies from Outcrop, Poorly Sorted Wackestone (Outcrop on Bois D'Arc Creek, x 40 ppl)

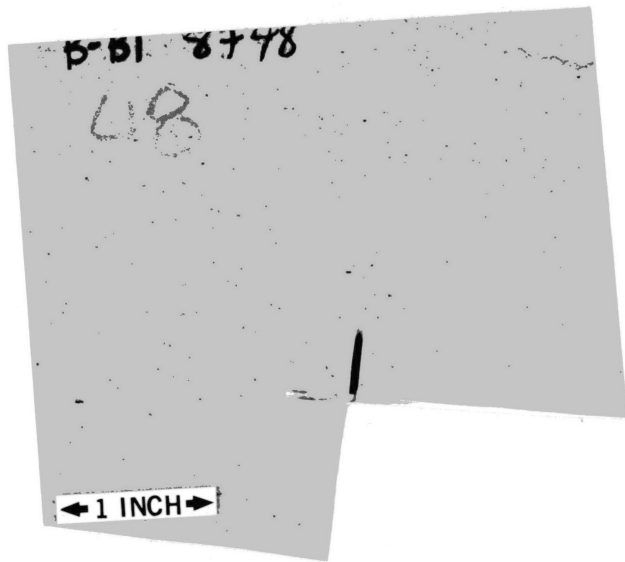


Figure 14. Intermound Facies, Grainstone with Oriented Grains. (Phillips Brooks B, 8748)

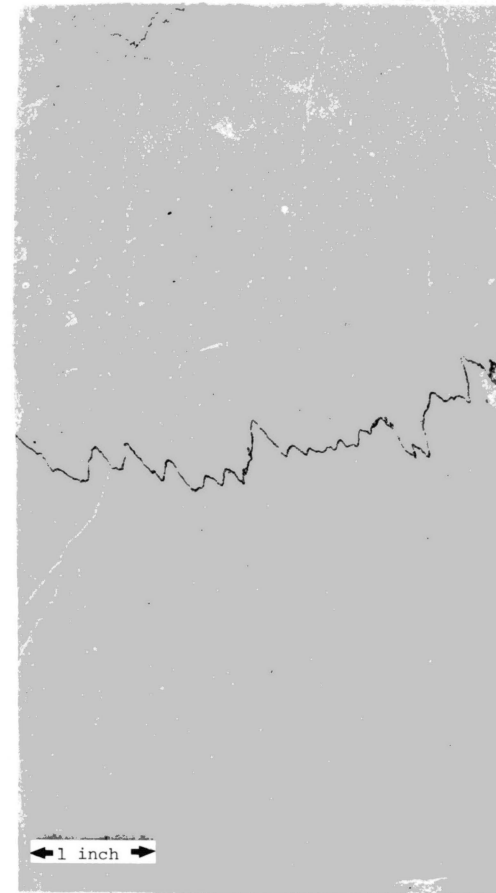


Figure 13. Intermound Facies, Notice Inclined Grain Orientations in the Upper Half of the Core Piece. (Phillips Brooks B, 8743)

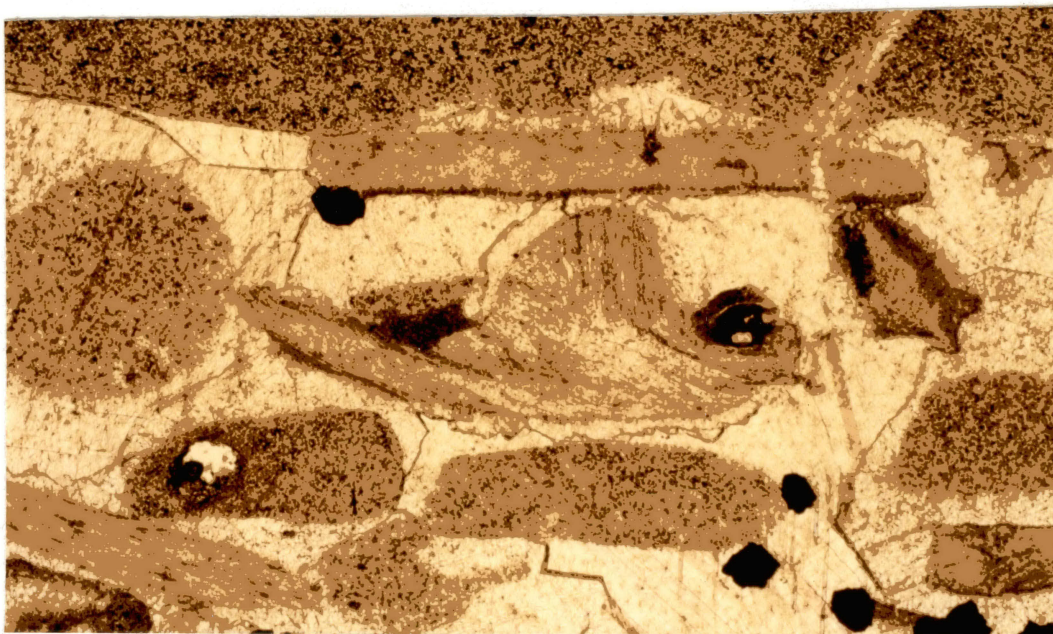


Figure 15. Photomicrograph of a Grainstone in the Intermound Facies; Black Grains are Pyrite.
(Gulf Schroeder, 6291, x 40 ppl)

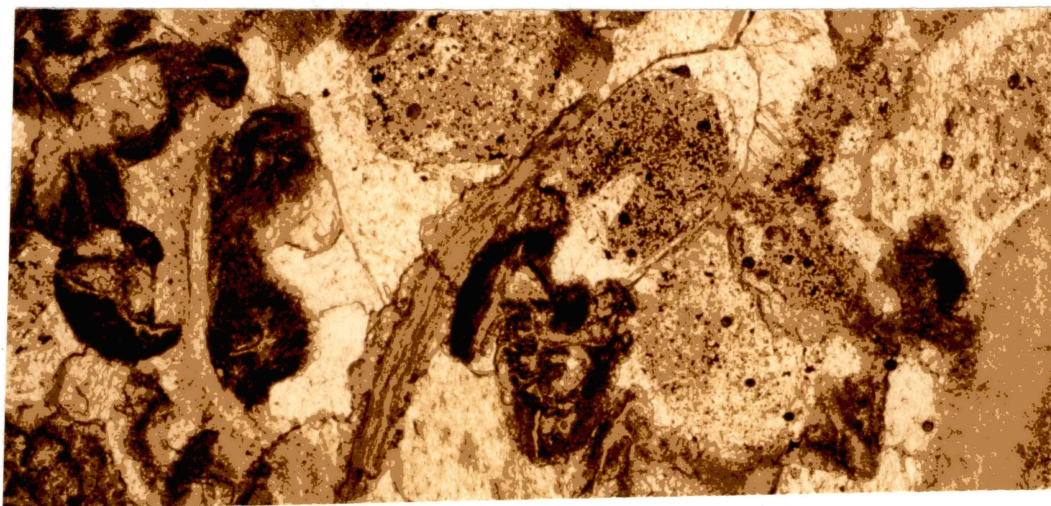


Figure 16. Photomicrograph of a Moderately Sorted Grainstone in the Intermound Facies. (Gulf Wright Heirs #1 B, 6341, x 40 ppl)

moderate. Different sizes and kinds of faunal components make well-sorted sands an improbable occurrence. Currents also orient grains. Orientation generally is horizontal or inclined, or inclined and imbricated. These orientations result in planar or crossbedded textures.

Capping Facies

Actual recognition of a capping facies must be based partly on stratigraphic position, because of lithic similarities between the capping and intermound facies. Where well-sorted grainstone overlies a mound facies, the term capping facies is applied (Wilson, 1975). In the Frisco, light-colored, well-sorted packstone-grainstone has been observed above the mound facies in numerous outcrops and cores. The term "capping facies" can be applied, although the rock's texture essentially is the same as the intermound facies (Figure 17-18).

Crestal Boundstone and Organic Veneers

Crestal boundstones have not been observed in the Frisco. A scattering of coral debris was observed in several cores and outcrops, but their development does not seem to be widespread. The mound may not have grown into the active wave base or into the photic zone, which explains the lack of crestal boundstones. Also, the intense competition with crinoids may have prevented colonization by corals.

Organic veneers also were not observed in the Frisco.



Figure 17. Crossbedded Capping Facies. (Outcrop on Bois Creek)

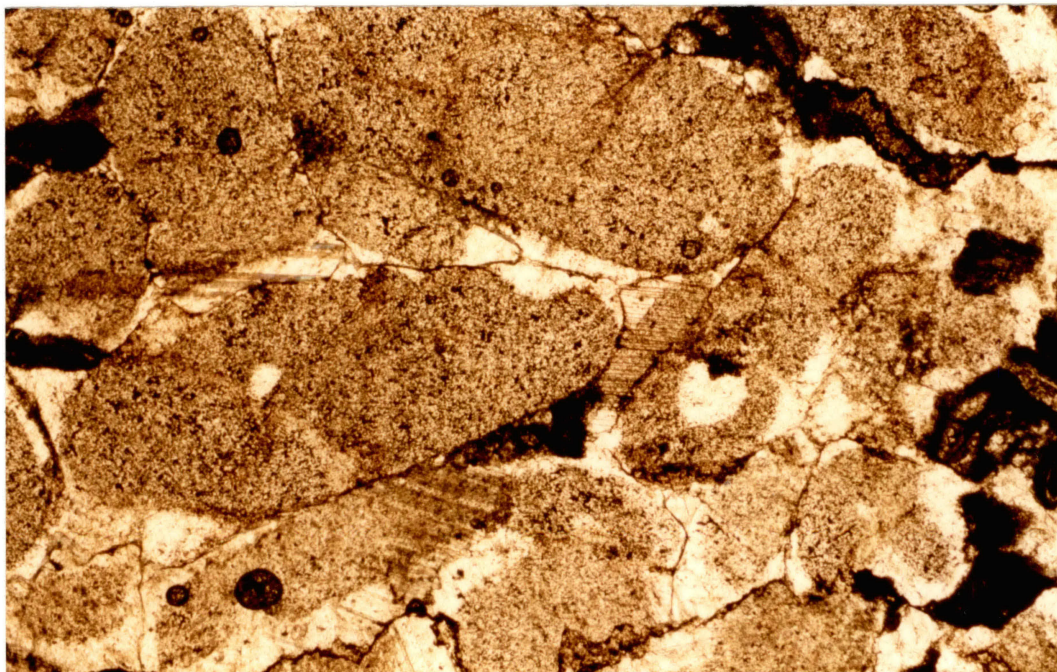


Figure 18. Photomicrograph of the Capping Facies,
Bryozoan Grains are Crushed by the Crinoid
Fragments. (Apexco Curtis 2, x 40 ppl)

Submarine cementation may have helped stabilize the mound. Bryozoans may have provided stabilization by encrusting the mound. Crinoids' root system or holdfasts also may have stabilized mound.

Interfacies Relationship

Reworking of sediments by currents may have spread or smeared facies. In several cores, abrupt change in textures indicates intertonguing of facies. Several cores also have mound facies above intermound facies, a fact which suggest that mound facies are not limited to stratigraphic position.

Determination of extents of facies or the sizes of mounds is difficult. Even closely spaced wells may not give a good delineation of a facies' extent or the areas of individual mounds. It is likely that there are a variety of mound sizes dependent upon pre-Frisco topography.

Thickness of the mound facies generally is less than that of associated facies. Mounds were limited in upward growth by slow subsidence rates (Adler, 1971). When this occurred, the mounds were inundated by the intermound facies and the capping facies (Wilson, 1975).

Summary

The mound development in the Frisco is summarized in Figure 5-7. Pre-Frisco erosion created a pattern of topographic highs and lows. Due to the nature of the

topography crinoids flourished on the slopes and crests of mounds. Crinoids baffled the sediment forming a muddy mound facies. Intermound facies developed as sediment was shed from the mounds in areas where baffling was not occurring. The intermound facies eventually inundated the mound facies creating a capping facies. Criteria for determining facies are shown in Table II.

Crinoid Paleoecology

Crinoids are the most abundant grain in the Frisco. Percentages of crinoids may vary along different facies. Intermound and capping facies generally have more crinoid fragments than mound facies.

In the Frisco current formed structures are observed by orientation of crinoid fragments. Orientation of ossicles are imbricate, inclined, and horizontal. When currents were not effective, orientation was random, and in thin section, ossicles appear circular or oblate.

Sediment Production and Crinoids

Crinoids in the Frisco were important in supplying sediment which was produced during their life and death. A ten-armed crinoid has been estimated to have contained 600,000 skeletal elements (Clark, 1915). Tasch (1973, p. 748) stated "recent pentacrinoids have up to 25 million ossicles," - an ample supply of sediment. Upon death the coelum fibers, which hold the crinoids together,

TABLE TWO
 CRITERIA FOR FACIES IDENTIFICATION IN THE FRISCO

	Mound	Intermound	Capping
Poorly Sorted			
Well Sorted			
Fossils Fragmented			
Well Preserved Fossils			
Current Formed Structures			
Massive Bedding			
Micrite Dominant			
Sparry Calcite Dominant			
Neomorphism Indicated			
Mudstone/Wackestone			
Grainstone/Packstone			

disintegrate allowing ossicles and calyx plates to be moved by currents. Disintegration of coelum fibers takes place under both aerobic and anaerobic conditions (Cain, 1968).

Crinoids also produce sediment during their life. Crinoid's arms can break or fall off. When an arm is lost, regeneration of an arm takes place. A variety of reasons for arm loss is known: 1. crinoids may shed arms during ontogeny (life cycle), 2. during predation, organisms grasping the crinoid can cause arms to break off, 3. unstable conditions such as low oxygen concentrations and elevated temperatures can cause arms to fall off, 4. large storms with extended wave bases may damage crinoids and break off parts of the skeleton (Tasch, 1973).

Crinoids also act as sediment bafflers. Baffling occurs when distribution of crinoids is dense (Wilson, 1975; Cain, 1968). Baffling by crinoids was important in growth and stabilization of mounds in the Frisco. Baffling prevented currents from winnowing mud away, allowing accumulation of mud and continued colonization of crinoids.

Crinoid Ecology

Optimum conditions for profuse crinoidal growth were necessary during Frisco deposition. Important parameters for crinoidal growth are animal/substrate relationship, salinity, water circulation, water depth, water temperature, and feeding mechanism.

Substrate is an important limiting factor for most sessile organisms, but modern day crinoids are not limited by substrate.

"Eel grasses, algal organisms, rock and mud substrates, shell and shell debris, sponges and corals are among the attachment sites for modern crinoids." (Tasch, 1973, p. 750)

A variety of substrates for crinoids is obvious, but Marr (1963, p. 347) states, "that the greatest variability and abundance occurs on muddy bottoms."

A range of tolerable salinities for crinoid survival is 24 parts per thousand to 36 parts per thousand (H. L. Clark, 1915). The normal salinity of sea water is approximately 35 parts per thousand; hence, restricted conditions would be detrimental to crinoids' existence.

Well aerated and well circulated water is necessary for crinoids to flourish (A. M. Clark, 1957). Stagnant water would curtail oxygen severely limiting crinoidal growth. Fewer numbers and species of crinoids exist in deep water than in shallow water (Tasch, 1973). Currents and waves in shallow water increase water circulation which in turn enhances oxygen concentrations.

Crinoid's filter feeding system relies on suspended food matter for nourishment i.e. phytoplankton and zooplankton. Abundant suspended food matter and low sedimentation rates are beneficial to filter feeders, especially crinoids (Sokolova, 1959). Particulate matter which could not be consumed would clog crinoidal filtering systems.

Paleo-conditions for profuse crinoidal growth are summarized below:

- muddy substrates
- normal salinities - 35 p.p.t.
- well-circulated conditions
- low turbidity/low sedimentation

The preceding conditions probably were present during Frisco deposition.

Crinoids as Sedimentary Particles

Two conflicting ideas exist when discussing crinoid ossicles as sedimentary particles; upon decomposition gases evolved are trapped allowing the crinoid fragments to become buoyant, or gases are not trapped and buoyancy does not occur. If buoyancy occurred, there would be widespread dispersion of columnals.

Experiments conducted on the crinoid Antedon bifida show that the density in Antedon did not decrease. In fact, the density increased initially, and followed by a very slight decrease in density (Figure 19), (Cain, 1968). No trapping of carbon dioxide was observed and Antedon did not become buoyant.

Facies in the Frisco would not have developed if crinoid fragments had been buoyant; because widespread distribution of crinoid fragments would have occurred, creating a sheet-like deposit.

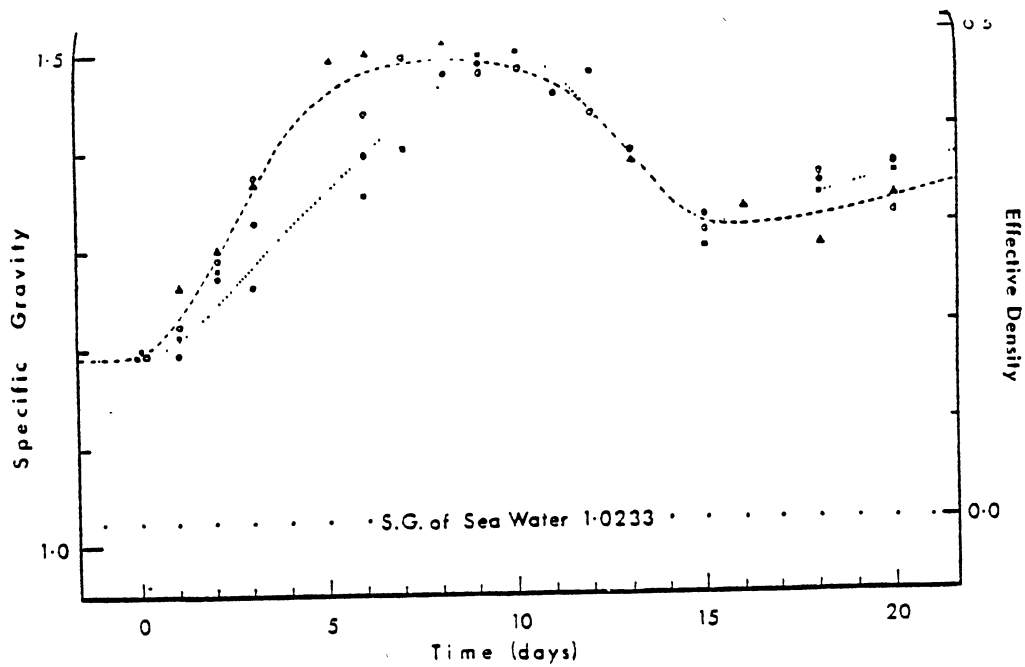


Figure 19. Graph of the Density Increase in the Crinoid *Antedon bifida*, After Death, the Dashed Line Represents Aerobic Decomposition, the Dotted Line Represents Anaerobic Decomposition (from Bain, 1968)

C

Petrology and Petrography

Numerous cements, sedimentary structures, and varieties of textures were observed in the Frisco; these features are supportive of the crinoidal mound model for the depositional environment of the Frisco Formation.

Matrix/Cement

The matrix seen in thin section varied from 100% micrite to 100% sparite. Mud content suggests the baffling by crinoids. Baffling by thickets of crinoids allowed mud to accumulate even under high energy conditions (Wilson, 1975).

Sparite can be attributed to persistent^e current activity that winnowed mud and left moderately sorted sands. Subsequent cementation of these sands by syntaxial overgrowths around crinoids resulted in abundant sparite. A relationship between spar and micrite is exhibited in Figure 20. The line drawn separates the mound facies from the intermound facies.

Sedimentary Features

Horizontal oriented grains can be observed in the intermound and capping facies. Megascopic orientation is present as subtle laminations. Crinoids, trilobites, bryozoans, and brachiopods can be horizontally oriented (Figure 21). Horizontally oriented grains are more common than

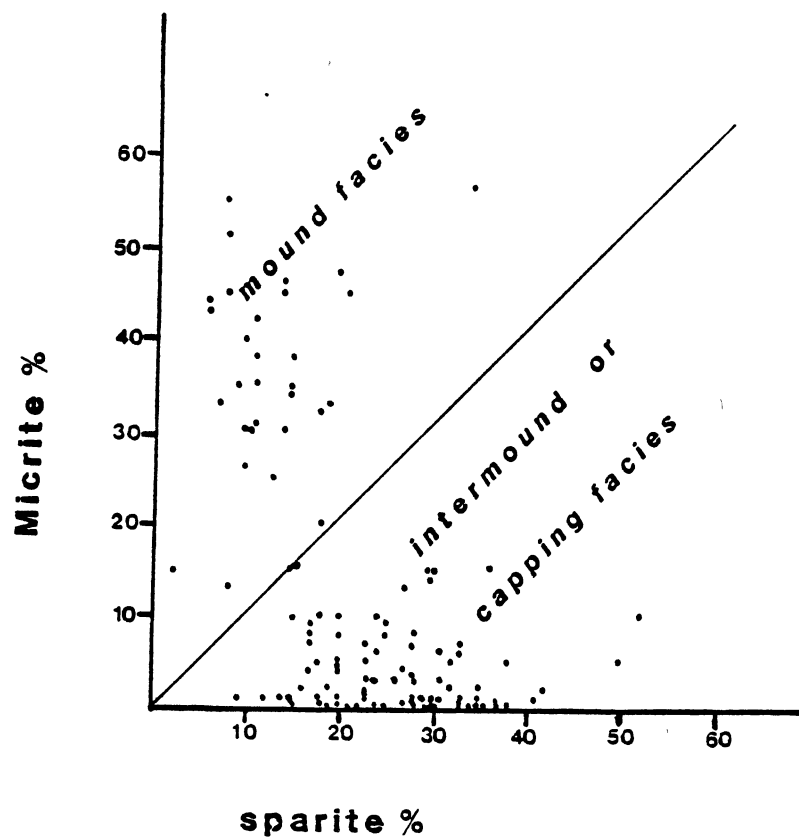


Figure 20. Graph of Sparite vs. Micrite, all Data from Thin Section Analyses.

horizontal laminations. Sparry calcite generally is the cement where horizontal features are observed.

Inclined grains or laminations are observed in the intermound and capping facies (Figure 22). No micrite has been reported in rocks with inclined orientations.

Massive bedding was observed in core and outcrop (Figure 23). Massive bedding is common in the mound facies, but it also appears in the other facies.

Fair to moderate sorting was found in the intermound and capping facies (Figure 24). Poor sorting is characteristic of the mound facies; because of the baffling, there was little chance to sort sediment (Figure 25). Grain size was dependent on the maturity of the crinoid and the type of grain. Grain size from the arm plates vary when compared to grains from the stem or calyx. Likewise, immature crinoid grains will vary in size, especially compared to a mature adult.

Frisco Fauna

The Frisco grains are almost entirely skeletal fragments. Crinoid fragments are the most abundant grain with percentages ranging from 10 to 70. The size varied greatly; large fragments were 2 cm in diameter, and small fragments were less than .1 mm. The mean size of crinoid fragments was .4 mm. The ecological significance of crinoids is discussed in the "Paleoecology of Crinoids" section.

Bryozoans are an important faunal element in the

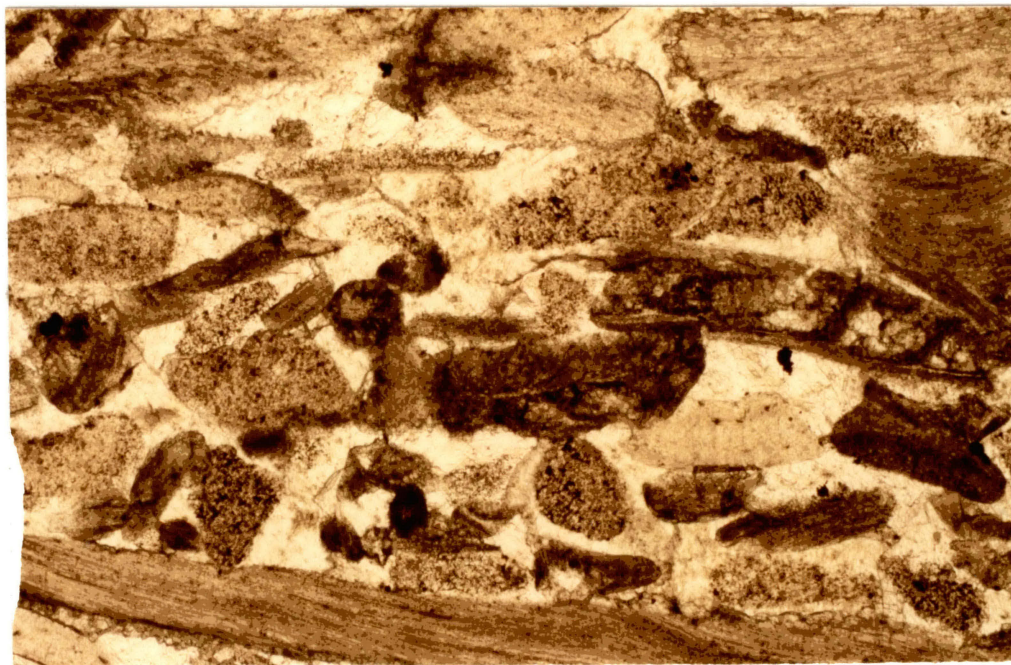


Figure 21. Horizontally Oriented Grains (Midwest McManus, 8109, x 40 ppl)

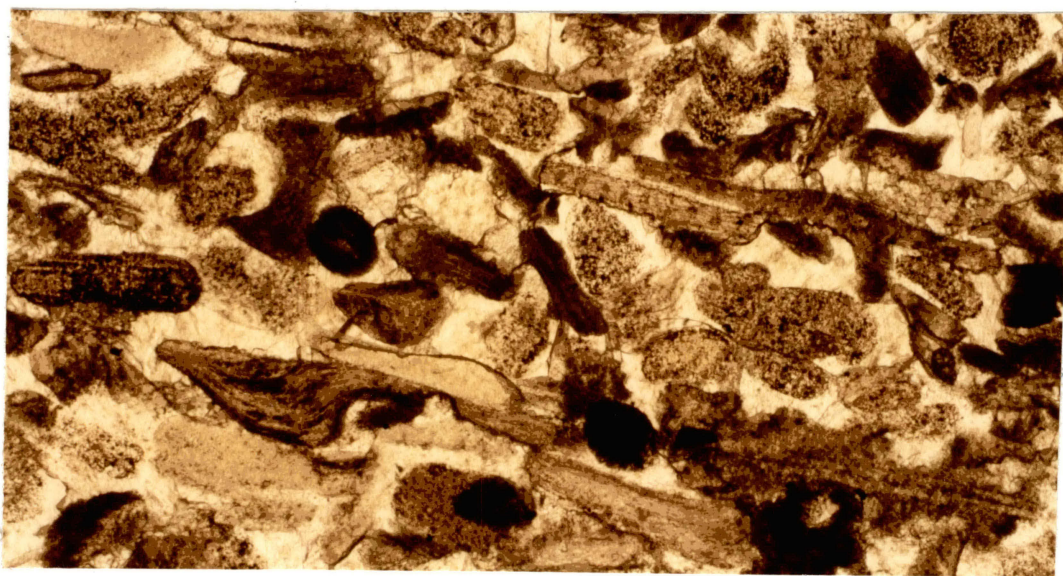


Figure 22. Inclined Grain Orientation (Midwest McManus, 8111, x 40 ppl)



Figure 23. Massively Bedded Mound Facies. (Outcrop on Bois D'Arc Creek)

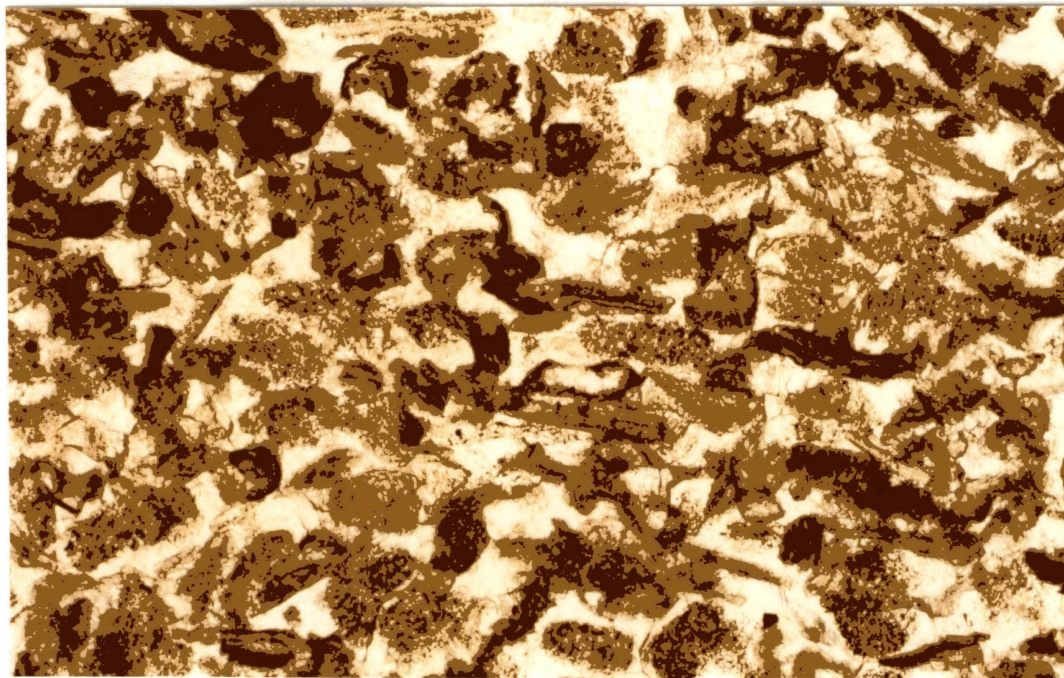


Figure 24. Well Sorted Grainstone. (Midwest McManus, 8111, x 20 ppl)

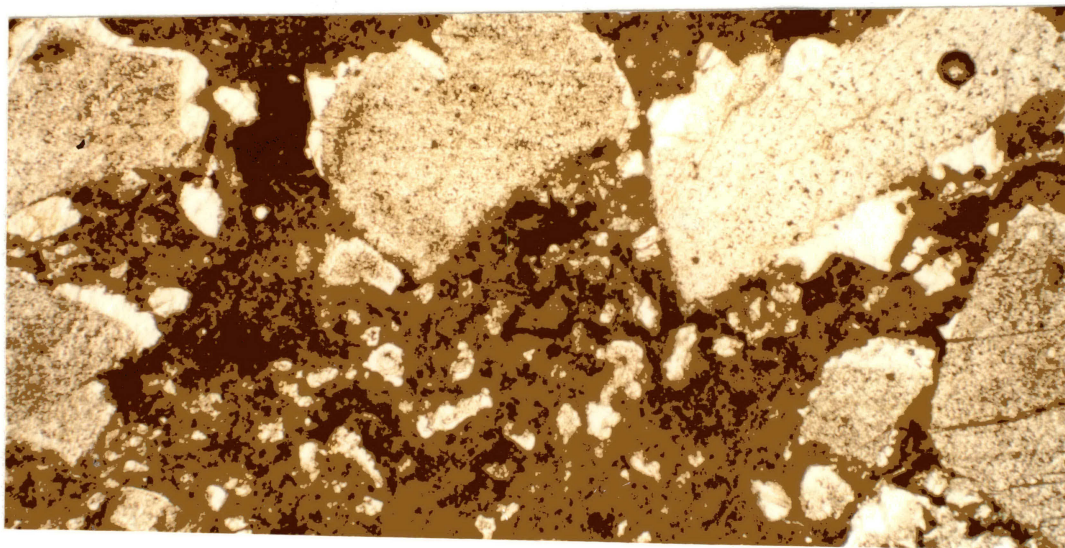


Figure 25. Poorly Sorted Wackestone. (Outcrop on Bois D'Arc Creek, x 20 ppl)

Frisco. Crinoids and bryozoans have similar ecological niches; both are filter feeders, feeding on phytoplankton and zooplankton. Bryozoans were not restricted to specific facies, but bryozoans in the mound facies were observed to be less fragmented than in other facies (Figure 26-27). Primary porosity can be preserved in bryozoan's zooecia. Bryozoans may have encrusted and stabilized mounds. As framework grains bryozoans (2-35%) were second to crinoids. The size of bryozoans range from 5 cm. to less than .1 mm.

The distribution of brachiopods (0-22%) did not suggest a specific facies. Articulated valves were not seen. Trilobites (0-5%) and gastropods (0-3%) also appear in the Frisco (Figure 28). Trilobites and gastropods also do not appear to be facies indicators.

Both rugose and tabulate corals appear in several cores and in outcrops (Figure 29). Paleo-conditions were not favorable for profuse coral growth (0-5%). Strong competition from crinoids may have prevented corals from colonizing.

Micritized grains and peloids appear in the intermound facies. Peloids also were found in association with ooliths. In one core, several ooliths appear in the intermound facies. Shallow, agitated water is suggested by the presence of oolites.

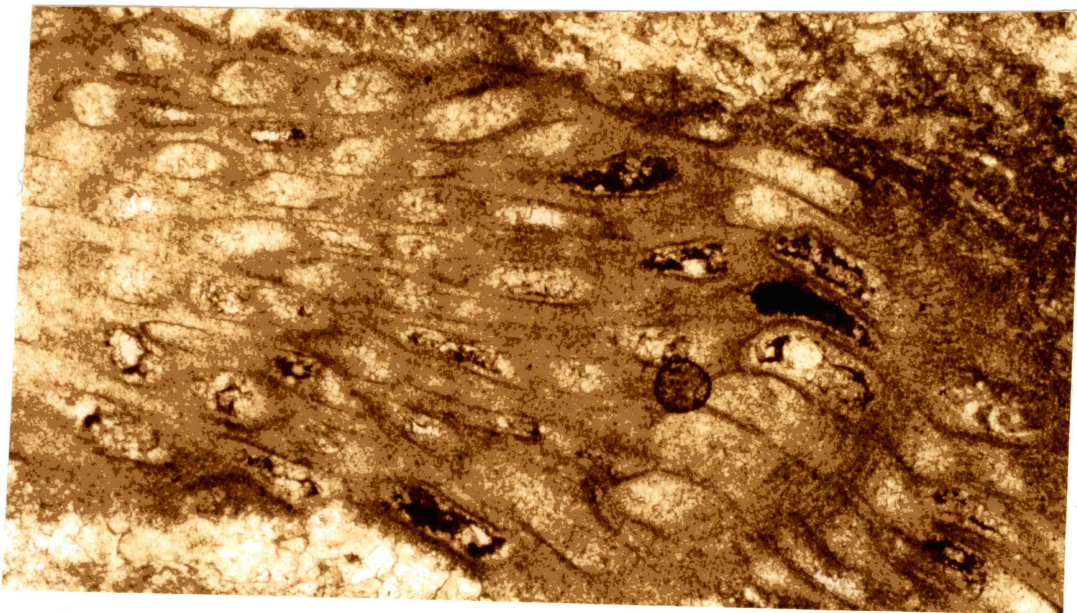


Figure 26. Unfragmented Bryozoan in the Mound Facies.
(Gulf Shaddix, 9215, x 40 ppl)

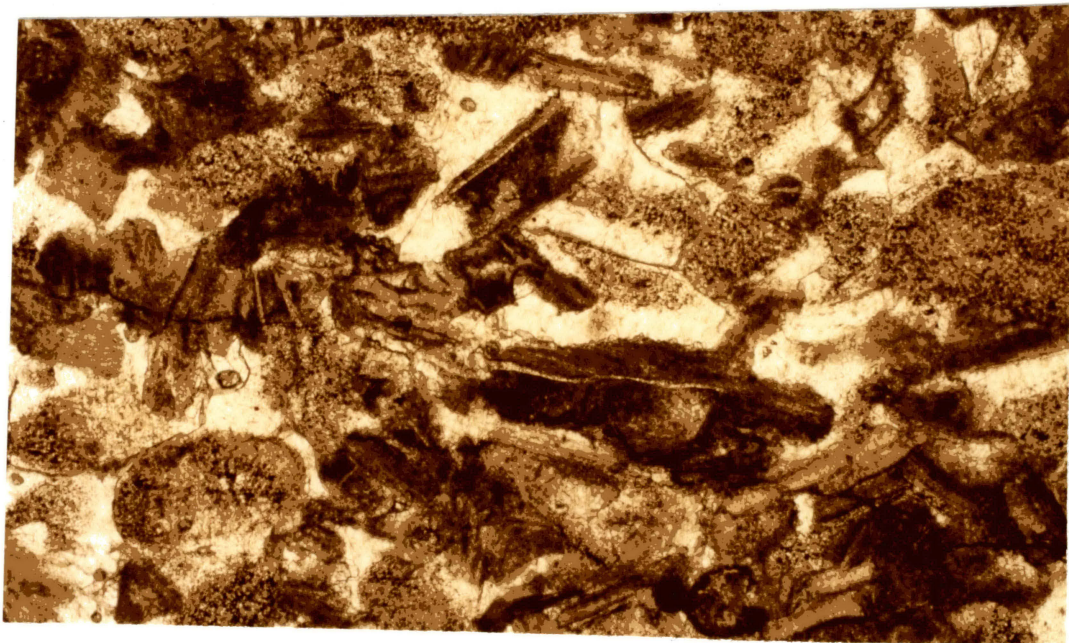


Figure 27. Fragmented Bryozoans in the Intermound Facies.
(Phillips Brooks B, 8755, 40 x ppl)

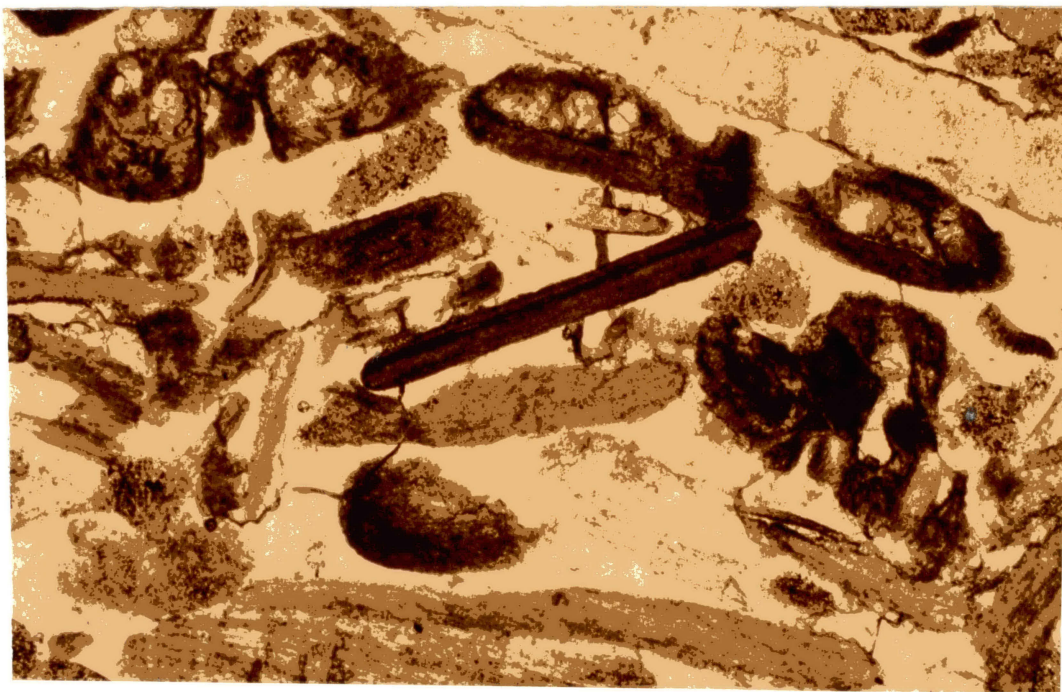


Figure 28. Diversity of Fauna, T=Trilobite Fragment, By=Bryozoan Fragment, B=Brachiopod Fragment (Midwest McManus, 8111, x 40 ppl)

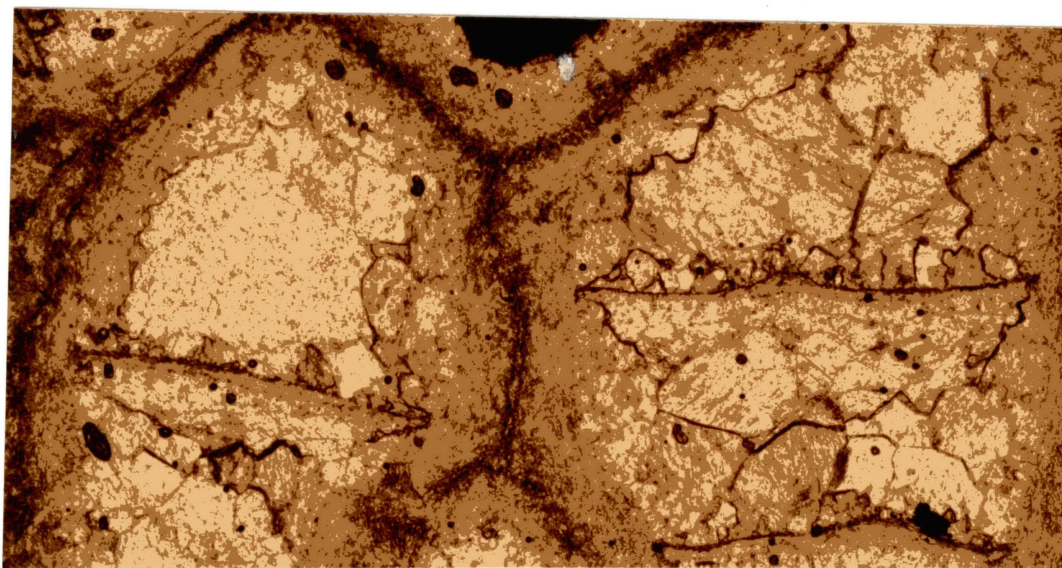


Figure 29. Drusy Spar in Coral Fragment (Apexco Curtis 2, 8588, x 40 ppl)

Diagenesis and Porosity

Cements

Cementation of the Frisco Formation was complex. The zonation of Frisco's monomineralic cement (calcite) aided in refining the paragenetic sequence. Two types of cement exist in the Frisco: sparry calcite and micrite.

Sparry Calcite Sparry calcite is present as overgrowths or drusy spar. The type of sparry calcite is determined by the substrate that the cement nucleated upon. Syntaxial overgrowths formed around single crystal crinoid fragments. Drusy spar formed around multi-crystal fragments (Figure 29). Drusy cements were observed in zoecia, corallites, brachiopod valves and trilobite fragments. Drusy cements also plugged vugs. The amount of drusy spar was minor in comparison to overgrowths around crinoid fragments.

Complex overgrowth patterns around most crinoid fragments were observed by cathodoluminescence.

Initially, overgrowth patterns appeared random. The c-axis in most crinoids was parallel to the vertical morphological axis (Evamy and Sherman, 1965). Calcite crystal growth favors the c-crystallographic axis. Fragments oriented with the thin section parallel to the c-axis/morphological axis (vertical section) show a larger amount of overgrowth than crinoid fragments which have their c-axis/morphological axis (basal section) perpendi-

cular to the thin section (Figure 30). Vertical sections may be serrated with multiple crystal terminations. The number of terminations decreases away from the crinoid fragment. If space is available the multiple terminations will coalesce into one (Figure 31). The multiple terminations probably resulted from the perforated surface of crinoids (Evamy and Sherman, 1965).

The abundant sparry calcite in the intermound and capping facies did not appear to have formed by neomorphism (new form) of micrite. Bathurst (1975) established criteria to distinguish cementation from neomorphism. Overwhelmingly, cementation criteria was met by the Frisco Formation:

1. interparticle spar in well-sorted sands (Figure 24)
2. two generations of cement (Figure 32)
3. mechanically deposited micrite is present but unaltered
4. sharp contacts (Figure 33)
5. geopetal structures are present
6. intercrystalline boundaries are plane interfacies with a high percentage of enfacial (180°) angles at triple points (Figure 33).

The sparry calcite in the mound facies may have formed by more than one process. Cementation of grains is apparent in Figures 11-12, but neomorphic textures are also present. Bathurst (1975) developed criteria for recognizing neomorphism; neomorphic textures present in the Frisco are:

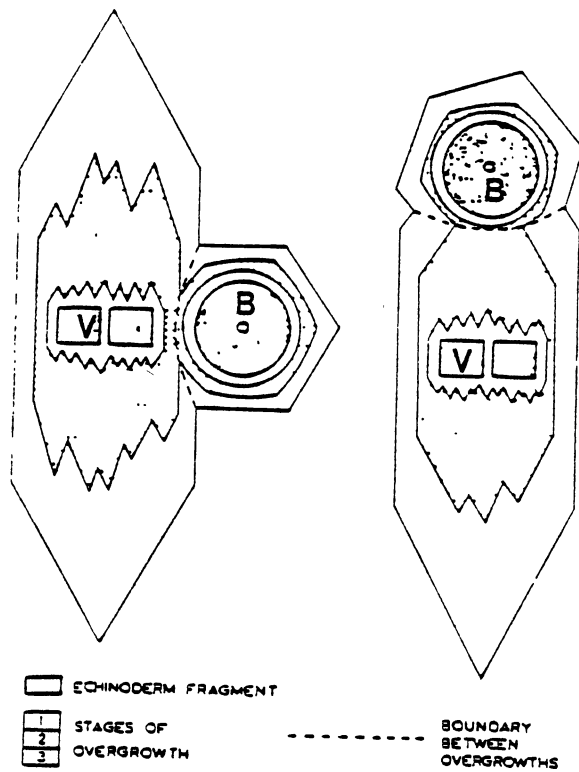


Figure 30. Difference in Overgrowth Pattern of Basal (B) and Vertical (V) Sections of Crinoids (Evamy and Shearman, 1965)

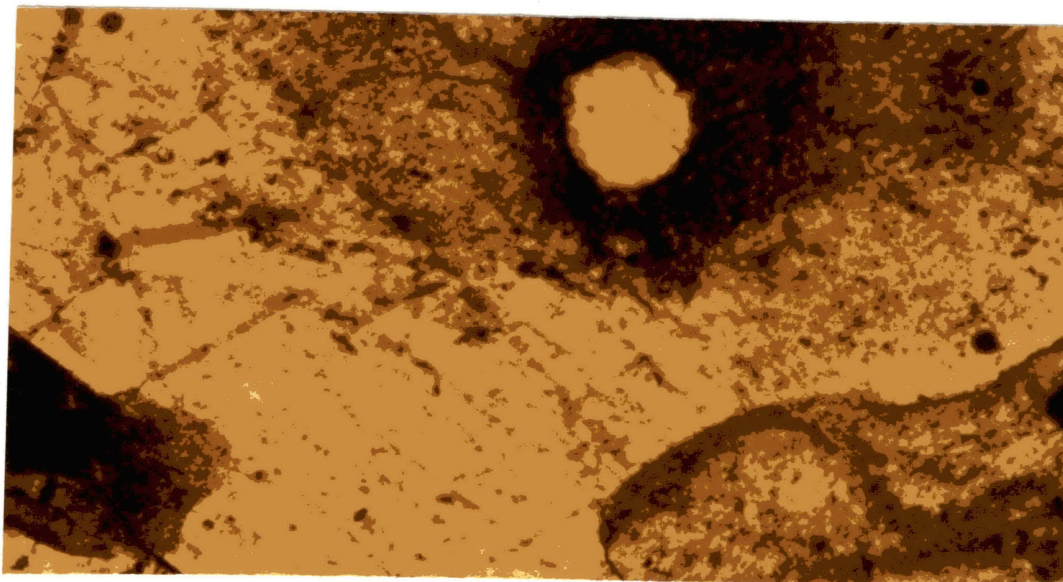
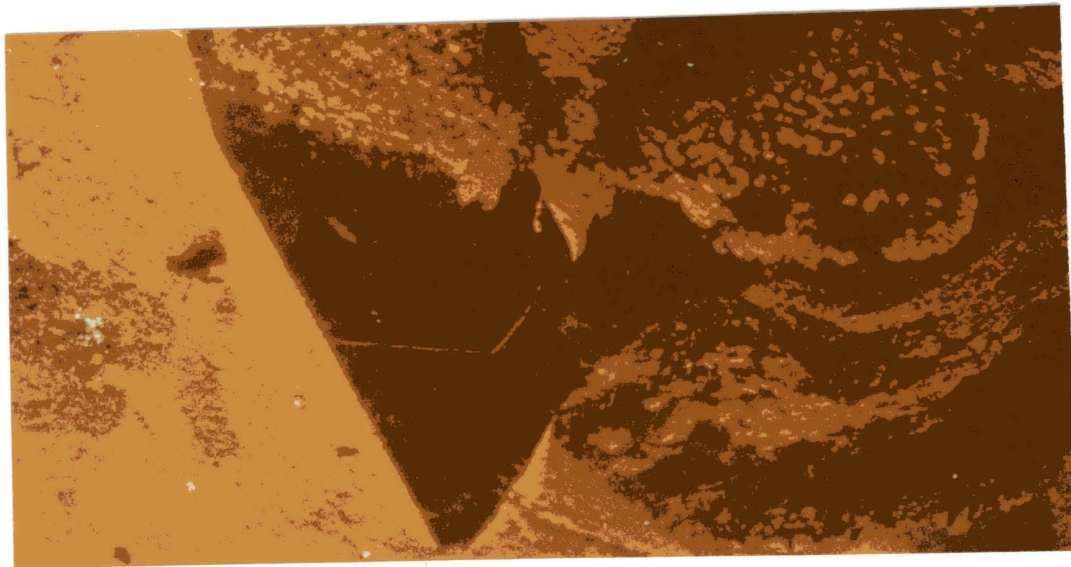


Figure 31. (a) Cathodoluminescent Microphotograph of Multiple Terminations (t) Coalescing into One (T). (Apexco Curtis 2, 8568, x 40)
(b) Plane Polarized Photograph of (a).

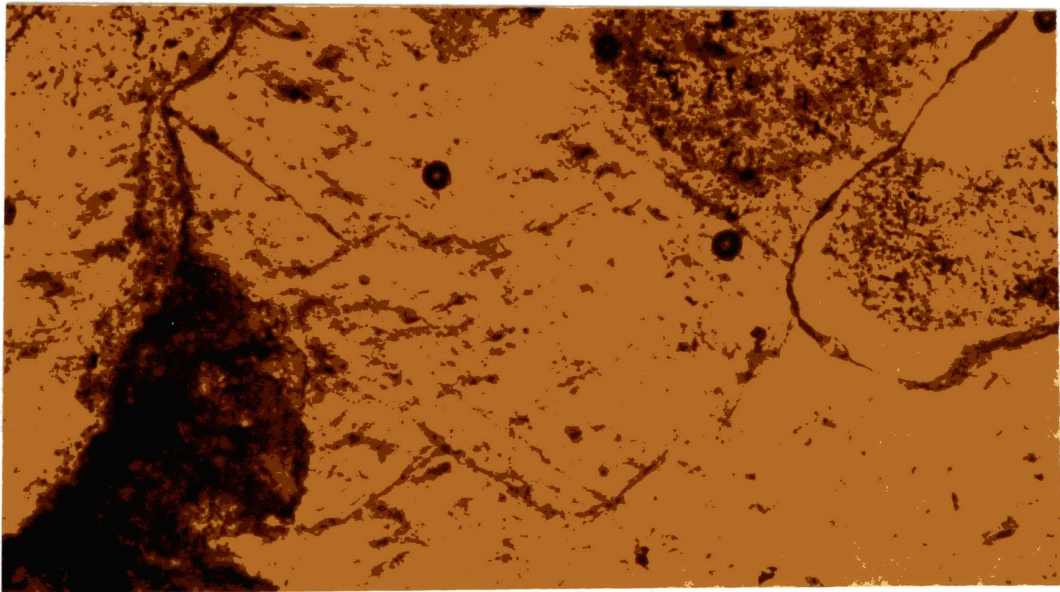
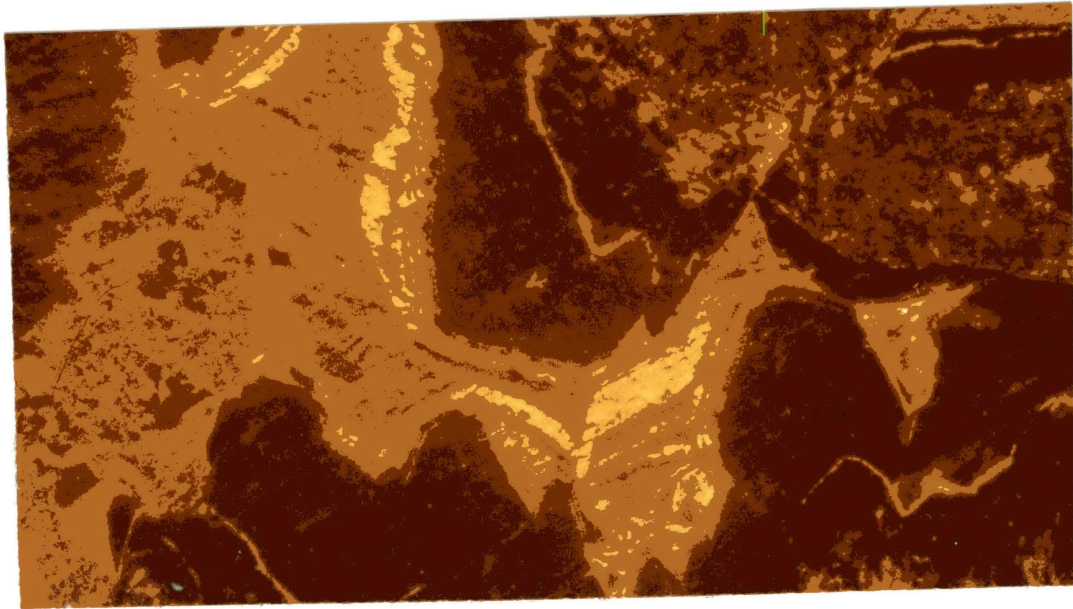


Figure 32. (a) Cathodoluminescent Photomicrograph of Multiple Zonations in Crinoid Overgrowths. (Gulf Holtzschue, 6359, x 40)
(b) Plane Polarized Photograph of 32.

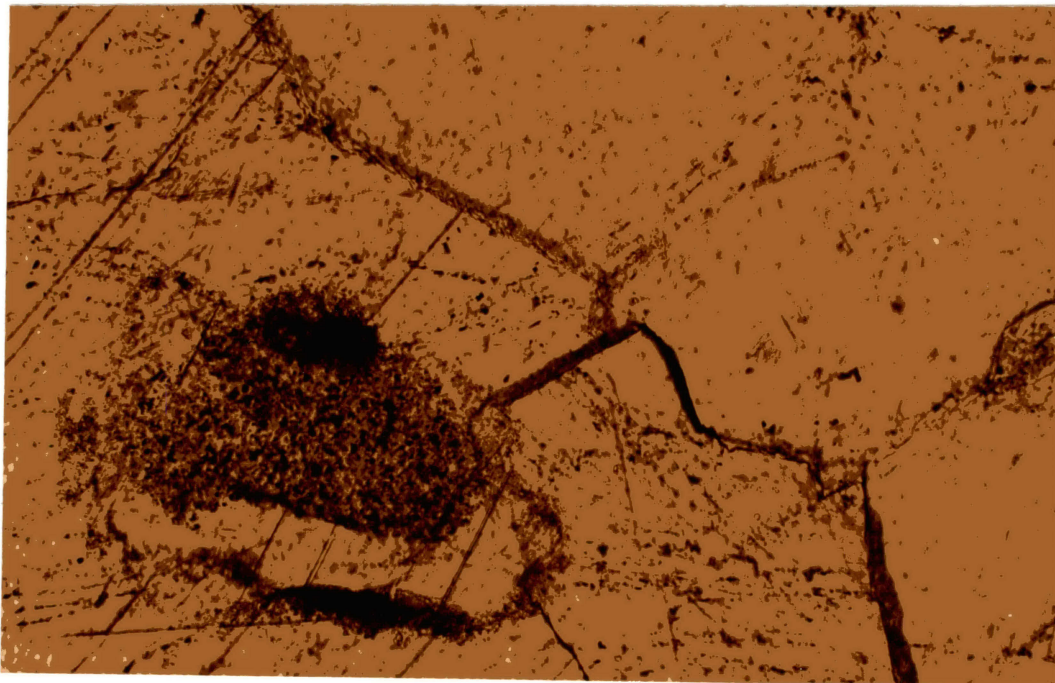


Figure 33. Photomicrograph of Sharp Contacts and Enfacial Angle (E) (Midwest McManus, 8090, x 100 ppl)

1. The first part of the document discusses the importance of maintaining accurate records of all transactions and activities. It emphasizes that this is essential for ensuring transparency and accountability in the organization's operations.

2. The second part of the document outlines the various methods and tools used to collect and analyze data. It highlights the need for consistent and reliable data collection processes to support effective decision-making.

3. The third part of the document focuses on the role of technology in data management and analysis. It discusses how modern software solutions can streamline data collection, storage, and reporting, thereby improving efficiency and accuracy.

4. The fourth part of the document addresses the challenges associated with data security and privacy. It stresses the importance of implementing robust security measures to protect sensitive information from unauthorized access and breaches.

5. The fifth part of the document discusses the importance of data quality and integrity. It notes that high-quality data is crucial for generating meaningful insights and making informed decisions.

6. The sixth part of the document explores the various applications of data analysis in different business contexts. It provides examples of how data can be used to identify trends, optimize processes, and improve customer satisfaction.

7. The seventh part of the document discusses the ethical considerations surrounding data collection and analysis. It emphasizes the need for transparency, consent, and responsible use of data to build trust and maintain a positive reputation.

8. The eighth part of the document provides a summary of the key points discussed throughout the document. It reiterates the importance of data in driving organizational success and the need for a data-driven culture.

9. The final part of the document offers recommendations for future research and practice. It suggests areas where further exploration is needed to advance the field of data management and analysis.

1. gradational contact between sparite and micrite,
2. crystal boundaries range from curved to wavy,
3. floating relics of micrite in sparite (Figure 11),
and
4. few triple junctions with enfacial angles.

Some of the syntaxial overgrowths in the mound facies may have had a dual origin as cement near the crinoid fragment and as neomorphic replacement near micrite.

The cathodoluminescent quality of sparry calcite is an indication of chemical variations within the cement and the redox potential present during cementation. Zonations of nonluminescence, bright luminescence, and dull luminescence (Figure 34) are dependent on the amounts of Fe (quencher) and Mn present in the calcite lattice (Grover and Read, 1983). While chemical analysis was not performed on the Frisco Formation, several generalizations can be applied to the zonation of cement: 1. non-luminescent cement probably has low Mn^{++} and Fe^{++} values; oxidizing conditions during cementation prevented reduction of Mn^{+++} , Mn^{+++} , Fe^{+++} , and introduction of those ions in the calcite lattice, 2. the bright luminescent cement probably resulted because of an increase in Mn^{++} in comparison to Fe^{++} , in the calcite lattice, 3. dull luminescent cement represents an increase in Fe^{++} into the calcite lattice (Grover and Read, 1983).

Figure 35 suggests that the cementation history of the Frisco Formation was a complicated event. Changes in pore-water chemistry were reflected in the luminescent quality

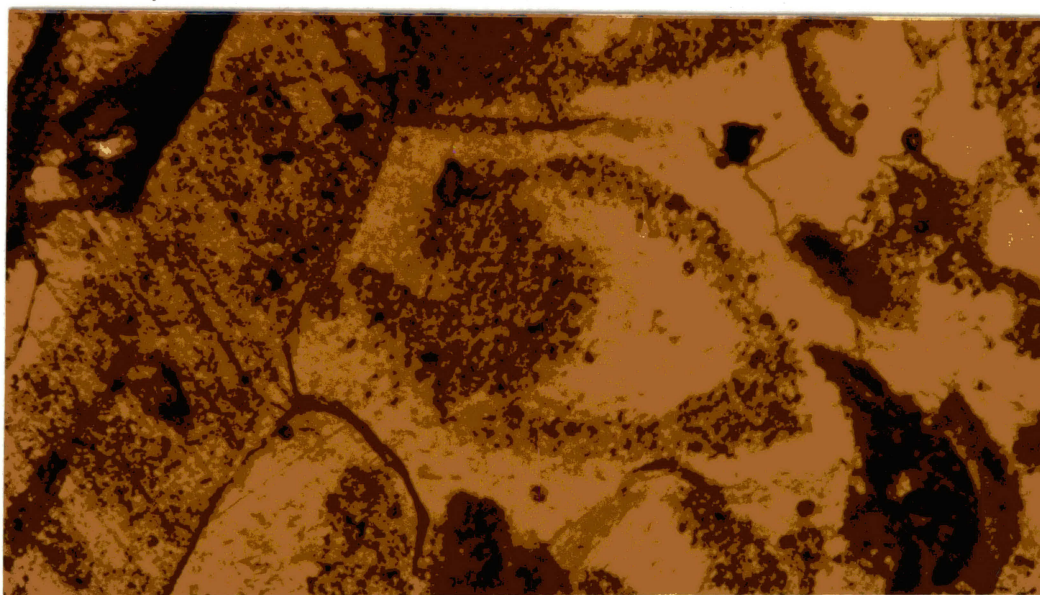


Figure 34. (a) Cathodoluminescent Microphotograph Showing Non-Luminescent, Bright Luminescent, and Dull Luminescent Sequence of Cementation in the Frisco. (Apexco Curtis 2, 8553, x 40)
(b) Plane Polarized Photomicrograph of (a).

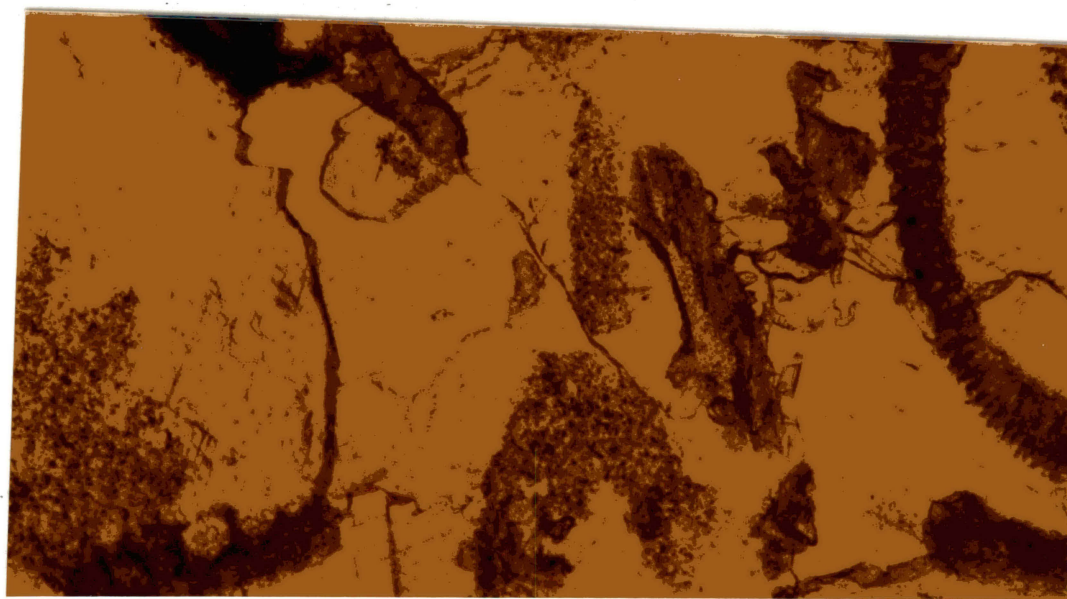


Figure 35. (a) Cathodoluminescent Photomicrograph Showing at Least Nine Different Zones of Cement, Multiple Episodes of Non-, Bright, and Dull Luminescent Cement are Present. (Gulf Streeter, 7032, x 40)
(b) Plane Polarized Photomicrograph of (a).

of the cement. The general sequence is a nonluminescent cement, followed by a bright orange luminescent cement and concluding with a dull luminescent cement. The preponderance of the dull luminescent cement implies that most of the sparry calcite in the Frisco Formation formed in a reducing environment i.e. the subsurface.

Micrite Two types of micrite are present in the Frisco: primary and secondary. In several areas microspar appears, but categorization of micrite by size was not performed. The presence of microspar represents aggrading neomorphism.

Crinoids baffling in the mound facies allowed the accumulation of primary micrite. Primary micrite in the intermound and capping facies represents incompletely winnowed sands. Xenotopic equigranular calcite is the composition and morphology of primary micrite (Figure 36).

Secondary micrite was not present in the Frisco Formation at the time of deposition. It represents disaggregation of overlying material by dissolution. Secondary micrite generally is found in or near vugs or areas of dissolution. Unlike primary micrite, secondary micrite is not equigranular, and it may contain other minerals other than calcite (Figure 37-38).

Porosity

The reservoir-quality is directly related to the distribution of porosity in the Frisco. Facies and the

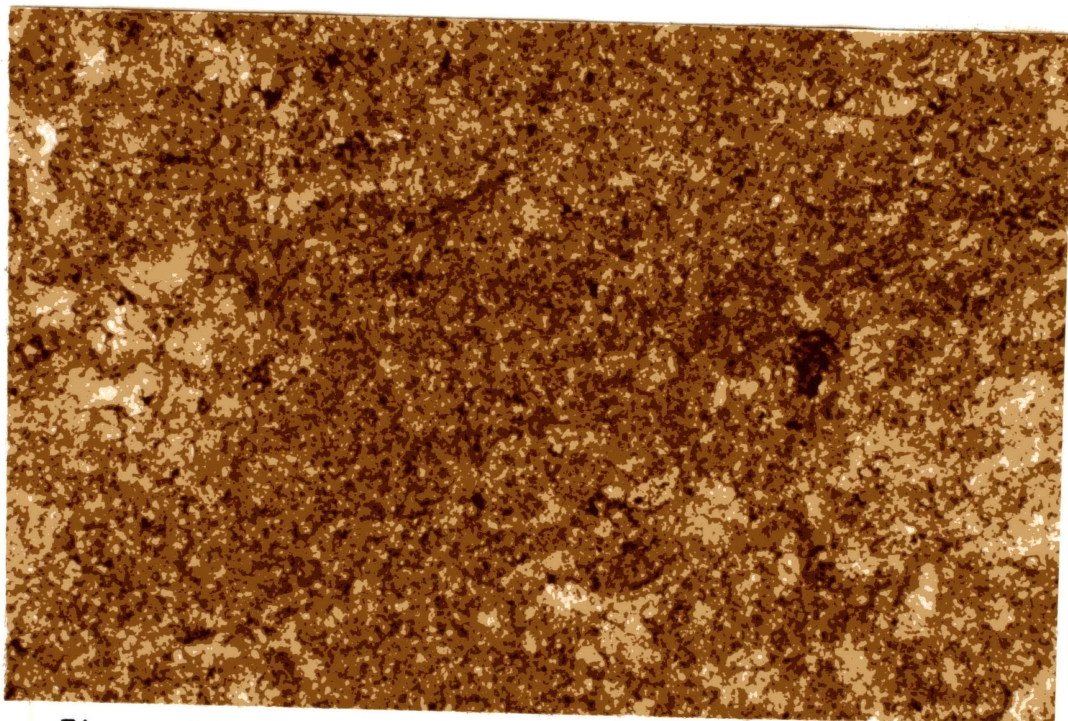


Figure 36. Photomicrograph of Primary Micrite (Gulf Shaddix, 9206, x 100 ppl)

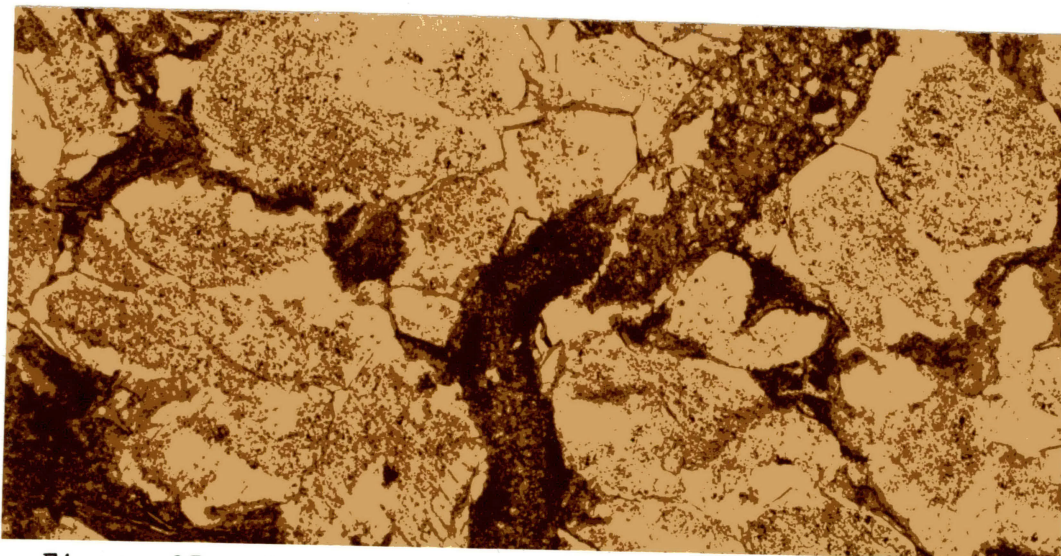


Figure 37. Secondary Micrite in the Intermound Facies, the Micrite is Not Equigranular or Pure Calcite. (Gulf Streeter, 6986, x 40 ppl)

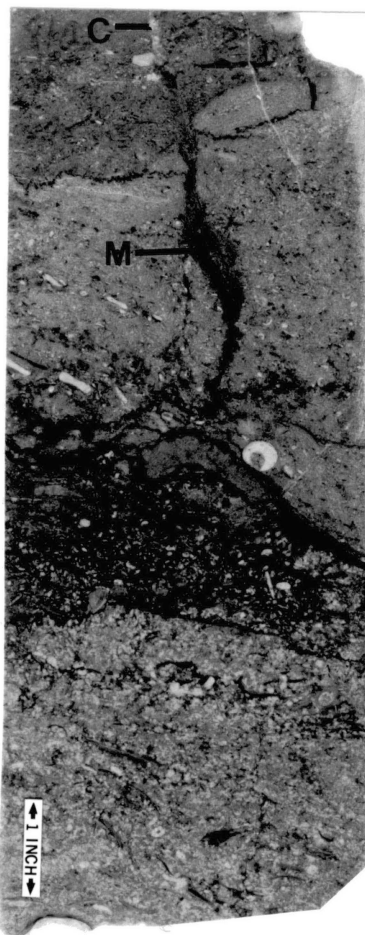


Figure 38. Secondary Micrite (M) Filling a Vug, Note Sparry Calcite (C) Filling the Uppermost Portion of the Core Piece. (Midwest McManus, 8101)

post-Frisco unconformity usually controlled the amount and type of porosity. Two types of porosity exist in the Frisco: fabric and non-fabric selective porosity.

Fabric Selective Porosity Three types of fabric controlled porosity have been observed in the Frisco: interparticle porosity, intraparticle porosity, and enlarged intraparticle porosity. Interparticle and intraparticle porosity are primary; enlarged intraparticle porosity is secondary.

Interparticle porosity is present in the Frisco (Figure 39) but in very small amounts. At the time of deposition a large amount of interparticle porosity was present in the intermound and capping facies, but it was virtually destroyed by overgrowths around crinoid fragments. In the mound facies interparticle porosity is low.

Intraparticle porosity is contained in the zooecia of bryozoans and to a lesser degree the lumen of crinoid ossicles (Figure 40). Widespread intraparticle porosity is unlikely in the intermound and capping facies due to the fragmentation of bryozoans. In the mound facies and near the mound facies fragmentation was less, preserving intraparticle porosity.

Enlargement of the intraparticle pores is the most widespread effective porosity in the Frisco (Figure 41-42). Solutions dissolved zooecia walls creating additional pores and interconnection between pores. Solutions dissolved some

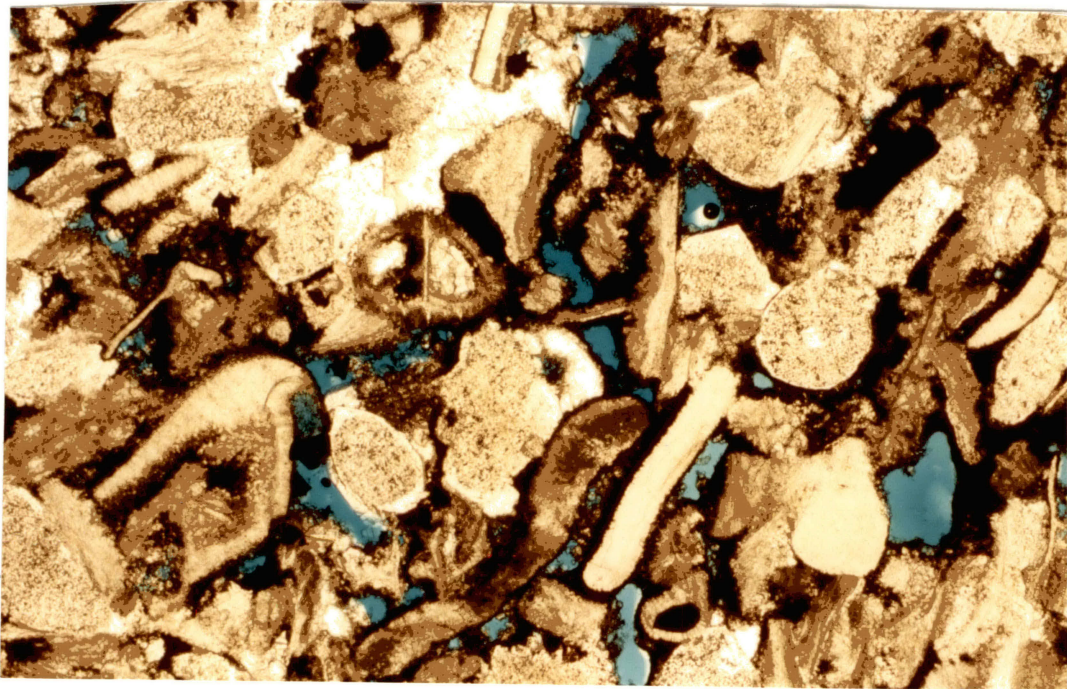


Figure 39. Enlarged Interparticle Porosity in the Intermound Facies. (Gulf Streeter, 7028, x 40 ppl)

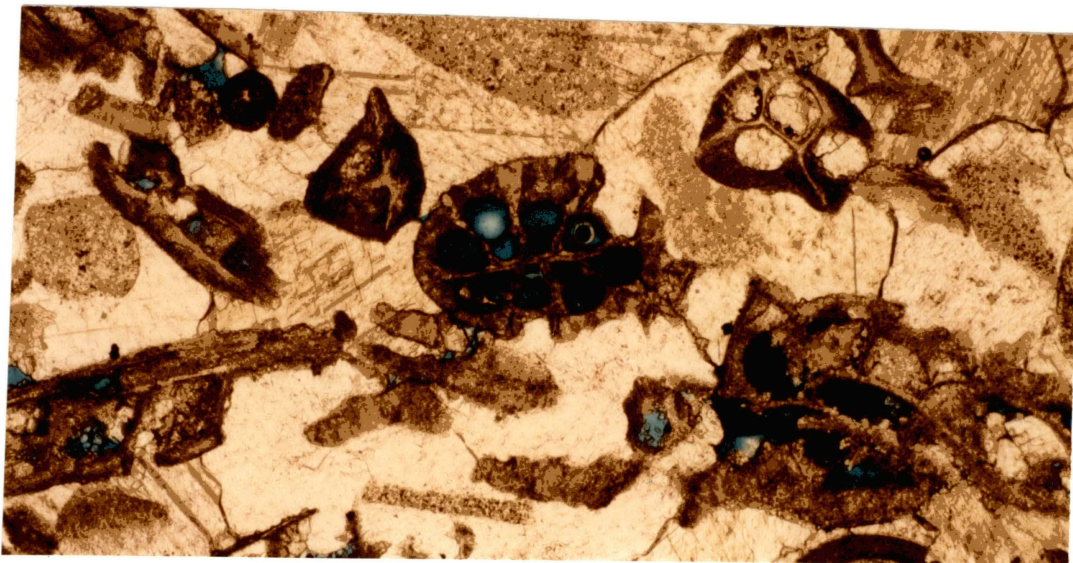


Figure 40. Intraparticle Porosity Preserved in the Zooecia of Bryozoans. (Gulf Streeter, 7036, x 40 ppl)

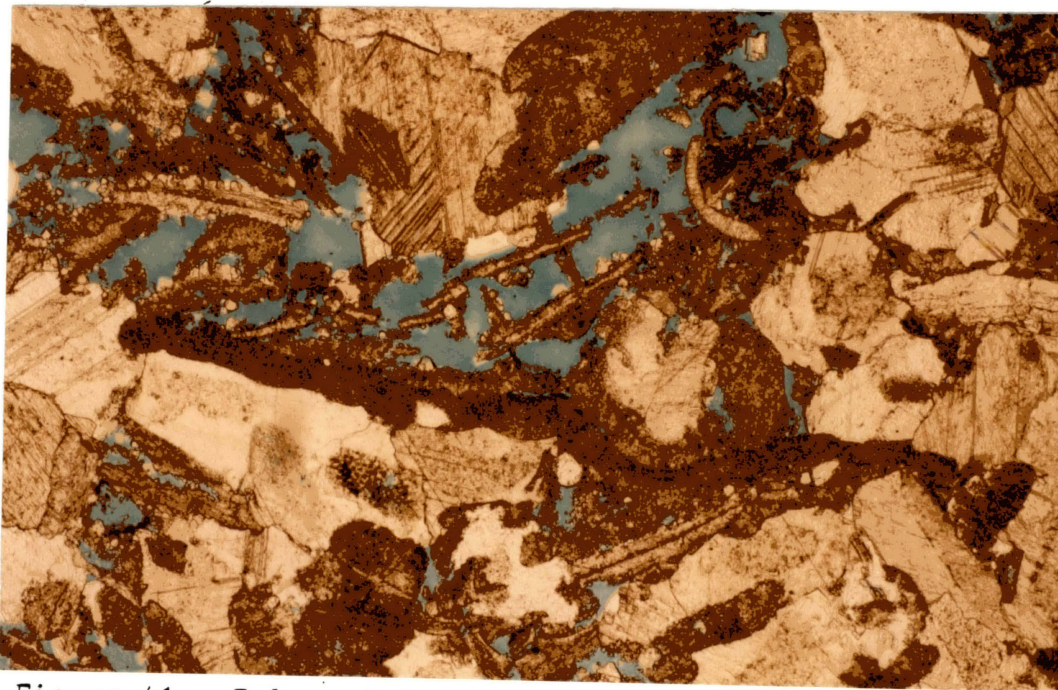
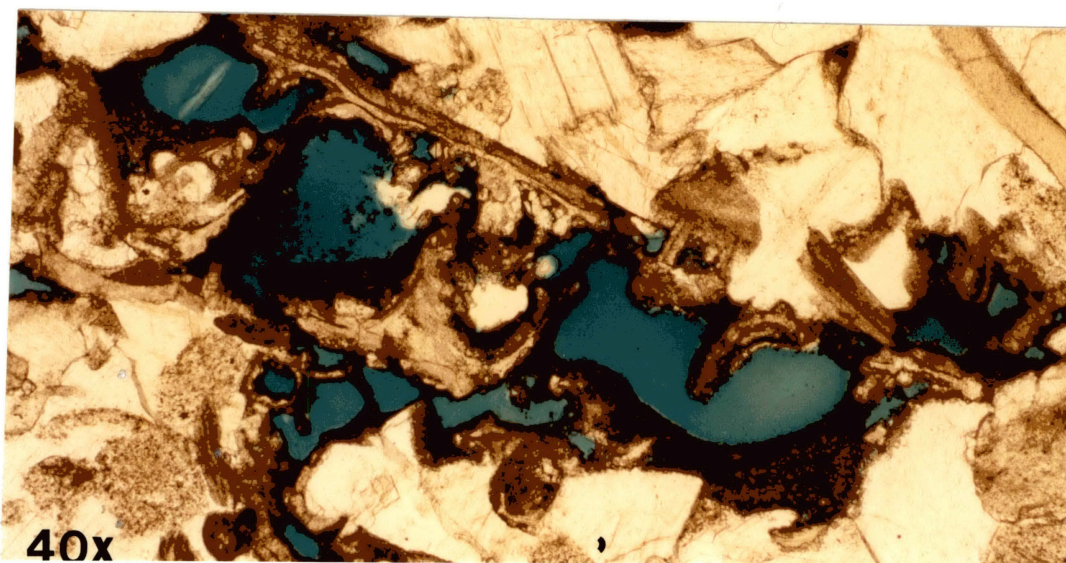


Figure 41. Enlarged Intraparticle Porosity, The Zooecia Walls Have Been Dissolved. (Gulf Streeter, 7018, x 40 ppl)



40x
Figure 42. Enlarged Intraparticle Porosity (Gulf Streeter, 7032, x 40 ppl)

fragments completely, creating vuggy porosity. It is probable that the solutions were related to the unconformity.

Non-Fabric Selective Porosity Vuggy porosity is the most effective porosity in the Frisco (Figure 43-44). Vertical to subvertical oriented vugs can be common. Vugs are observed in all facies. Overlying material or sparry calcite partially or totally filled some vugs (Figure 45-46).

Many fractures are present in the Frisco, but the majority of them are cemented with calcite (Figure 47).

Porosity Controls Some porosity was developed in every facies, but the amount and the type of porosity was largely determined by the facies. Some porosity was enhanced during the post-Frisco unconformity.

Initial porosities in the intermound and capping facies may have been as high as 40%. Preservation of this porosity is rare because of rapid cementation. In the intermound and capping facies intraparticle porosity was low due to the fragmentation of grains; enlargement of the intraparticle porosity generally was insignificant. When lime mud is present in the intermound facies cementation by sparry calcite was not as rapid or complete. Fluids were then permitted to percolate through possibly yielding vuggy porosity. The large amounts of lime mud in the mound facies created little interparticle porosity. Intra-

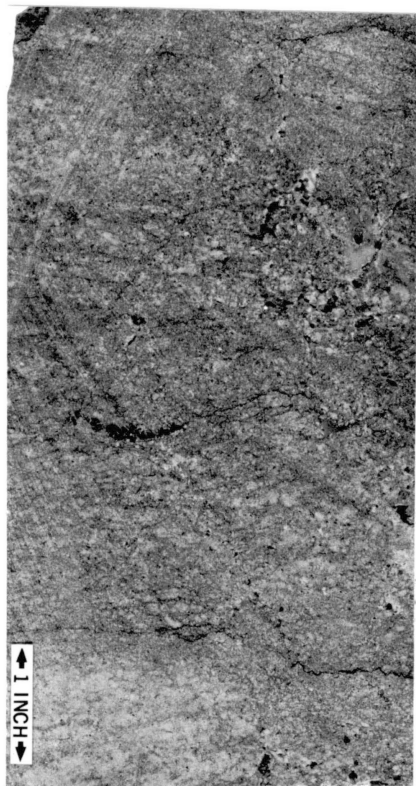


Figure 43. Vuggy Porosity (V) (Apexco Curtis 2, .8555)

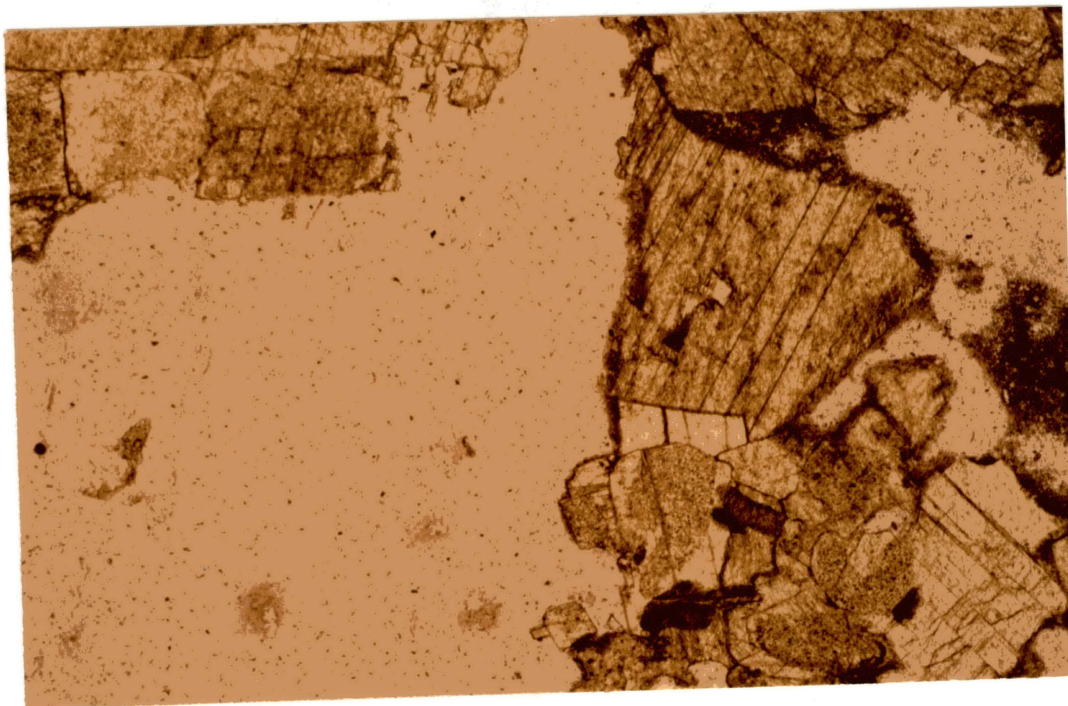


Figure 44. Vuggy Porosity (V) (Apexco Curtis 2, 8575,
x 40 ppl)

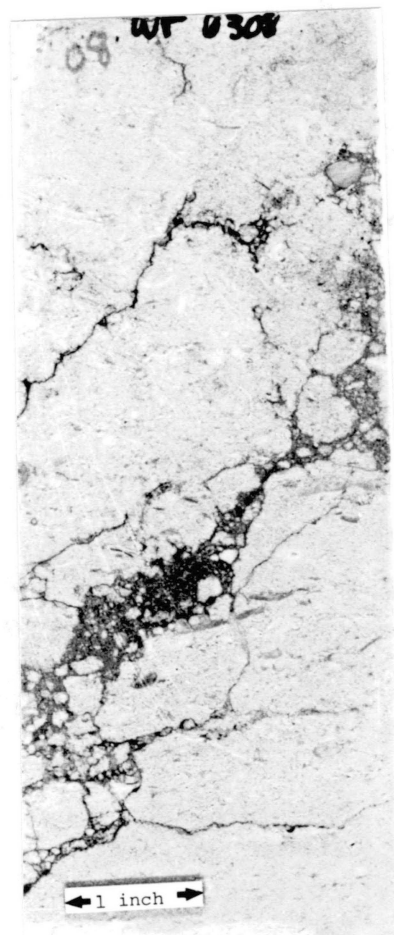


Figure 45. Overlying Material Which Has Percolated Down During the Post-Hunton Unconformity. (Gulf Wright Heirs, 6308)

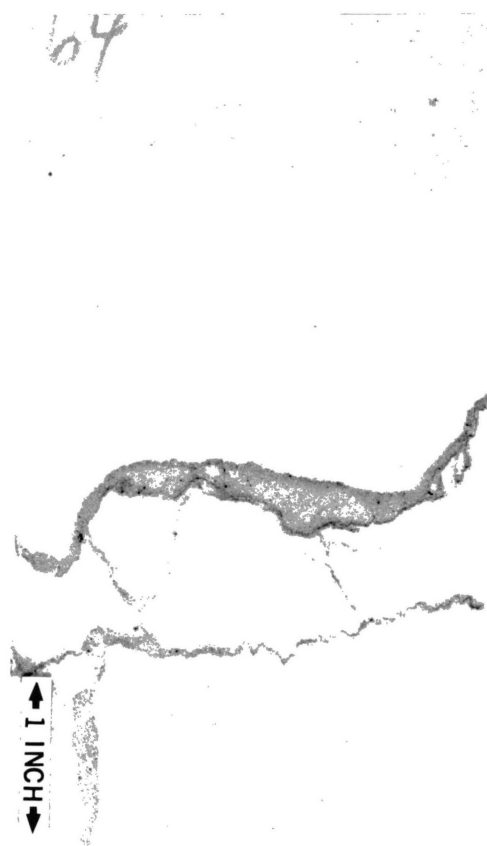


Figure 46. Sand Filling A Vug; Misener Fm. (Sandstone)
Overlies the Frisco in this Core. (Gulf
Wright Heirs, 6308)

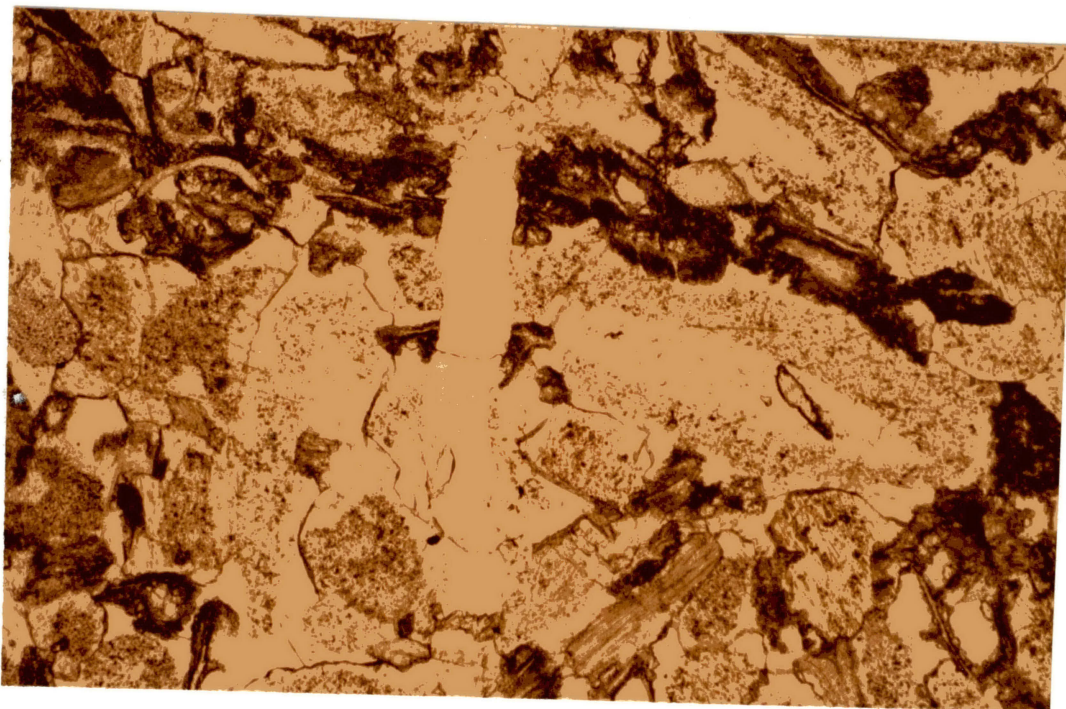


Figure 47. Fracture Filled with Sparry Calcite. (Gulf Streeter, 6986, x 40 ppl)

particle porosity is prevalent, but the interconnection of pore spaces generally are insignificant. Movement of fluids through the mound facies does not appear to be extensive; as a result, porosity was not greatly enhanced. Though, vuggy and enlarged intraparticle porosity occasionally are present.

The unconformity may or may not have enhanced porosity. During the unconformity some porosity was destroyed as downward percolation of overlying material is common in areas affected by the unconformity (Figure 45-46). Although, it is probable that the majority of vugs and the enlarged intraparticle pores were produced during the post-Frisco unconformity.

Porosity in the Frisco varies greatly. The best porosity (primary and secondary) was observed in poorly winnowed intermound rocks that were deposited in close proximity to a mound. The lime mud reduced the amount and rapidity of sparry calcite cementation. Fragmentation of bryozoans would have been less in short distances from the mound. The chance for enhancement of porosity greatly increased with larger amounts of primary porosity.

Paragenetic Sequence

A generalized paragenetic sequence was constructed by using petrographic techniques facilitated with cathodoluminescence (Figure 48). Variations in the sequence occur, but they were not widespread. Partial cementation appears to have occurred before any other diagenetic

Generalized Paragenesis in the Frisco

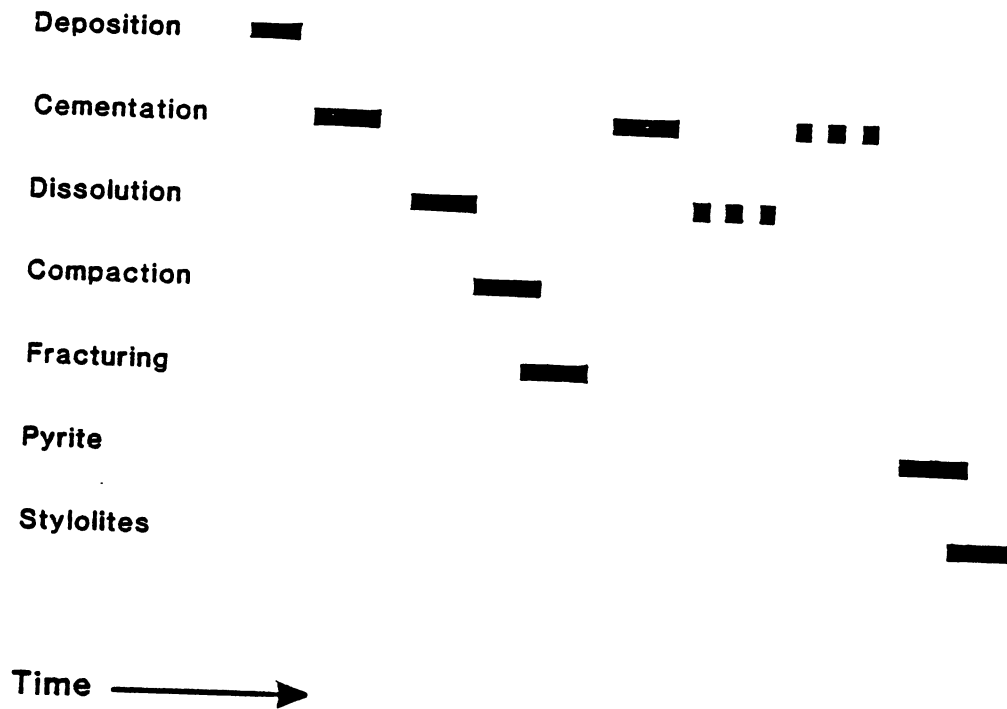


Figure 48. Paragenesis of the Frisco

event. After initial cementation, a dissolution stage was dominant in the Frisco (Figure 49-50). Compactional occurred after a second generation of cementation (Figure 51-52). The timing of fractures is difficult to determine; clear cross-cutting relationships are rare, but most fractures appeared to have formed after compaction (Figure 53-54). Continued cementation is seen as bright and dull luminescent cements filling fractures and truncating across compacted grains (Figure 53-54). Late dissolution was indicated in several thin sections as corrosion of bright and dull cements (Figure 55). Pyrite appears late and usually is seen in association with stylolites or as a replacement and displacement of grains (Figure 56-57). Stylolitization was a late compaction event. Stylolites were observed to cut across all fabrics of the rock suggesting late formation (Figure 58). The timing of neomorphism is difficult to establish; it may have been a continuing event in the Frisco.

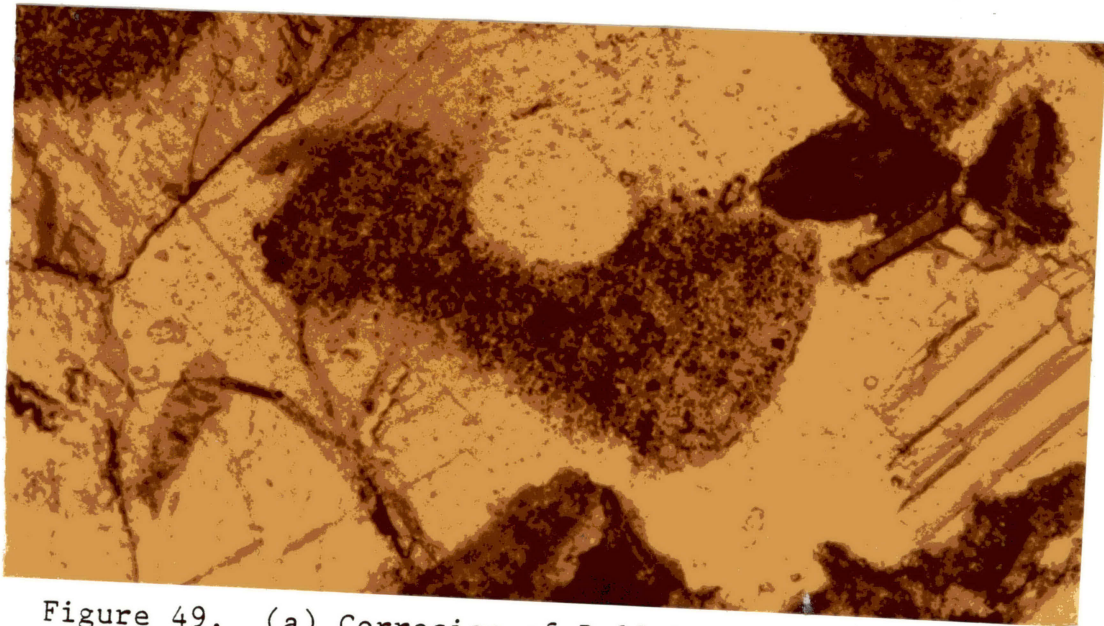
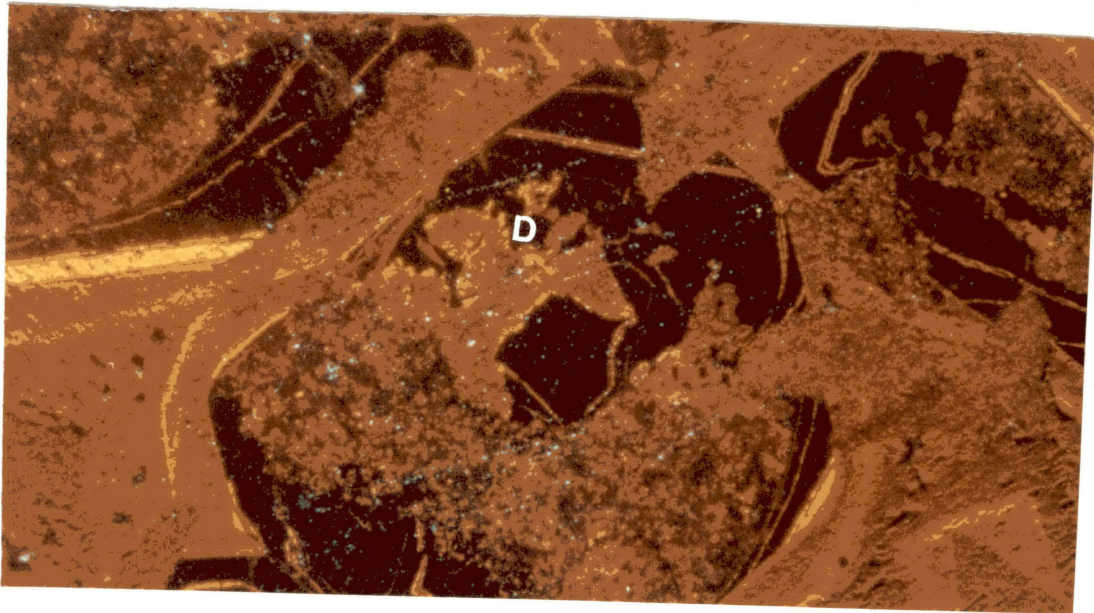


Figure 49. (a) Corrosion of Dull Luminescing Cement (D) Indicating Dissolution. (Gulf Streeter, 7032, 40 x Cathodoluminescence)
(b) Plane Polarized Photomicrograph of (a).

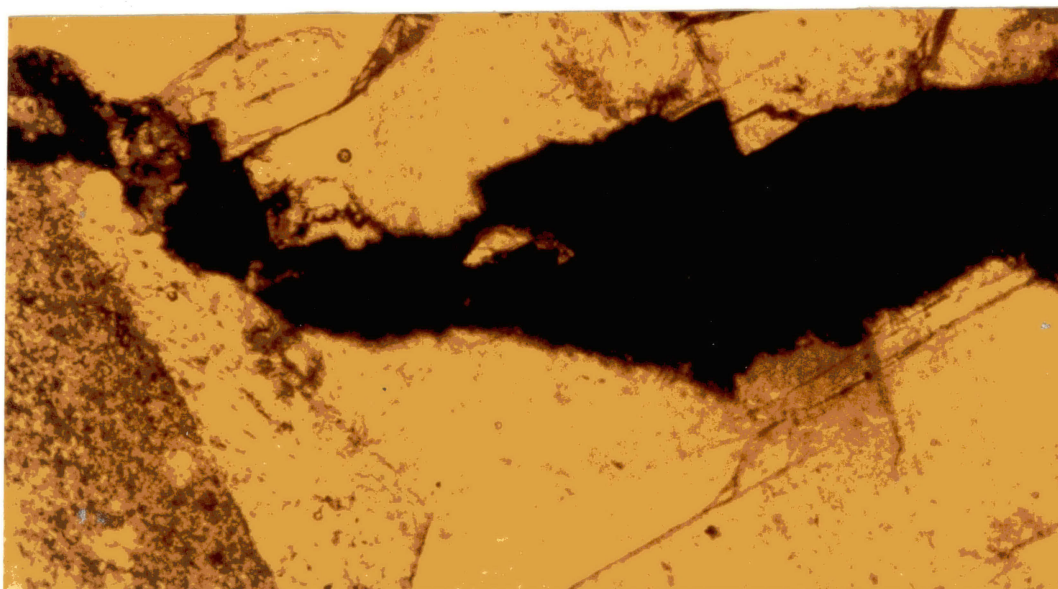
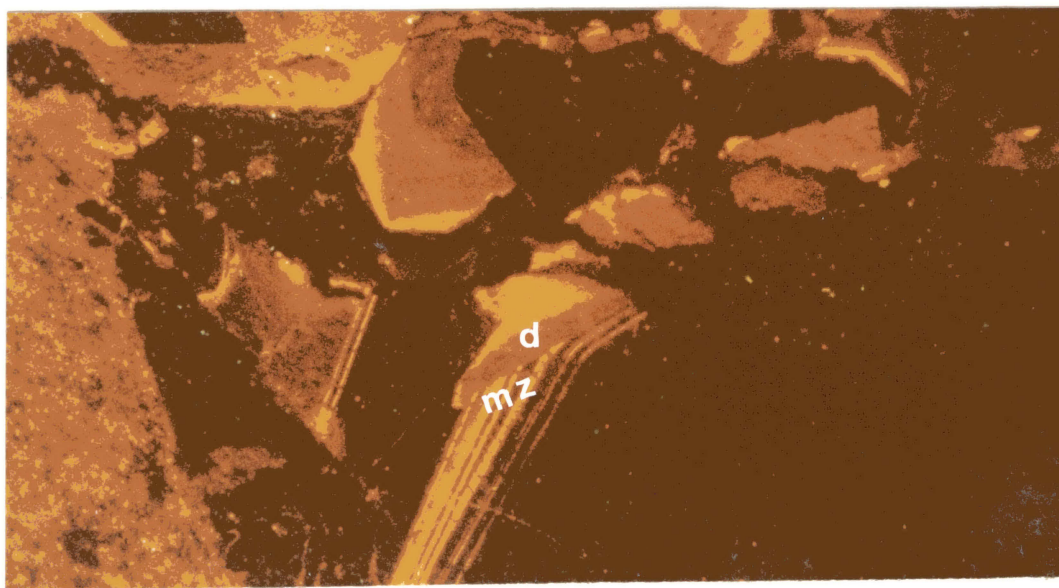


Figure 50. (a) Dissolution Followed by Re-Cementation, Multiple Zoned Cements (mz) Truncated on Dull Luminescent Cement (d). (Jones and Pellow Boyd, 6509, x 40)
(b) Plane Polarized Photomicrograph of (a), Black Material is Hydrocarbons.

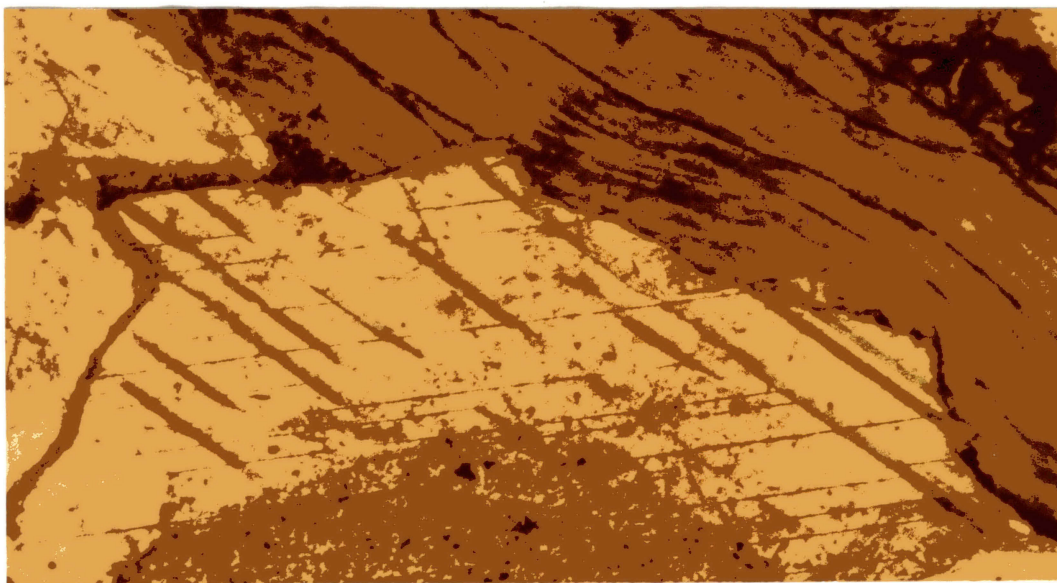
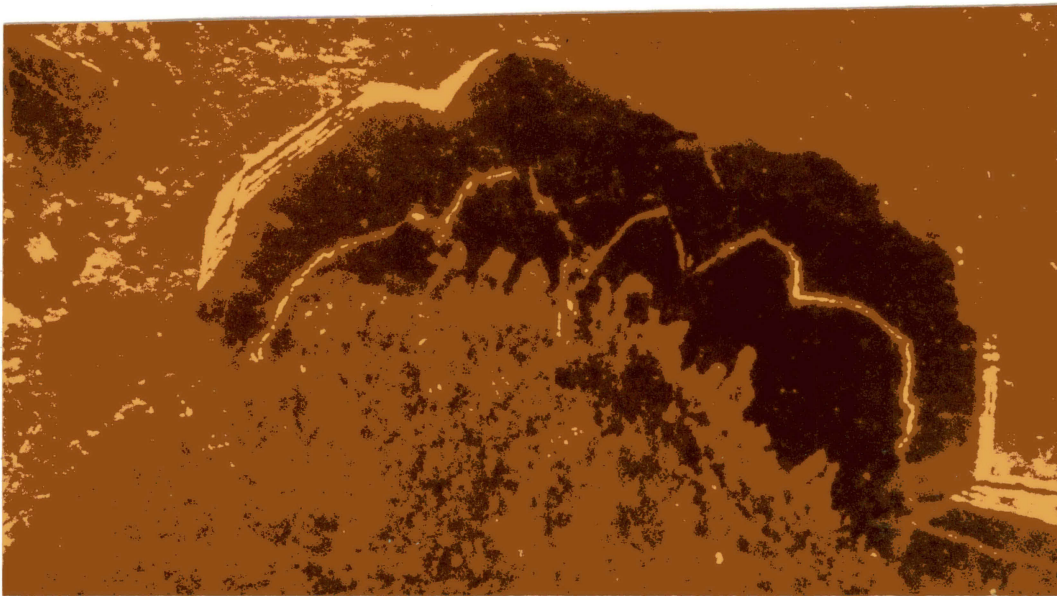


Figure 51. (a) Cathodoluminescent Photomicrograph of Cementation Occuring Before Compaction, Note Decrease in Terminations Away From Crinoid Fragment. (Gulf Holtzschue, 6359, x 40)
(b) Plane Polarized Photomicrograph of (a).

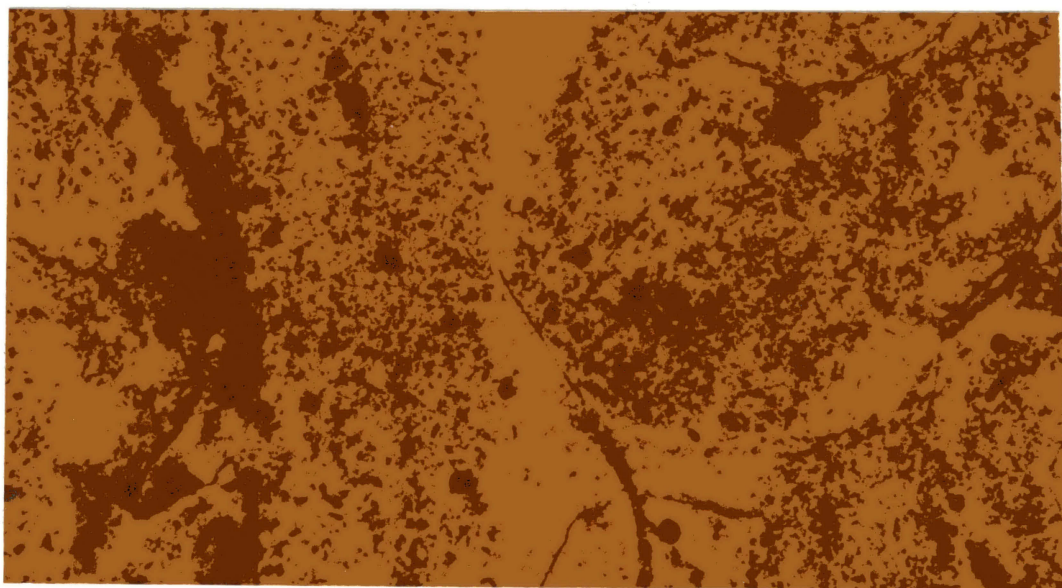
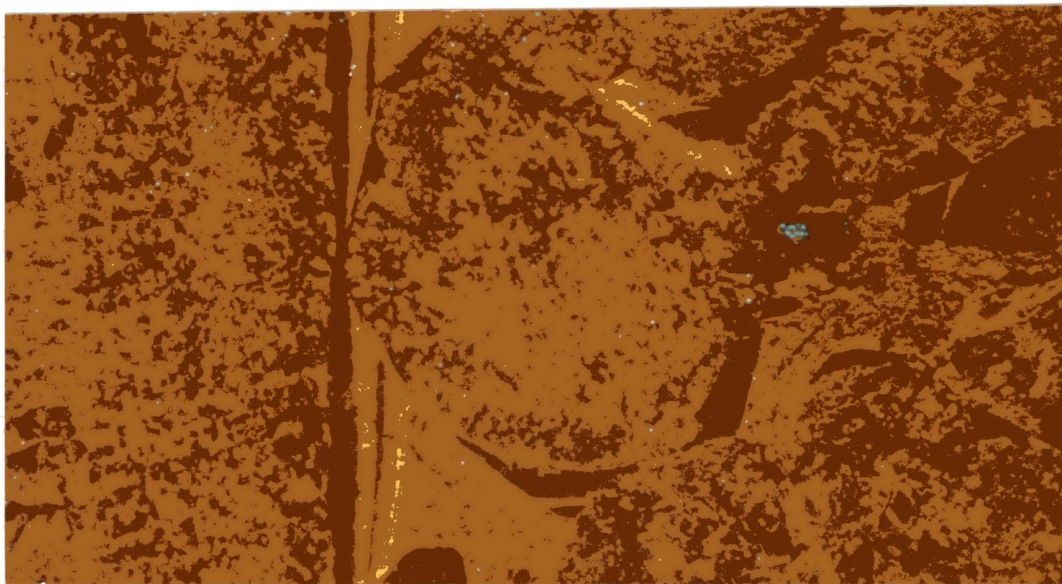


Figure 52. (a) Cathodoluminescent Photomicrograph Showing
Compaction Occurring After Some Cementation.
(Shaddix, 9223, x 40)
(b) Plane Polarized Photomicrograph of (a).

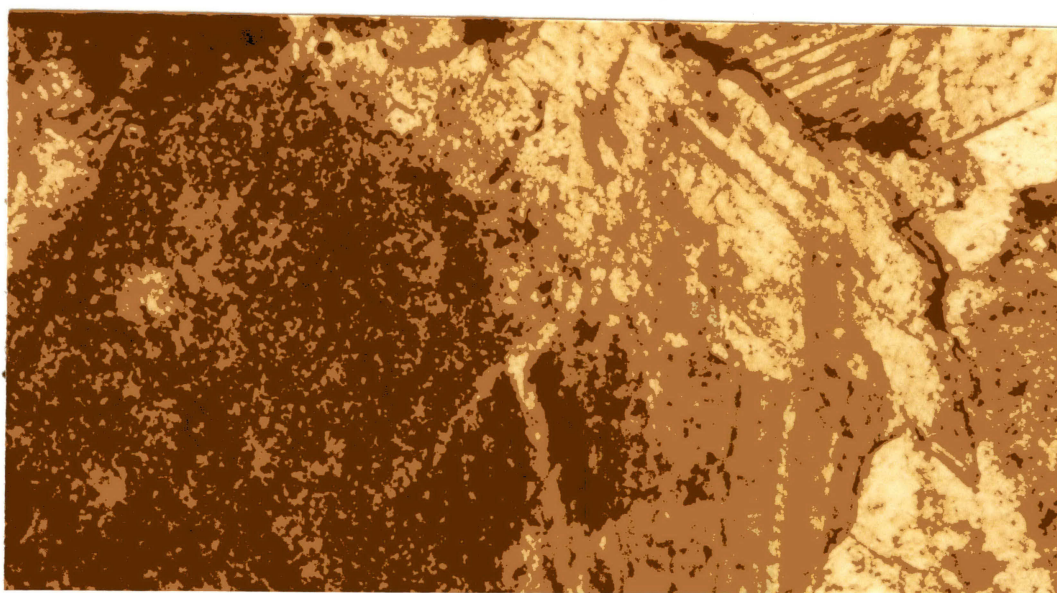
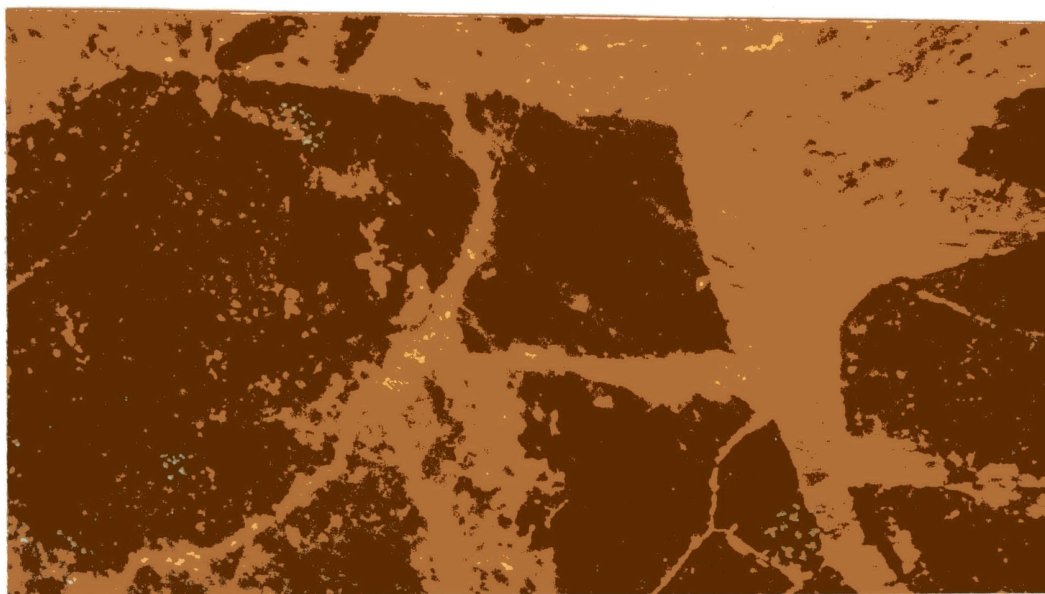


Figure 53. (a) Fractures Occurring After Non-Luminescent Cement. (Phillips Brooks B, 8727, x 40 Cathodoluminescence)
(b) Plane Polarized Photomicrograph of (a).

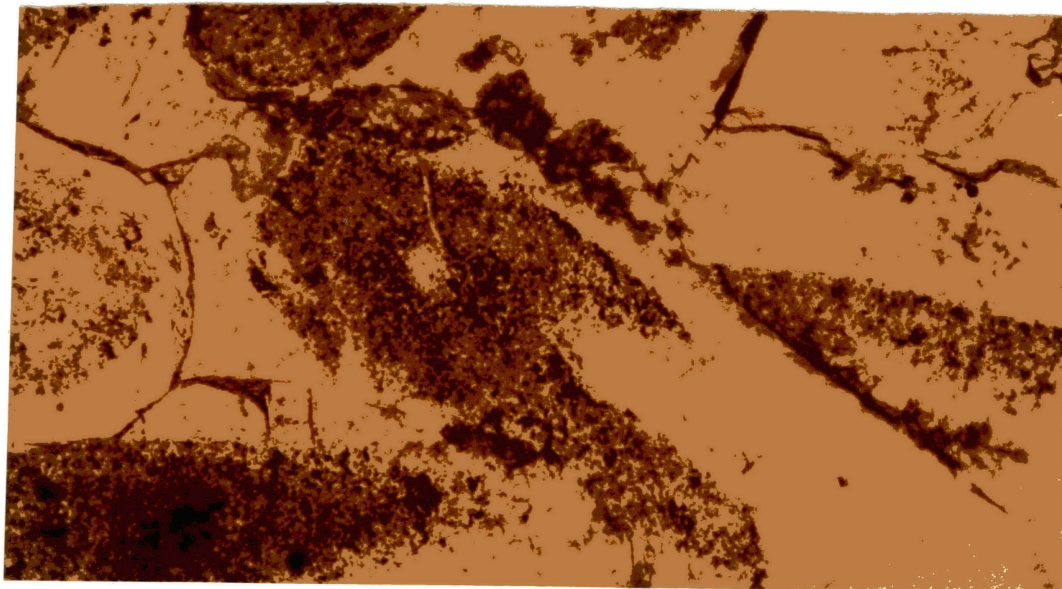
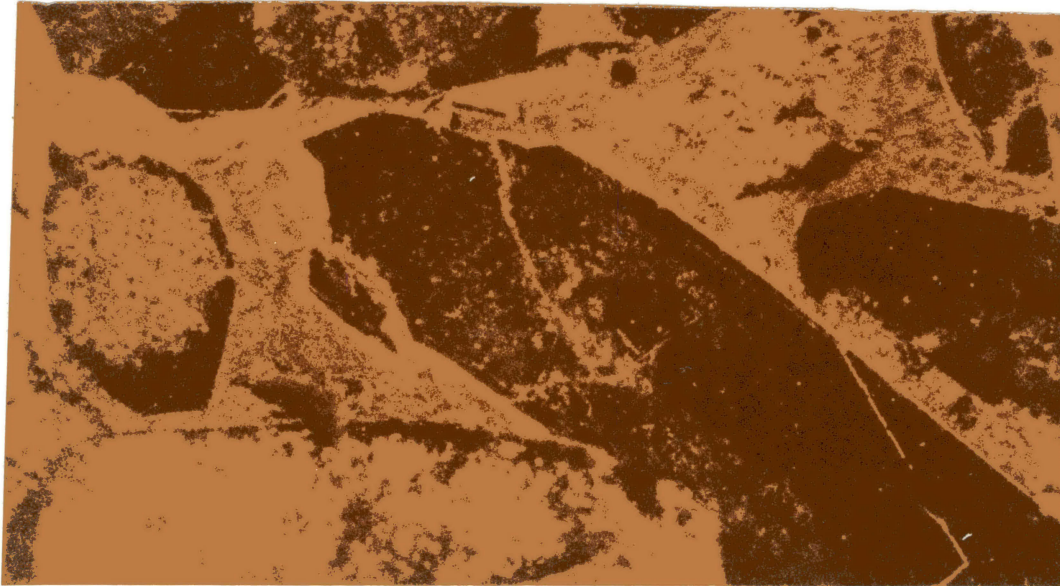


Figure 54. (a) Cathodoluminescent Photomicrograph Showing Fractures Occurring After Two Zones of Cement. (Jones and Pellow Boyd, 6509, x 40)
(b) Plane Polarized Photomicrograph of (a).

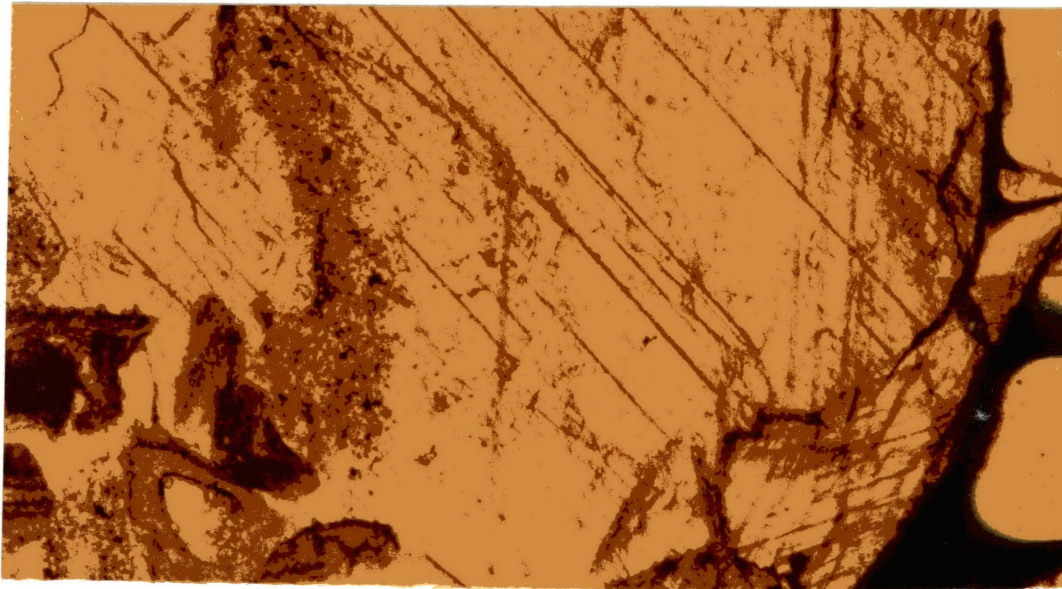
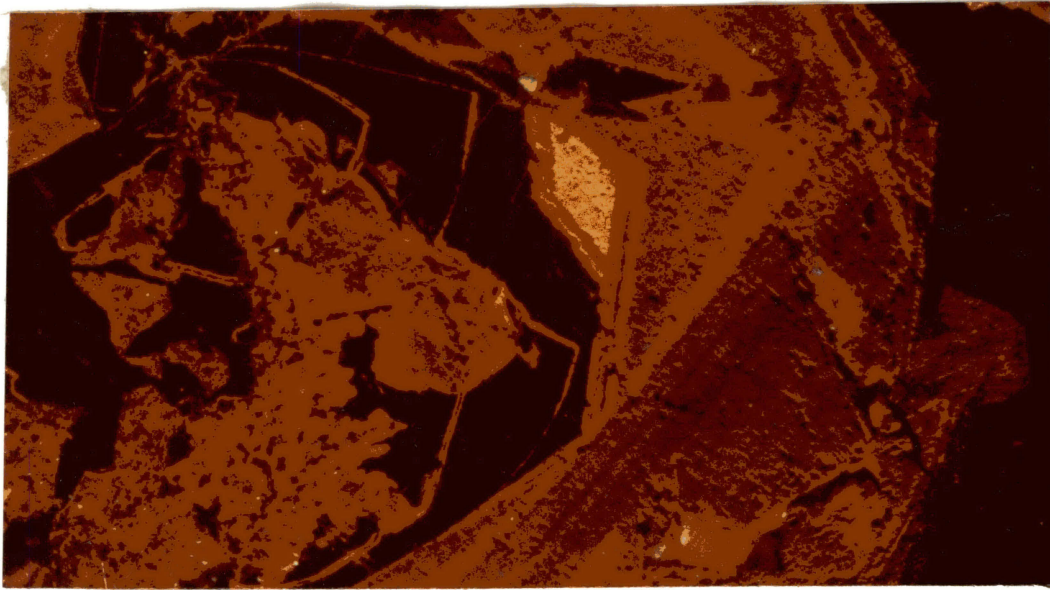


Figure 55. (a) Cathodoluminescent Photomicrograph Showing Two Stages of Dissolution. (Gulf Streeter, 7032, x 40)
(b) Plane Polarized Photomicrograph of (a).

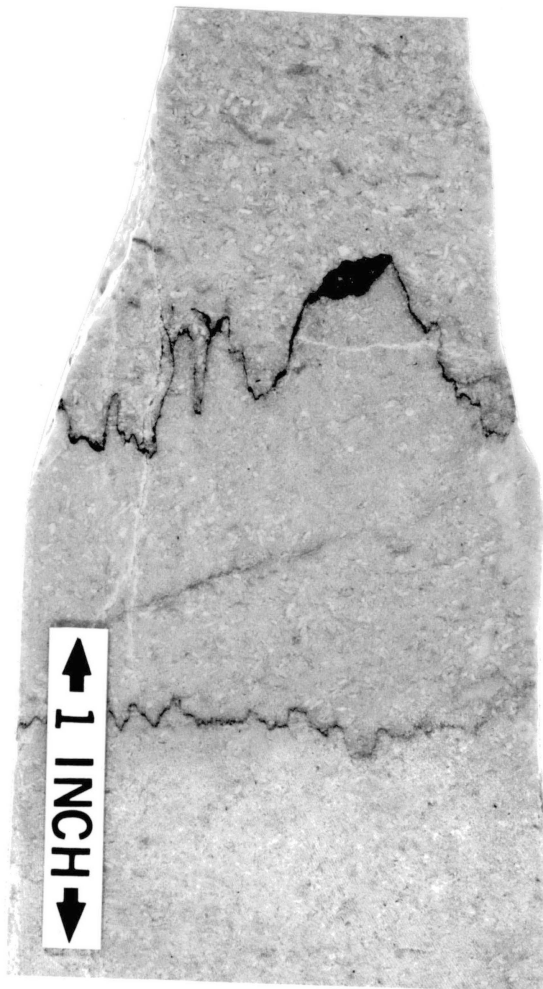


Figure 56. Pyrite in Stylolite
(Phillips Brooks B,
8751)

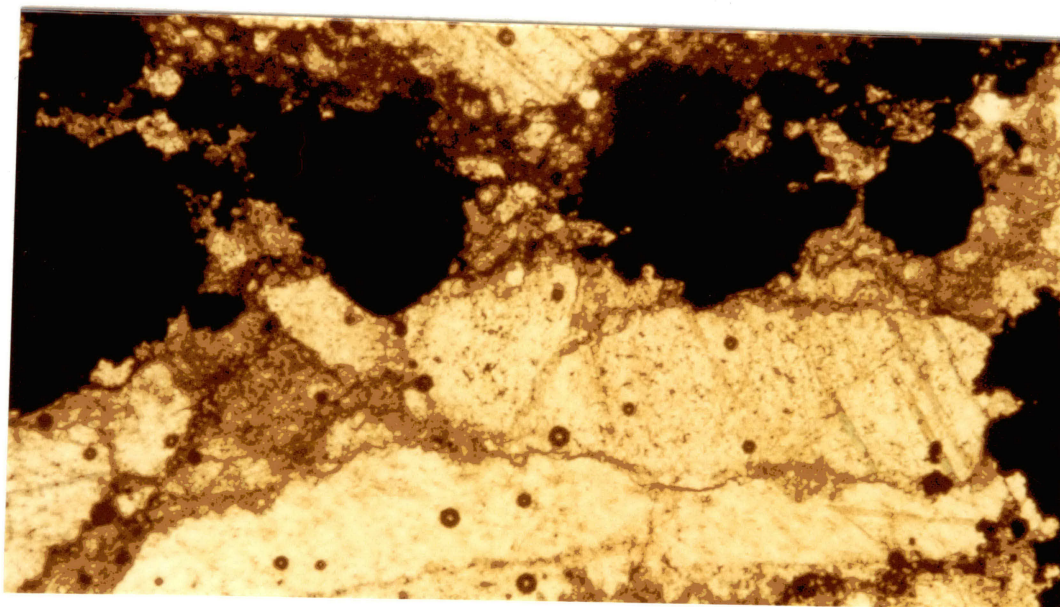
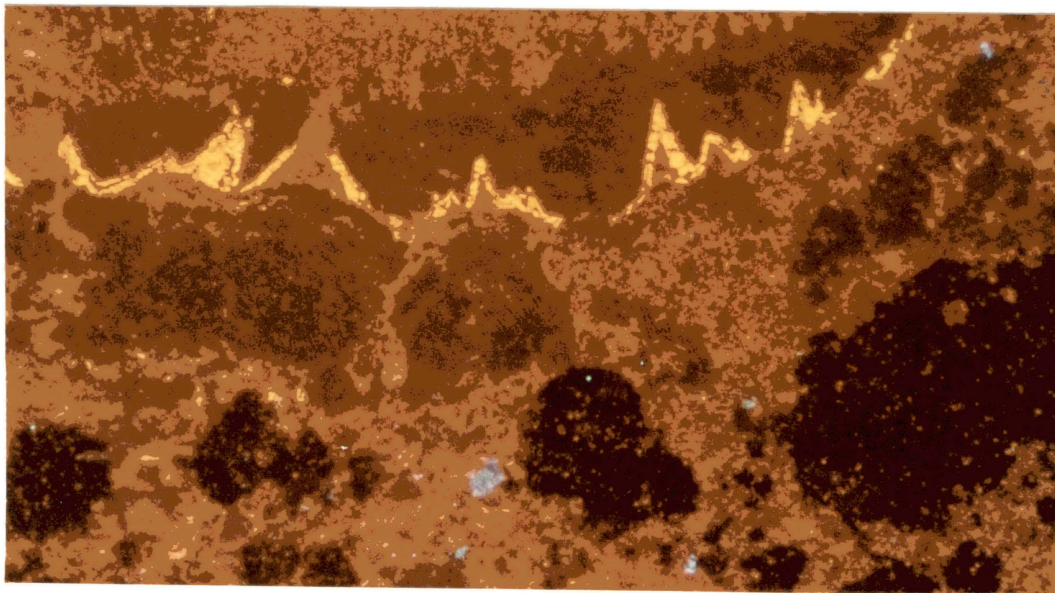


Figure 57. (a) Pyrite Replacing Calcite (Midwest McManus, 8074, 40 x Cathodoluminescence)
(b) Plane Polarized Photomicrograph of (a).

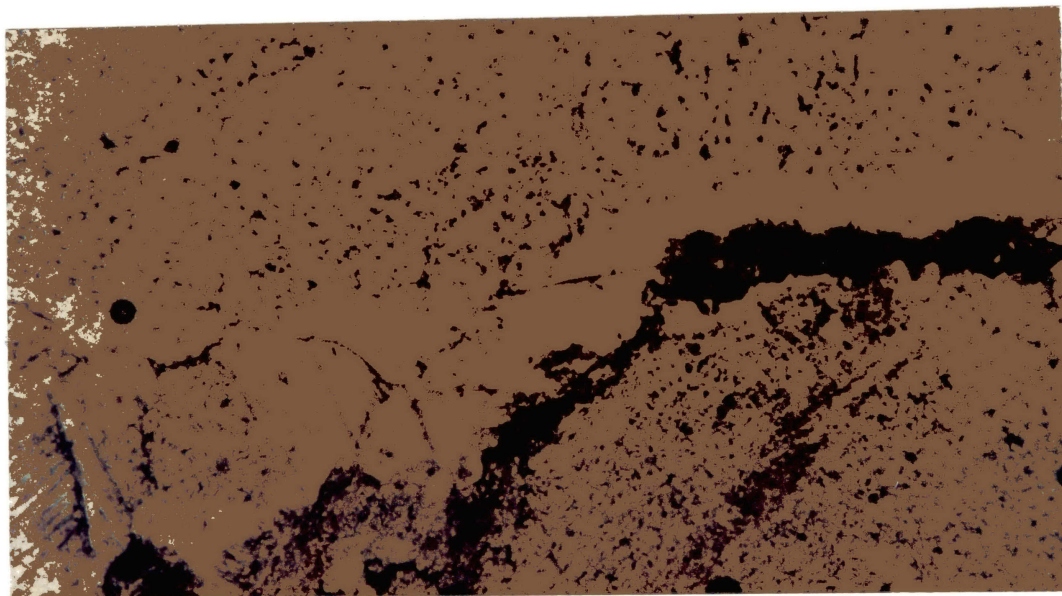
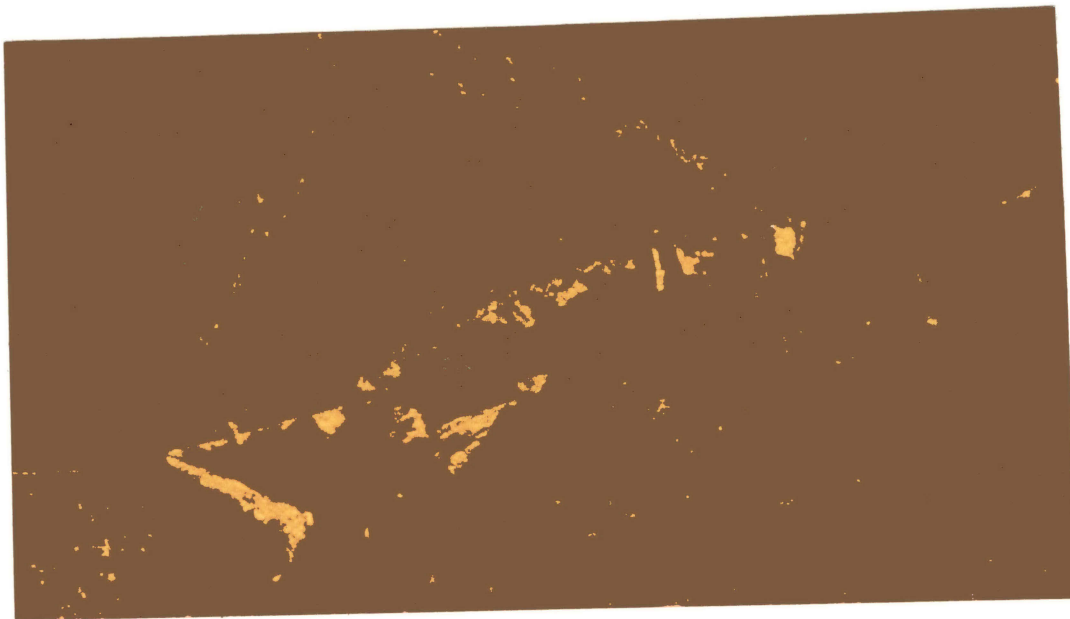


Figure 58. (a) Stylolite Cross-Cutting Fractures and Cement. (Apexco Curtis 2, 8525, 40 x Cathodoluminescence)
(b) Plane Polarized Photomicrograph of (a).

CHAPTER FIVE

HENRYHOUSE FORMATION

Introduction

An oolitic facies is an important and unique feature of the Henryhouse Formation in Central Oklahoma. Oil and gas are produced from the oolite; the name, Sooner Trend, has been used to consolidate the numerous field names in the area. The oolitic facies is unique in that it has limited regional extent, dual mineralogy, and a complicated diagenetic imprint. The oolite appears in a sand belt trending T13N-R4W to T19N-R10W, that parallels the axis of the Anadarko Basin (Figure 59). An oolitic facies has not been reported in any other region of the Henryhouse.

The mineralogic composition of the oolite is dolomite in the northwest and calcite in the southeast. No oolites were found with a mixture of dolomite and calcite. The mineralogy of the oolitic facies and associated facies was affected by diagenetic processes.

The oolitic zones are not continuous. Morgan (1983) mapped the extent of the calcitic oolite facies; it thins and disappears in the northwest direction (Figure 60). The pinchout may be due to a tidal channel (Morgan, 1983). Other explanations are post-Henryhouse erosion or the

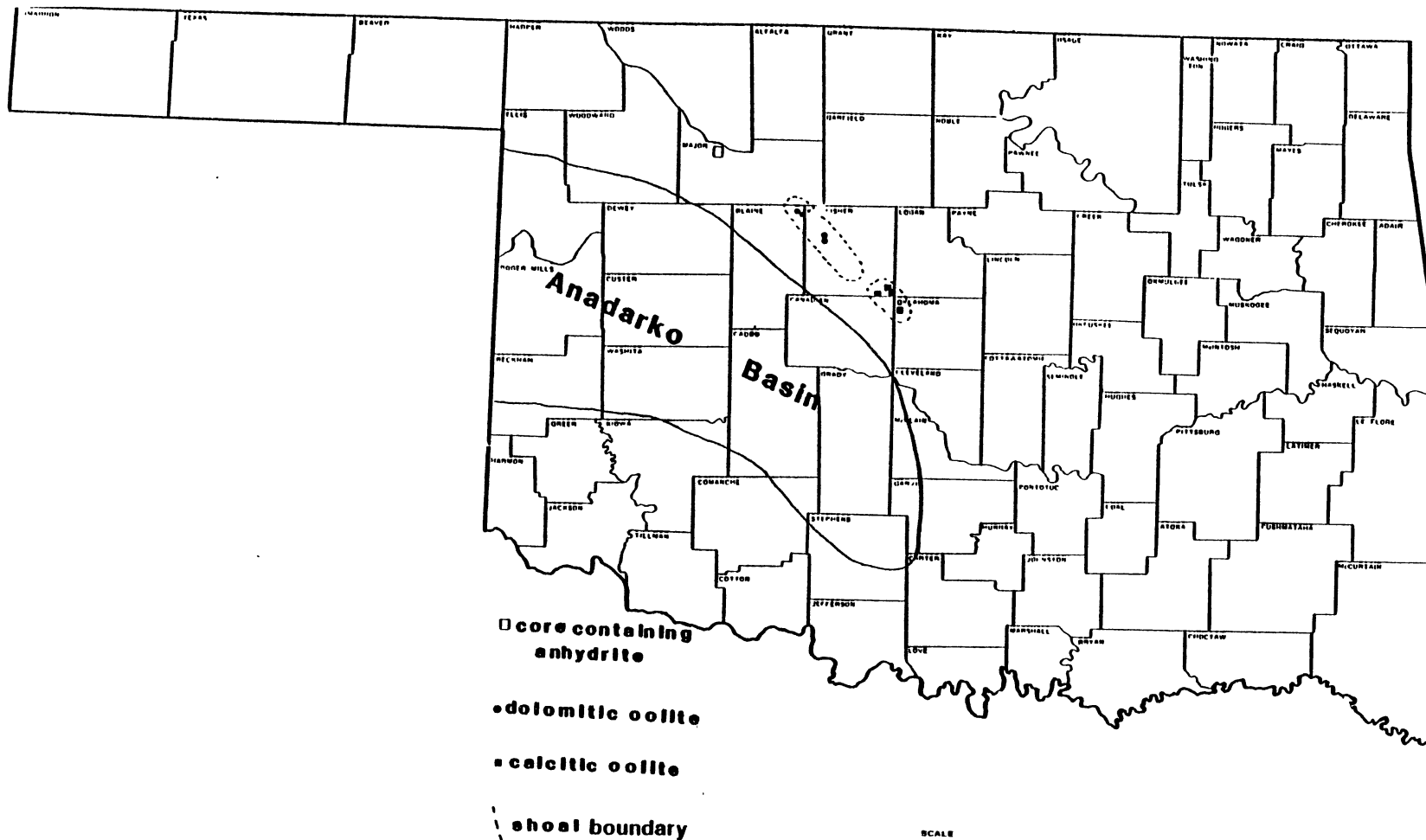
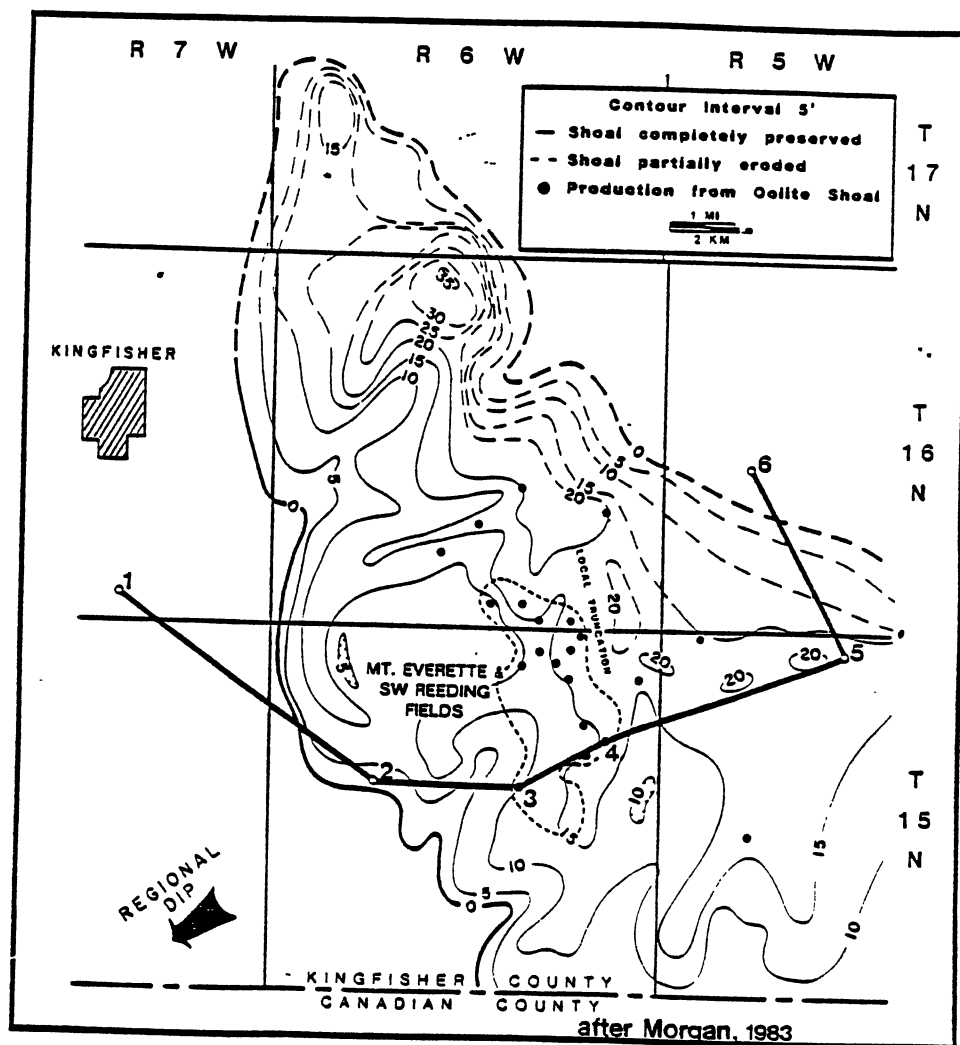


Figure 59. Oolitic Facies in the Henryhouse Which is Parallel to the Axis of the Anadarko Basin, Core Containing Anhydrite on Strike Line of Oolitic Facies.



facies were not syndepositional.

Depositional Model

Studies of recent oolites indicate that they form in agitated water (Leeder, 1982; Flugel, 1982; Bathurst, 1975). A slope break is necessary to concentrate currents that agitate the oolites (Ball, 1967). A regional slope break in the paleoslope probably is the explanation for the limited extent of the oolitic facies in the Henryhouse Formation. Depositional model of the Henryhouse in western Oklahoma suggests that the Henryhouse was deposited as a broad shallow ramp without a significant slope break (Beardall, 1983).

Several progradational sequences have been reported in the Henryhouse Formation (Beardall, 1983; Morgan, 1983). The oolitic facies is located near the top of one progradational sequence. Below the oolite is a subtidal facies and above the oolite is a lagoonal facies (Figure 61). These facies were deposited as a broad carbonate ramp (Figure 62).

Lagoonal Facies

The lagoonal facies may have been deposited in restricted conditions. Fossils are rare, but burrowing is present. The rock is a massive peloidal dolo-mudstone (Figure 63-65). In the northwest and the southeast, the texture of the lagoonal was severely altered by dolomitiza-

Vertical Sequence of the Henryhouse

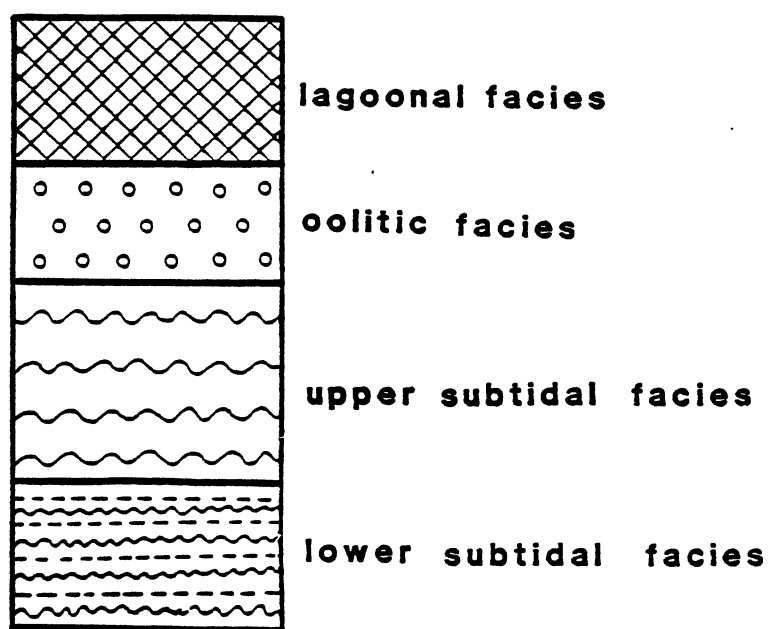


Figure 61. Typical Vertical Sequence of the Henryhouse Where Oolites are Present.

Depositional Model of the Henryhouse

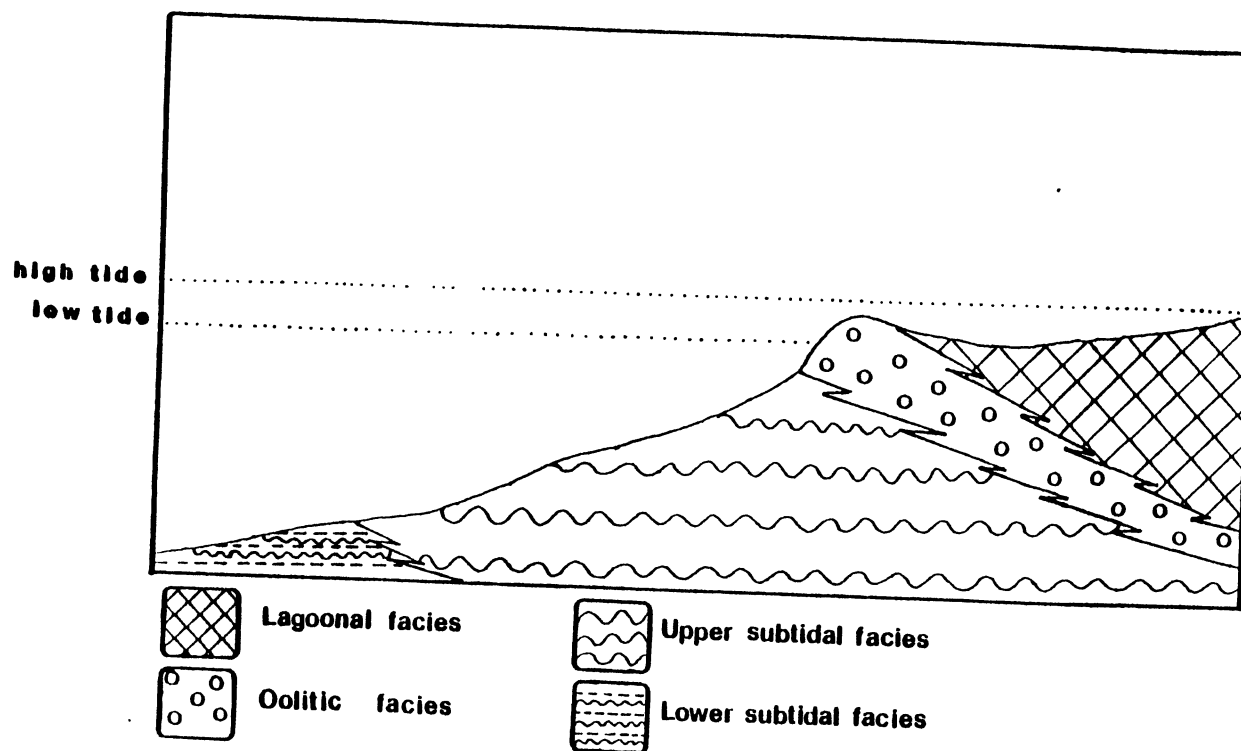


Figure 62. Depositional Model of the Henryhouse, Vertical Scale Greatly Exaggerated, Actual Slope Less Than 1° .

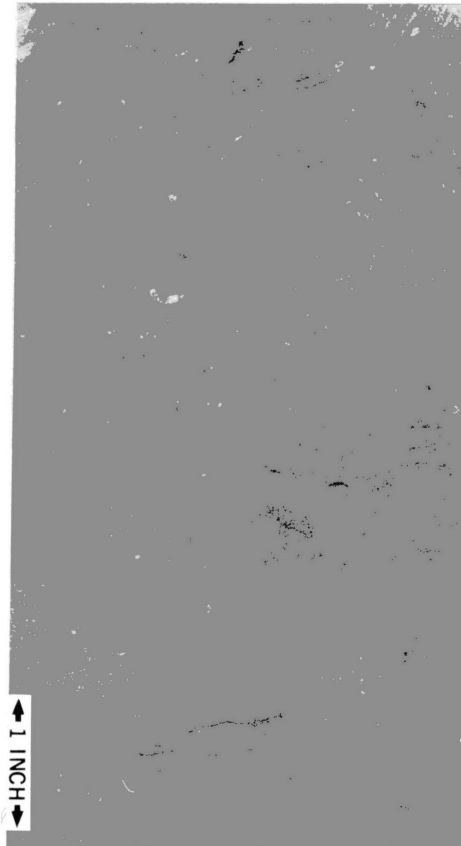


Figure 63. Lagoonal Facies, Mudstone with Bioturbation and Scattering of Fossil Fragments. (Eason Van Curen, 7140)

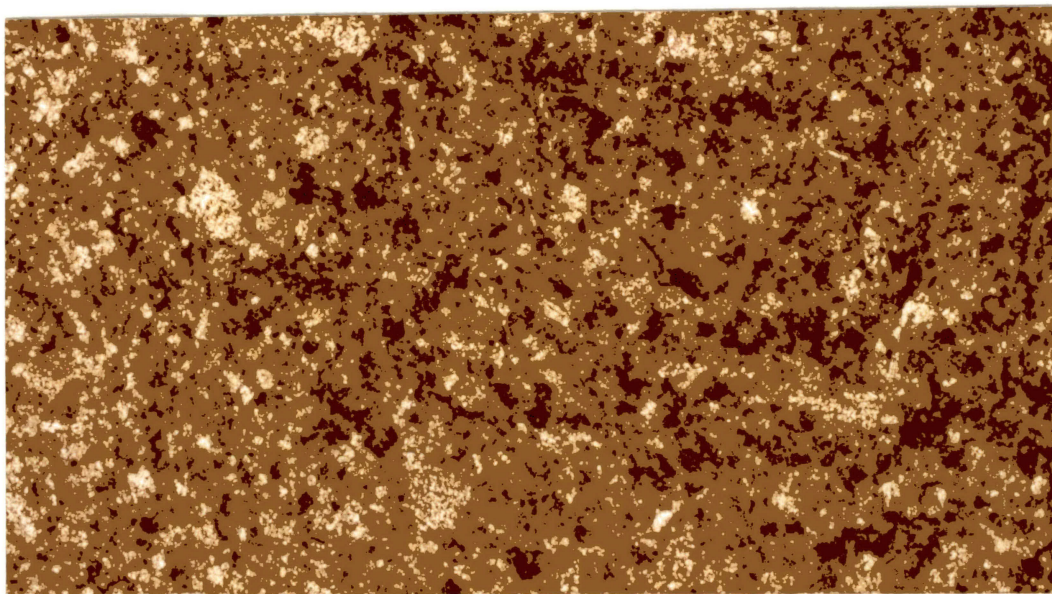


Figure 64. Photomicrograph of Lagoonal Facies, Abundant Peloids Are Characteristic of This Facies. (Eason Van Curen, 7140, 40 x ppl)

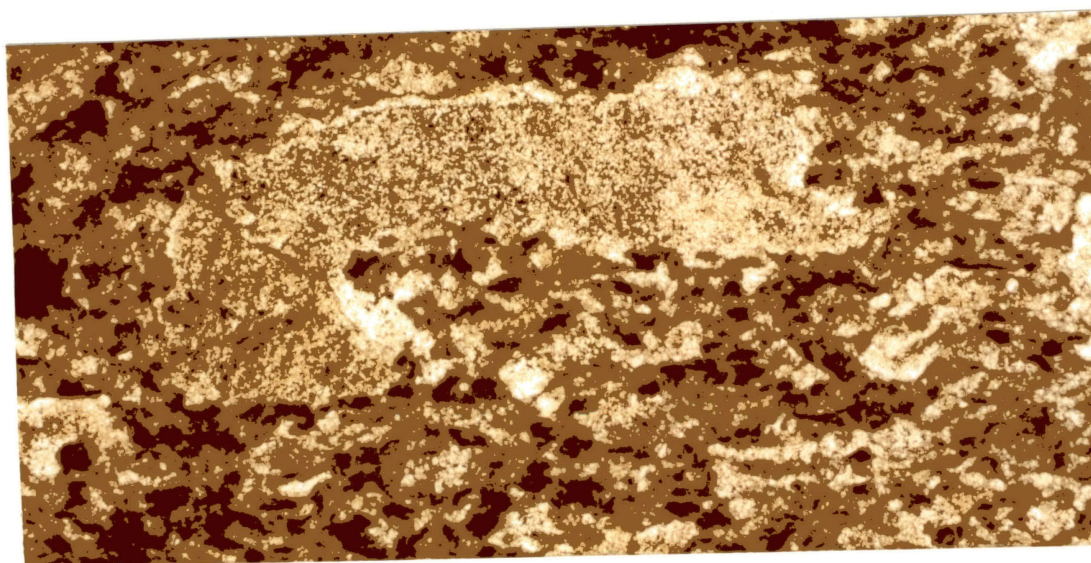


Figure 65. Photomicrograph of Lagoonal Facies, Echinoid Fragments Are Present. (Eason Van Curen, 7143, 40 x ppl)

tion. The lagoonal facies formed in quiet water, landward of the oolitic buildup.

Oolitic Facies

The oolitic facies contains abundant ooliths; occasionally, fossil fragments and peloids were observed. Crossbedding and horizontal laminations are common in the calcitic oolites (Figure 66-67). Dolomitization obliterates the textures in the dolomitic oolites (Figure 68-69). The rock is a grainstone. The shoal probably was deposited in the lower intertidal-upper subtidal environment.

Subtidal Facies

The subtidal facies occurs below and was deposited seaward of the oolitic facies. It can be divided into upper and lower units. The subtidal facies is dolomitic near the contact with the oolitic facies in both the northwest and southeast. Down section the dolomite percentage decreases until the rock is completely limestone. The upper subtidal facies is a packstone-wackestone; fossil fragments generally are pelmatozoans and brachiopods (Figure 70-71). The lower subtidal facies generally is a mudstone with a large diversity of fauna: pelmatozoans, brachiopods, trilobites, ostracodes and bryozoans (Figure 72-73). Fossils in both upper and lower subtidal facies tend to be well preserved. Both upper and lower subtidal facies were massive or hummocky-nodular bedded which is a

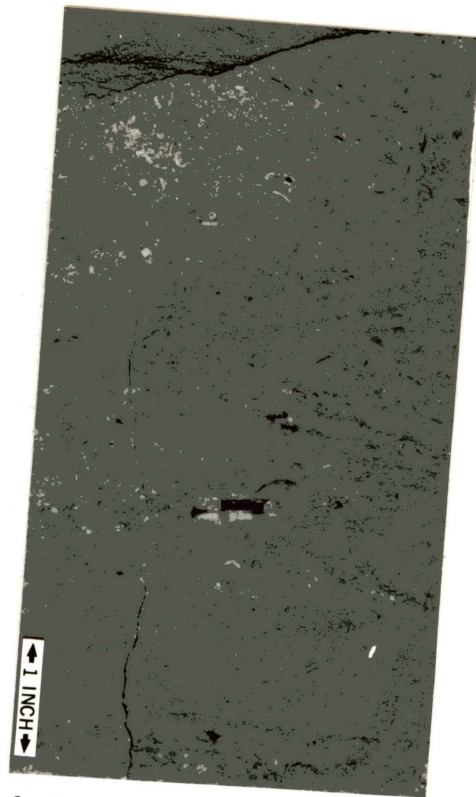


Figure 66. Calcitic Oolite Containing Herring Bone Crossbedding. (Eason Van Curen, 7146-47)

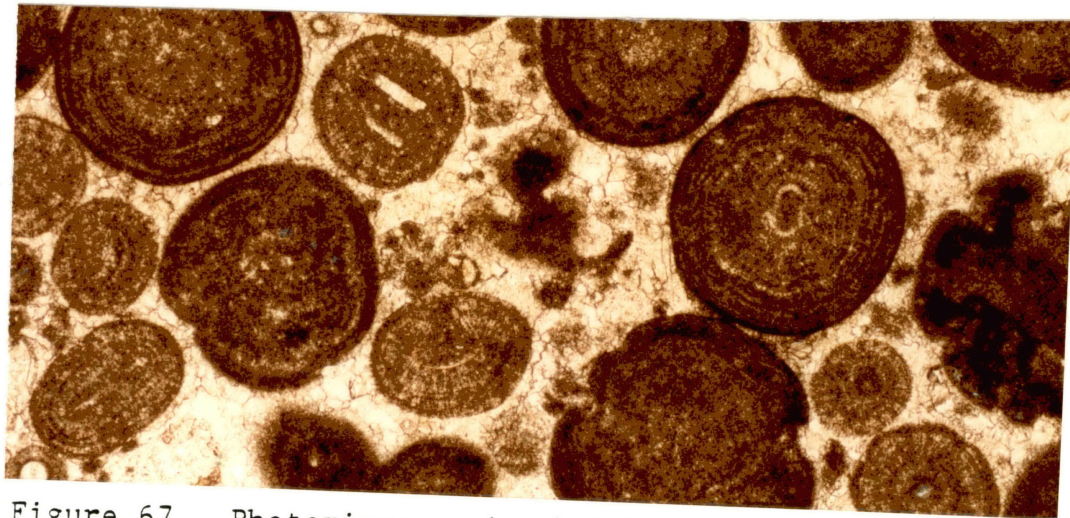


Figure 67. Photomicrograph of Calcitic Oolitic Facies, Note Isopachous Cement. (Kirkpatrick Cronkite, 7119, 40 x ppl)



Figure 70. Upper Subtidal Facies, Wackestone,
Note Preservation of Thin Valve of
a Brachiopod. (Kirkpatrick Cronkite,
7121)

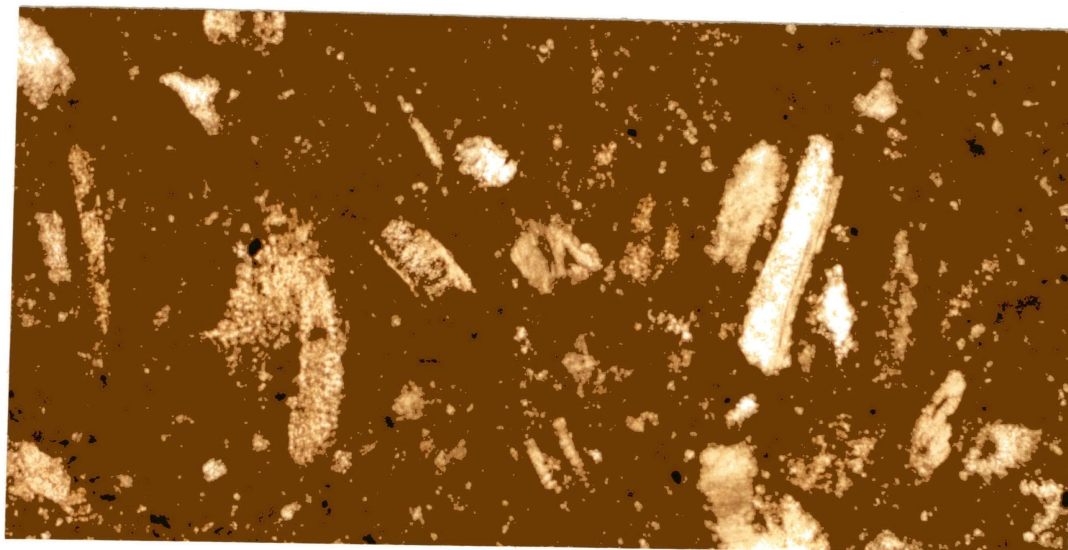


Figure 71. Photomicrograph of Upper Subtidal Facies.
(Jones and Pellow Farrel, 7797, 40 x ppl)

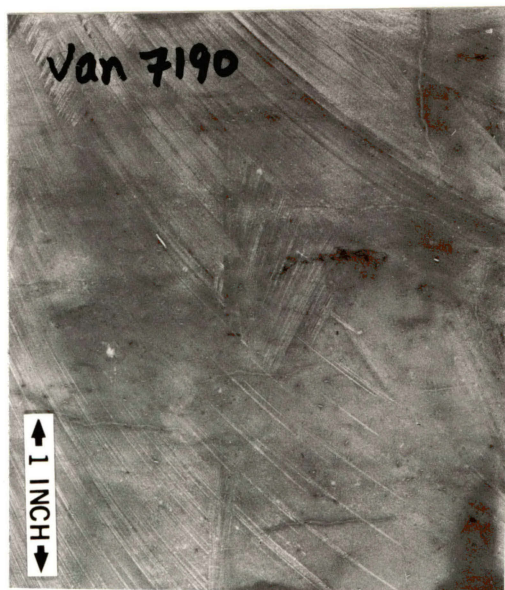


Figure 72. Lower Subtidal
Facies, Mud-
stone (Eason
Van Curan,
7190)

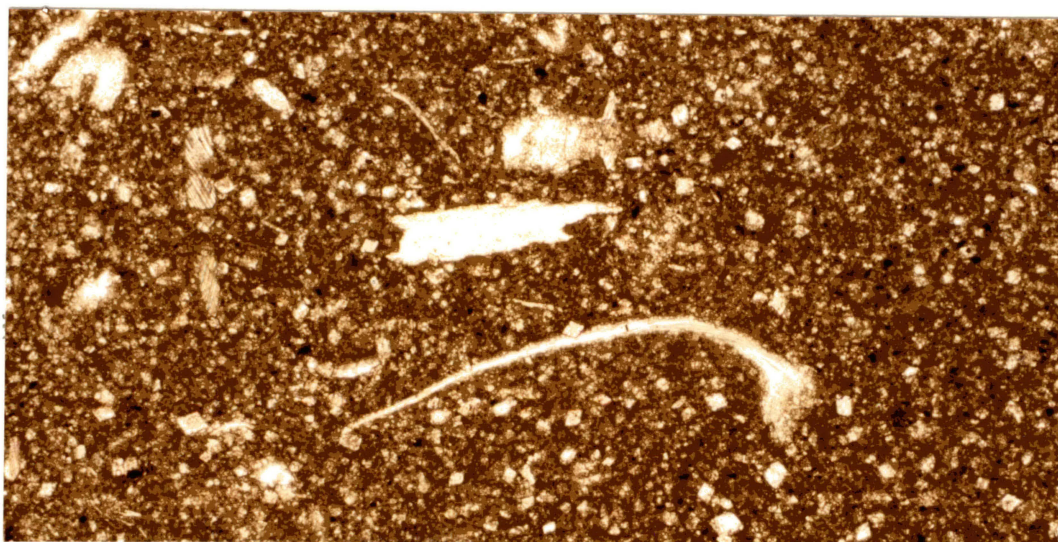


Figure 73. Photomicrograph of Lower Subtidal Facies
with Unfragmented Brachiopod Valve, Note
Predominance of Limpid Dolomite Rhombs.
(Texaco Thompsen, 8903, 40 x ppl)

result of incipient stylolitization (Figure 74). The subtidal facies represents a deepening of water.

Summary

The Henryhouse Formation was deposited on a shallow carbonate ramp. An oolitic sand belt is preserved in the Henryhouse; associated facies are a burrowed peloidal mudstone representing the lagoonal facies, a horizontal laminated and crossbedded grainstone indicative of the oolitic facies, and a massive to hummocky bedded packstone-wackestone-mudstone representative of the subtidal facies (Figure 62).

Dolomitization of the Henryhouse

Introduction

The present day oceans are saturated with respect to dolomite but precipitation has not been observed. Precipitation of ordered dolomite is difficult under surfacial conditions. Most sedimentary dolomite forms as a replacement of calcium carbonate and not as a primary precipitate. Cation hydration, slow kinetics and ionic pairing (ion complexing) all hinder the dolomitization process.

Rapid dolomitization results in aphanitic, poorly ordered, impurity-rich, cloudy rhombs (Land and Folk, 1975). Slow crystallization rates and low salinities result in clear, limpid, well-ordered rhombs but low super-

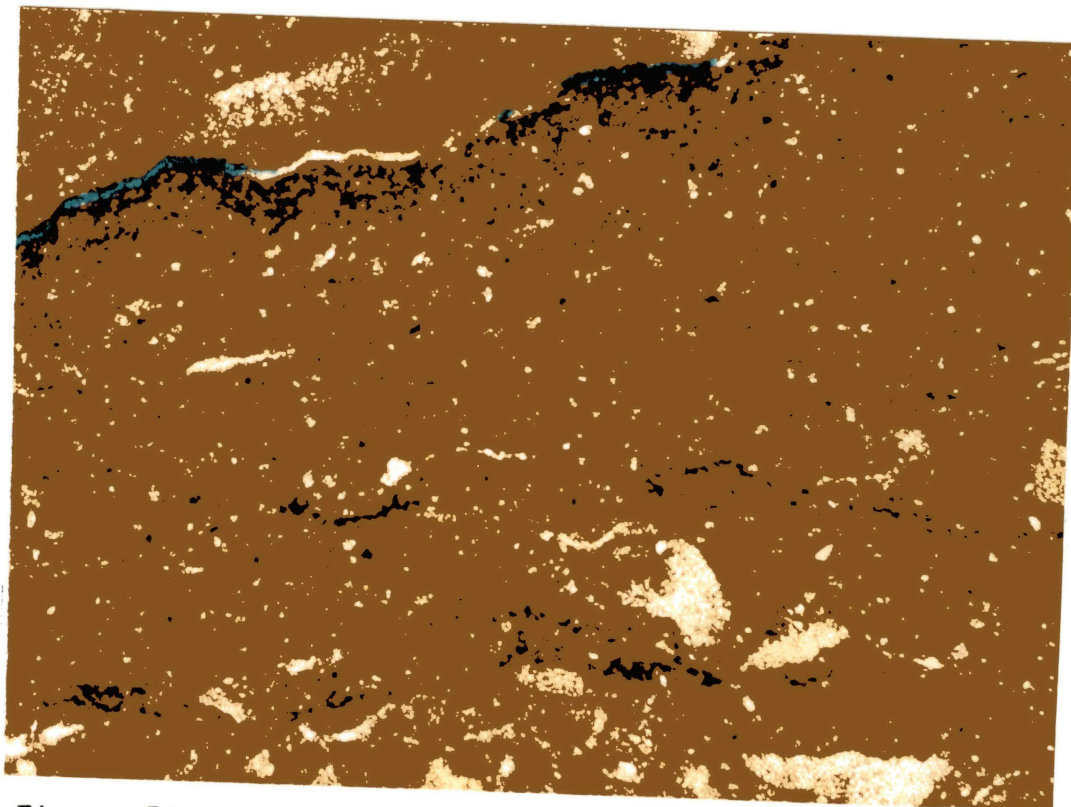


Figure 74. Photomicrograph of Incipient Stylolite,
Continued Pressure Solution Would Result
in Complete Dissolution of Carbonate and
Concentration of Insolubles in a Stylolite.
(Gulf Streeter 7143, 40 x ppl)

saturation favors overgrowths around existing crystals not nucleation of new crystals (Curtis, 1978).

Numerous theories have been postulated concerning dolomitization processes. These may be classified into three categories. These are evaporatic, freshwater/marine water mixing, and deep burial models.

Hypersaline dolomitization is reported in arid areas. High evaporation results in the precipitation of gypsum and anhydrite. As calcium is removed from the system, the Mg^{++}/Ca^{++} ratio increases to a ratio of 10:1 causing dolomitization of calcium carbonate sediments (Folk and Land, 1975). Hypersaline dolomite generally appears cloudy and anhedral.

Freshwater/marine water mixing dolomitization has been reported to occur when a freshwater lens moves into an area of hypersaline brines or seawater creating brackish waters with favorable Mg^{++}/Ca^{++} ratios (Figure 75).

"Much dolomite is formed by dilution of sea or sabkha waters by freshwater causing a tremendous drop in salinity but only a slight change in high Mg/Ca ratio". (Folk and Land, 1975, p. 62).

A mixture of 30% seawater with 70% freshwater lowers the salinity that inhibits ordered growth, but it allows Mg^{++}/Ca^{++} ratios to remain in the dolomite field (Badiozomani, 1973). Freshwater/marine water mixing allows longer periods of time for slow crystal growth. Freshwater/marine water mixing dolomite characteristically is limpid, well-ordered, and euhedral.

Deep burial (mesogenetic) dolomitization has been

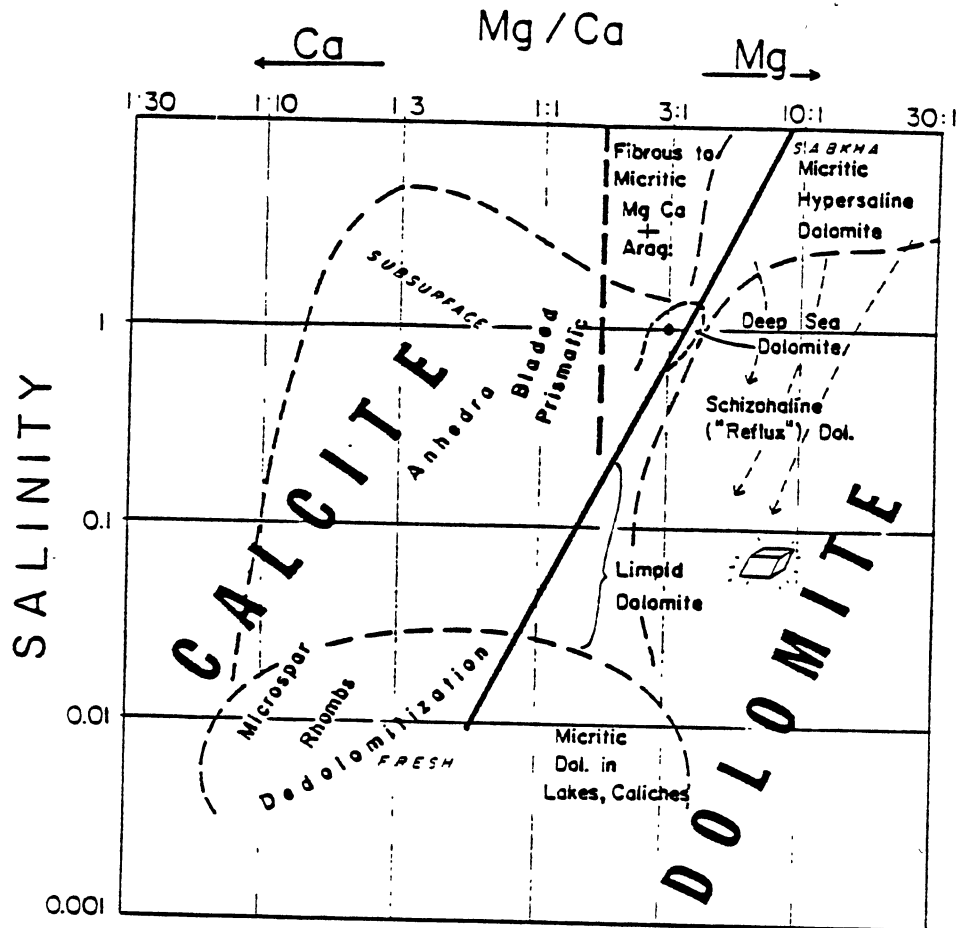


Figure 75. Fields of Occurrence of Dolomite Types, Note Mixing of Marine and Freshwater Results in a Salinity Drop While Remaining in Dolomite Field. (From Folk and Land, 1975)

advocated to explain dolomitization of large expanses of rock that were not affected by either hypersaline solutions or freshwater/marine water mixing. Several factors controlling dolomitization may be enhanced in the meso-genetic setting:

1. Increased temperature with increased depth increases dolomitization reaction rates.
2. The high hydration of Mg^{++} is removed with increasing temperature.
3. Increased reaction time for the dolomitization regime.
4. Effects of sandstone diagenesis may produce fluids conducive to dolomitization (Mg^{++} released from clay alteration) (Mattes and Mountjoy, 1980).

A variety of dolomite types has been reported for meso-genetic dolomite; one common form is baroque dolomite with curved faces.

Three episodes of dolomitization appear to have occurred in the Henryhouse Formation: hypersaline, freshwater/marine water mixing, and deep burial. The different types of dolomite are distinct.

Hypersaline Dolomitization

The scarcity of fauna in the lagoonal facies suggests restricted conditions and hypersalinity. When salinity increased gypsum and anhydrite were precipitated increasing Mg^{++}/Ca^{++} ratios. There are no evaporites preserved in the study area, but seasonal evaporites may have been present. Partially, or completely silicified anhydrite nodules are a

suggestion of hypersaline conditions which existed in the Henryhouse Formation in western Oklahoma (Beardall, 1983). A Henryhouse core containing anhydrite is along the strike of the oolite facies (Figure 59).

While evaporites are not present in the study area, evidence of hypersaline conditions were observed in the Henryhouse Formation:

- paucity of fossils
- euhedral quartz
- cloudy, anhedral rhombs
- enrichment in $^{13}\text{C}^{\circ}/\text{oo}$
- oolites.

In the northwest and southeast lagoonal facies, fossils are scarce. This suggests a harsh and hypersaline condition.

In several cores euhedral quartz is present (Figure 76). Euhedral quartz has been reported in association with calcitized sulfates (Friedman, 1980).

Cloudy, anhedral, dolomite rhombs suggest hypersalinity (Figure 77-78) (Folk and Land, 1975). The "dirty" appearance was a result of incorporation of impurities in the dolomite lattice during rapid dolomitization. Rapid dolomitization also accounts for the anhedral form of hypersaline dolomite.

Heavy $^{13}\text{C}^{\circ}/\text{oo}$ values have been reported for Holocene hypersaline dolomite (Mattes and Mountjoy, 1980). Although, extreme $^{13}\text{C}^{\circ}/\text{oo}$ values (Appendix I) have not been

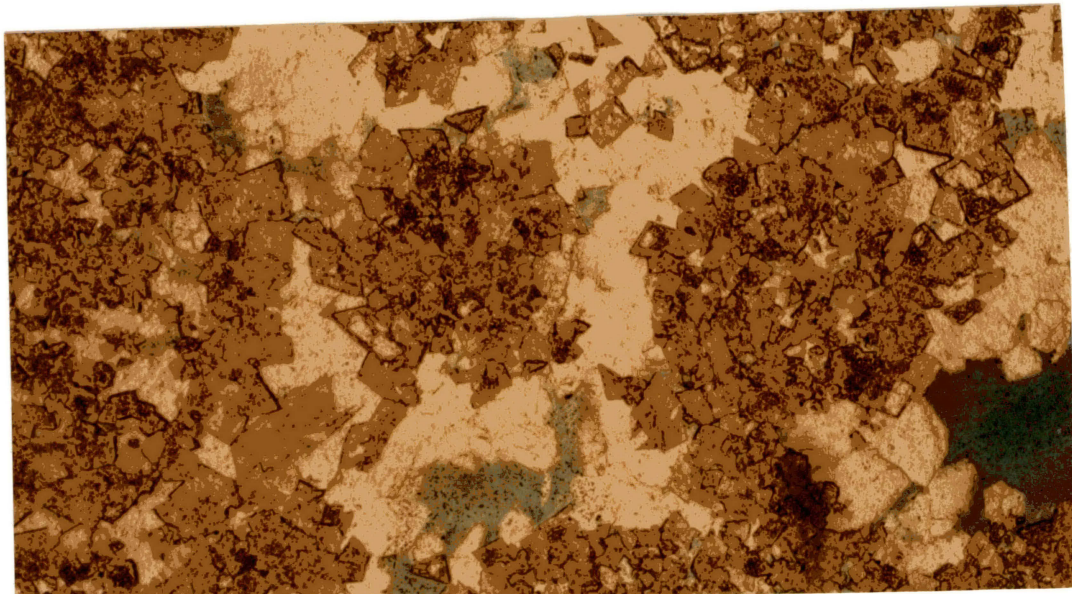
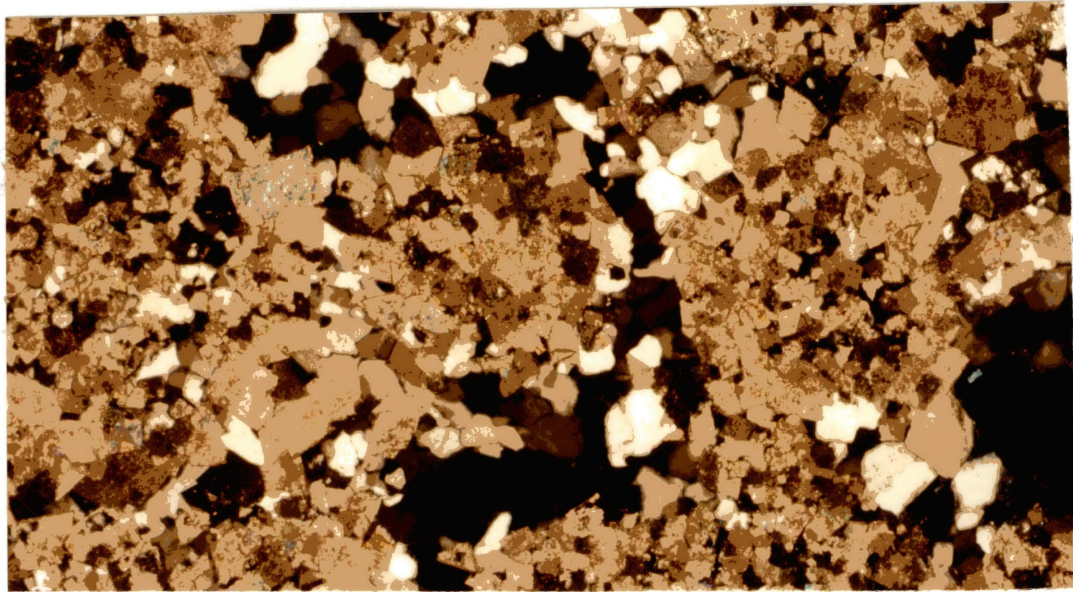


Figure 76. (a) Photomicrograph of Euhedral to Subhedral Quartz Surrounding Dolomitized Oololiths. (Shell Dill, 8531, 40 x CN)
(b) Plane Polarized Light of (a) (Shell Dill, 8531, 40 x CN)

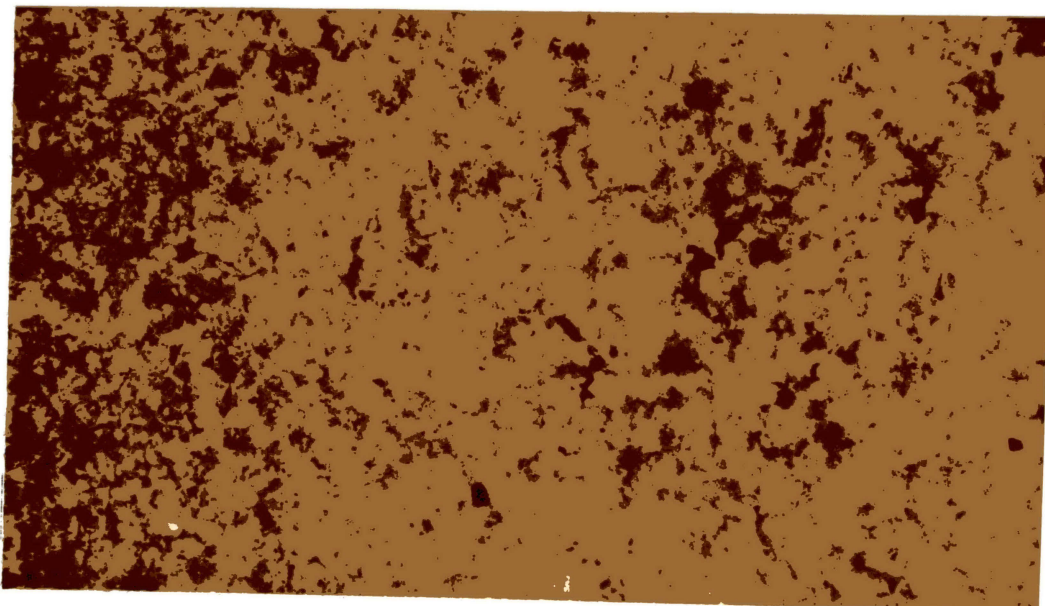


Figure 77. Photomicrograph of Cloudy Anhedral Dolomite in the Lagoonal Facies--Representative of Hypersaline Dolomite. (Duncan Garrett, 8739, 100 x ppl)

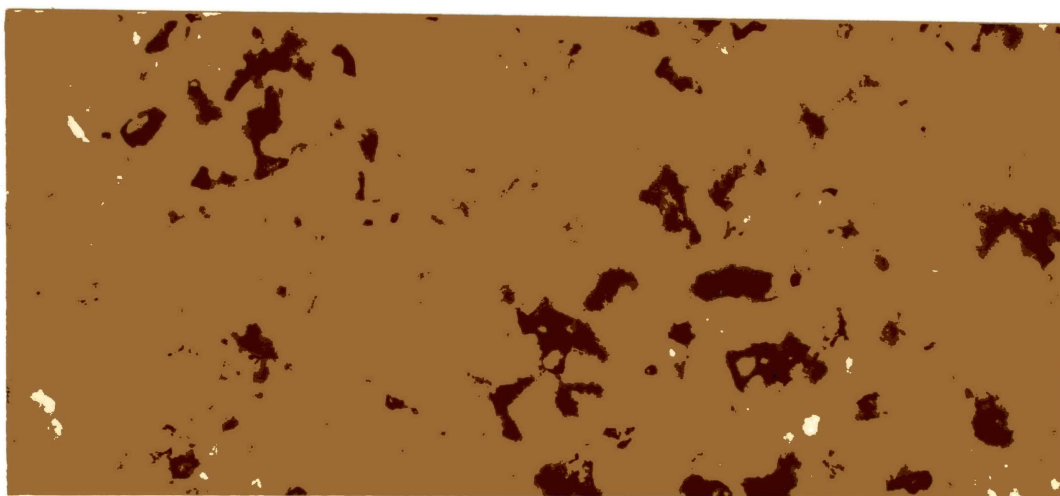


Figure 78. Photomicrograph of Cloudy Anhedral Dolomite--Representative of Hypersaline Dolomite, Clear Euhedral Dolomite--Representative of Marine/Freshwater Mixed Dolomite, Photomicrograph from Oolitic Facies. (Duncan Garrett, 8743, 100 x ppl)

reported in the Henryhouse, there appears to have been an enrichment of $^{13}\text{C}/\text{oo}$ in comparison to other dolomites (Figure 79). Isotopic analyses from the oolitic facies reflect more than one dolomitization process (freshwater/marine water mixing and hypersaline dolomitization). Isotopic values from the lagoonal facies were not examined, but they probably would have been heavier than the oolite due to the more extensive hypersaline dolomitization in this facies.

Ooliths are also indicators of hypersalinity (Friedman, 1980). Ooliths form in warm waters with elevated salinities. The oolitic shoal in the Henryhouse was emergent at times, possibly allowing the restricted conditions to occur in the lagoonal facies.

While each criteria is equivocal the combination of all suggest hypersaline dolomitization. Migration of dense hypersaline fluids dolomitized the lagoonal facies and partially dolomitizing the oolitic and subtidal facies (Figure 80).

Freshwater/Marine Water Mixing Dolomitization

It appears some of dolomite in the Henryhouse may have formed from freshwater mixing with seawater or hypersaline brines (Figure 81). Dilution of the brines or seawater with freshwater would have lowered the salinity with a slight decrease in the $\text{Mg}^{++}/\text{Ca}^{++}$ ratio (Figure 75). Some of the characteristics of Henryhouse dolomite suggesting a mixing model are:

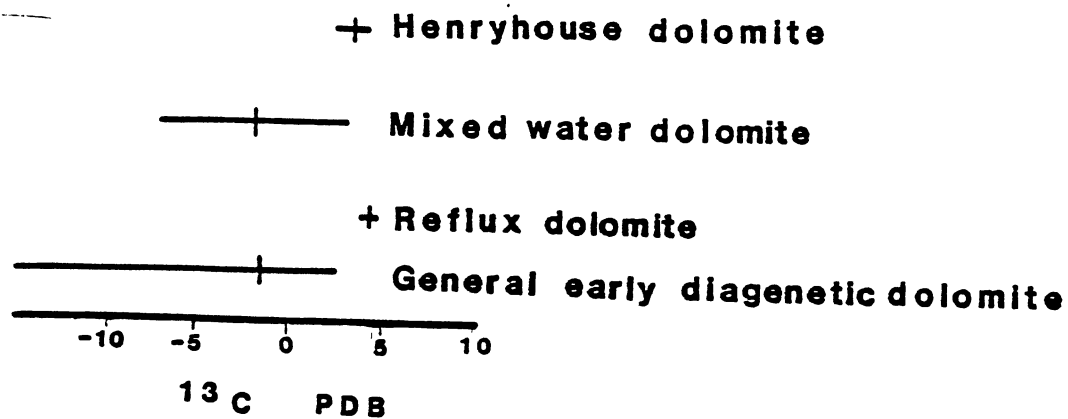
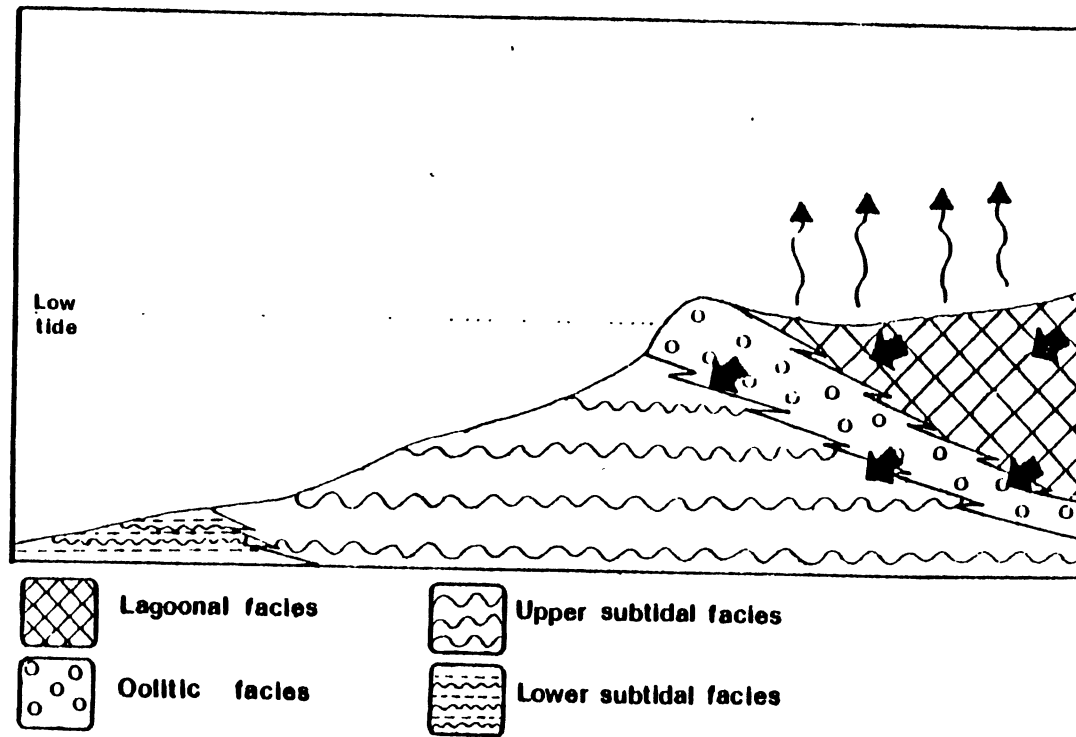





Figure 79. Bar Graph Comparing Henryhouse Carbon 13 Isotopic Values to Other Dolomites, Note Similarity of Henryhouse Dolomite to Reflux Dolomite. (other data from Mattes and Mountjoy, 1980)

Hypersaline Dolomitization of the Henryhouse



 Lagoonal facies  Upper subtidal facies
 Oolitic facies  Lower subtidal facies

 movement of hypersaline solutions

 evaporation at low tide

Figure 80. Hypersaline Dolomitization Model of the Henryhouse, Vertical Scale Greatly Exaggerated.

Mixed-Water Dolomitization of the Henryhouse

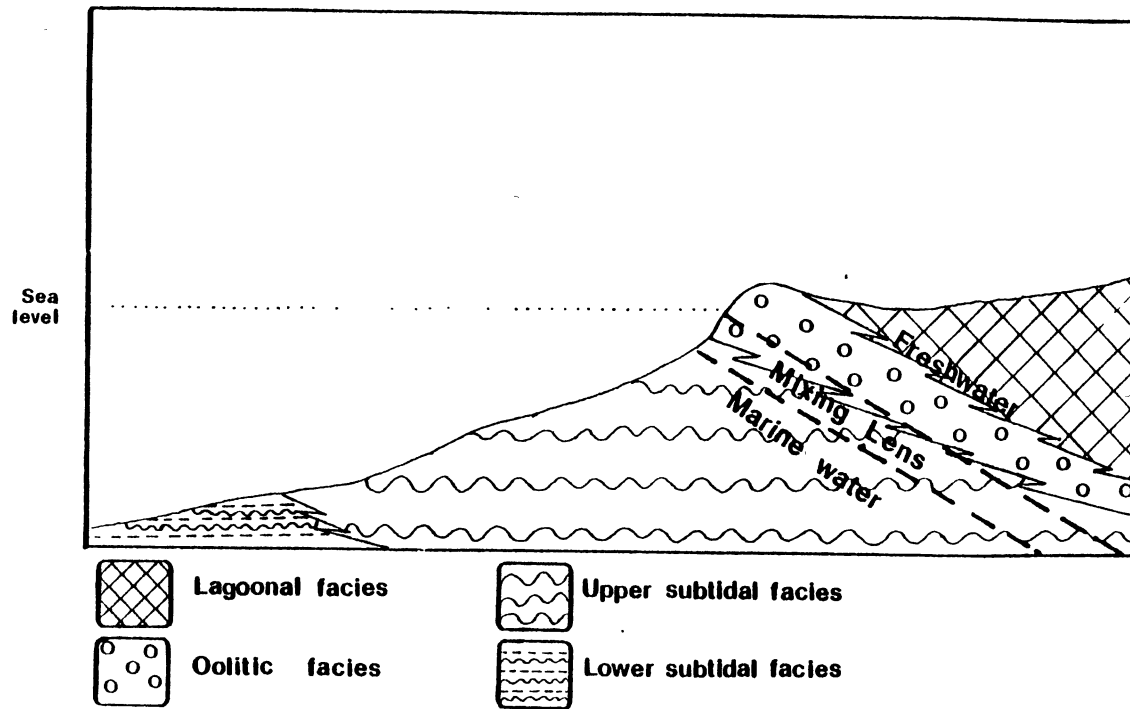


Figure 81. Freshwater/Marine Water Mixing Dolomitization Model, Vertical Scale Greatly Exaggerated.

- limpid, euhedral dolomite
- zoning
- light $^{18}\text{O}/\text{oo}$

Limpid, clear dolomite rhombs are indicative of a mixing environment (Folk and Land, 1975). Lower salinity conditions during dolomitization resulted in few impurities in the dolomite lattice. Longer periods of time in freshwater/marine water mixing dolomitization model resulted in clear, euhedral rhombs (Figure 82).

Zonation suggests two or more periods of dolomitization. Zoning consists of dark cloudy centers and limpid rims (Figure 83). The "dirty" centers formed during hypersaline conditions; the clear rims formed from freshwater/marine water mixing. The luminescent quality of the rhombs is similar to zoning in plane polarized light (Figure 84).

Depleted values in $^{18}\text{O}/\text{oo}$ indicate recrystallization at a high temperature or crystallization in the presence of isotopically-light water (freshwater) (Land, 1980). Oxygen isotopic values (Appendix I) are depleted in the Henryhouse (Figure 85). Freshwater/marine water mixing probably was responsible for this depletion.

Deep Burial Dolomitization

Baroque dolomite is observed as late dolomitization stage in the Henryhouse. The "lateness" is suggested by:

- crosscutting relationship in fractures

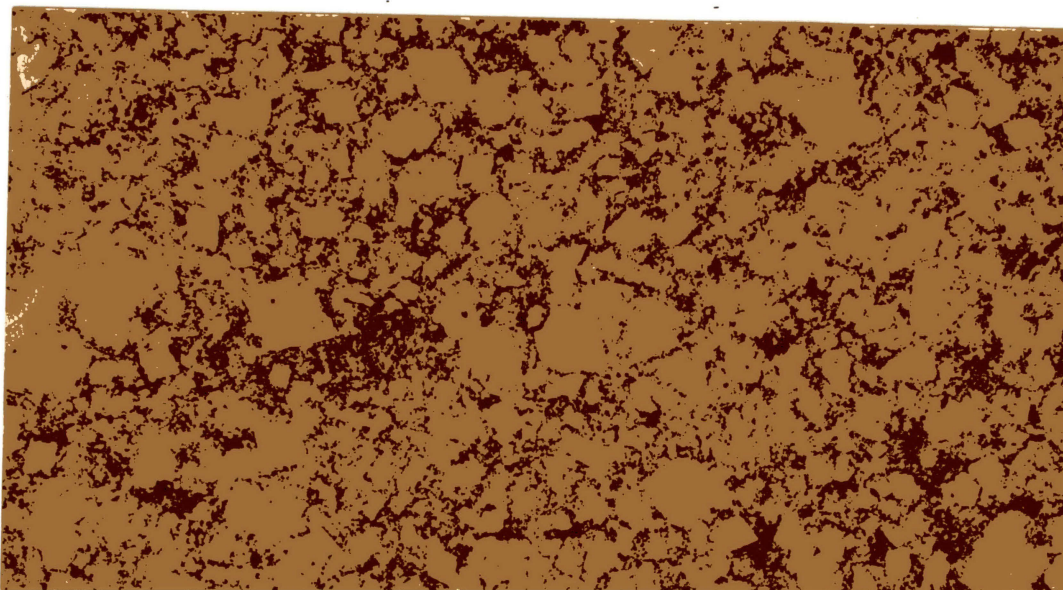


Figure 82. Photomicrograph Showing the Predominance of Limpid Euhedral Dolomite Subtidal Facies, Zoning is Not Prevalent. (Eason Van Curen, 7190, 10 x ppl)

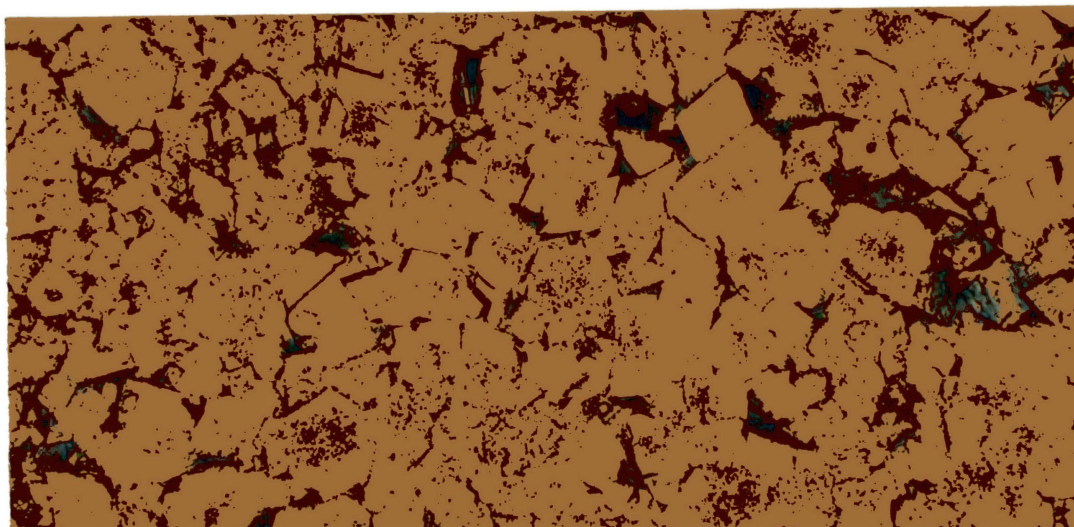


Figure 83. Photomicrograph Exhibiting Zoned Dolomite in the Oolitic Facies, Centers of Individual Rhombs are Cloudy, Rims are Clear. (Texaco Thompsen, 8867, 40 x ppl)

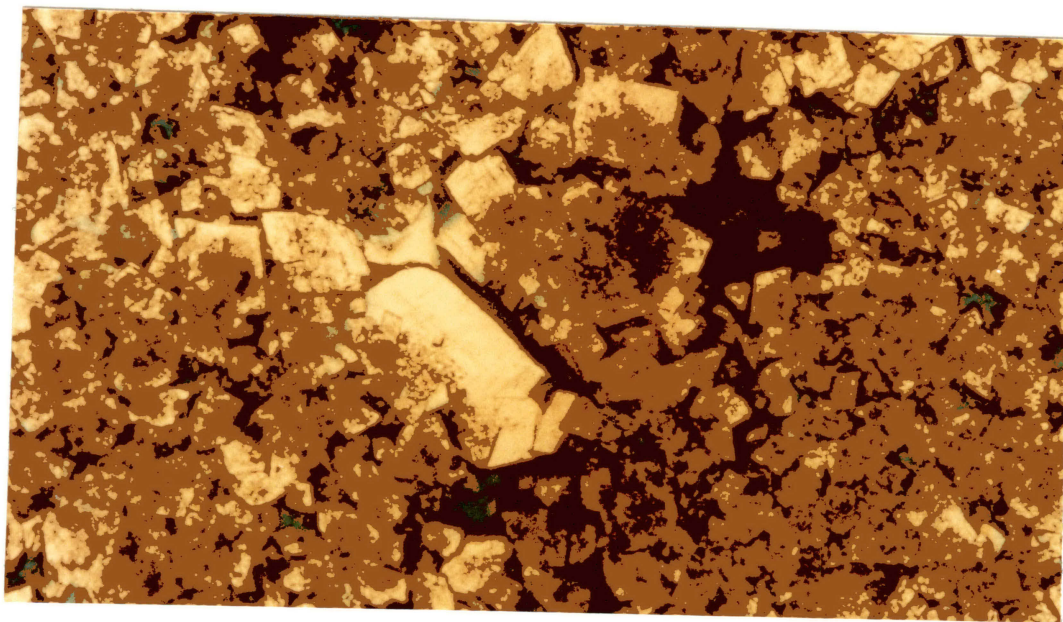
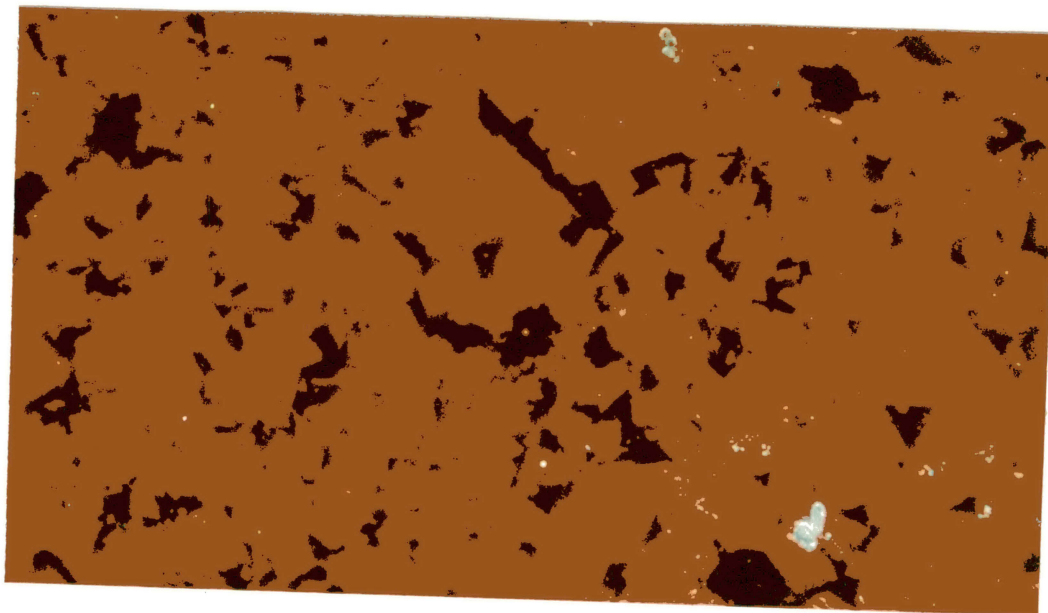


Figure 84. (a) Cathodoluminescent Photomicrograph Showing Zoning in Dolomite, Oolitic Facies. (Texaco Thompsen, 8868, 40 x)
(b) Plane Polarized Light of (a). (Texaco Thompsen, 8868, 40 x)

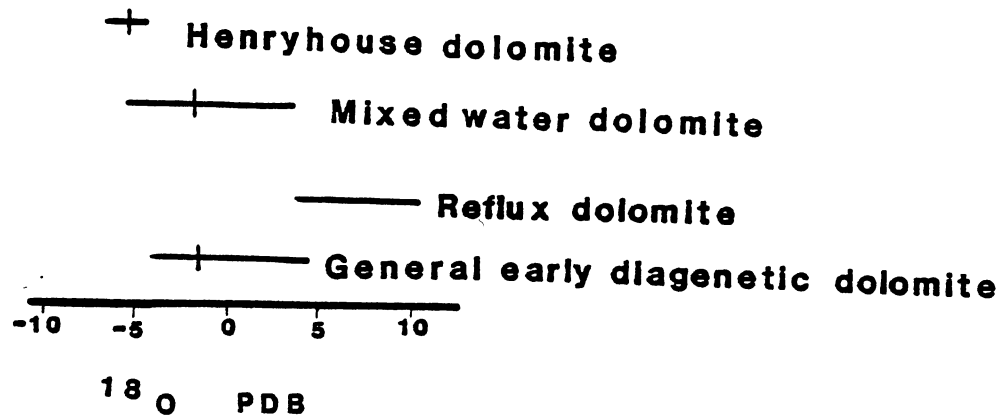


Figure 85. Bar Graph Showing Depletion of Oxygen 18 with Respect to Other Dolomites (additional data from Mattes and Mountjoy, 1980)

- filling secondary pore spaces (vugs and molds), and
- replacement of large grains.

Areas in the Henryhouse that contain healed fractures of baroque dolomite are post-lithification and usually post-stylolitization (Figure 86). Vugs and molds can also be filled with this dolomite. The pores generally are created after the second stage of dolomitization (freshwater/marine water mixing). Some large grains that resisted earlier dolomitization were successfully dolomitized by baroque dolomite (Figure 87).

Porosity Distribution and Its Relationship to Dolomite

The distribution of the dolomite and porosity is facies controlled. The following discussion examines the dolomite and its affect on porosity.

Dolomitization of the Lagoonal Facies

In the northwest portion of the study area the lagoonal facies (above the dolomitic oolite) was completely dolomitized, while dolomitization was incomplete in the southeast lagoonal facies (above the calcitic oolite) (Figure 88). The dolomite is dark and xenotopic. Zoned dolomite, limpid, euhedral dolomite, and baroque dolomite are rare in both areas but relatively more abundant in the northwest portion. In the lagoonal facies, the majority of the dolomite appears to have formed by hypersaline solutions.

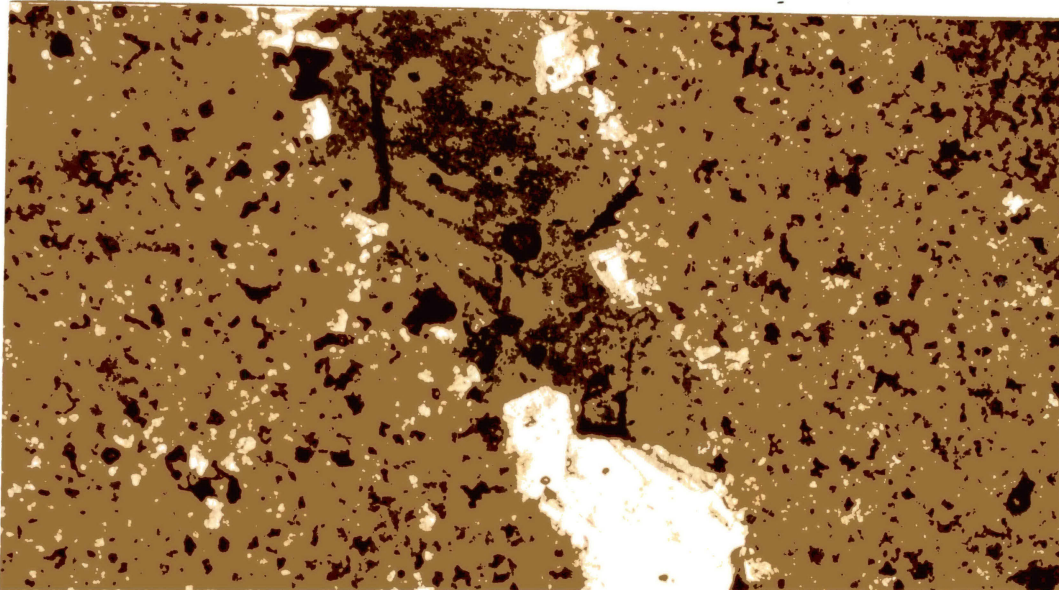


Figure 86. Photomicrograph of Baroque Dolomite Healing Fracture. (Duncan Garrett, 8749, 40 x (N))

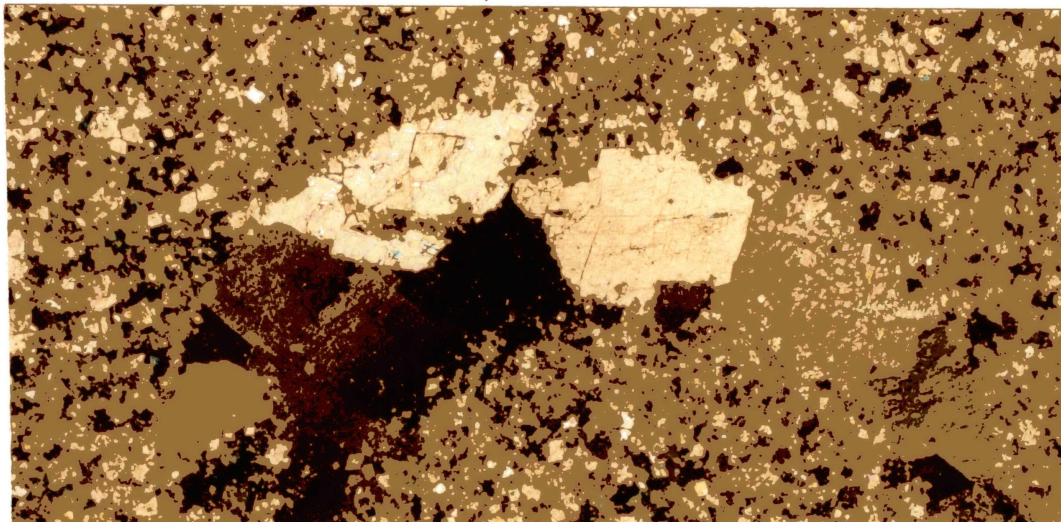


Figure 87. Photomicrograph of Baroque Dolomite Replacing Fossil Fragment. (Texaco Thompsen, 8876, 40 x (N))

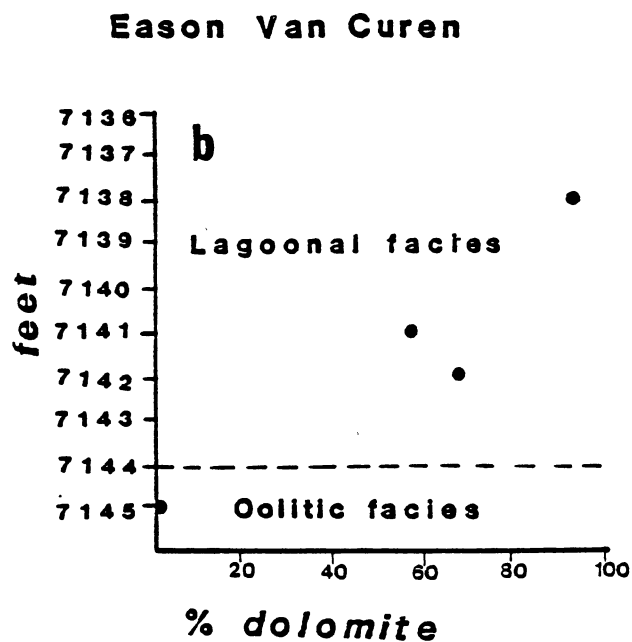
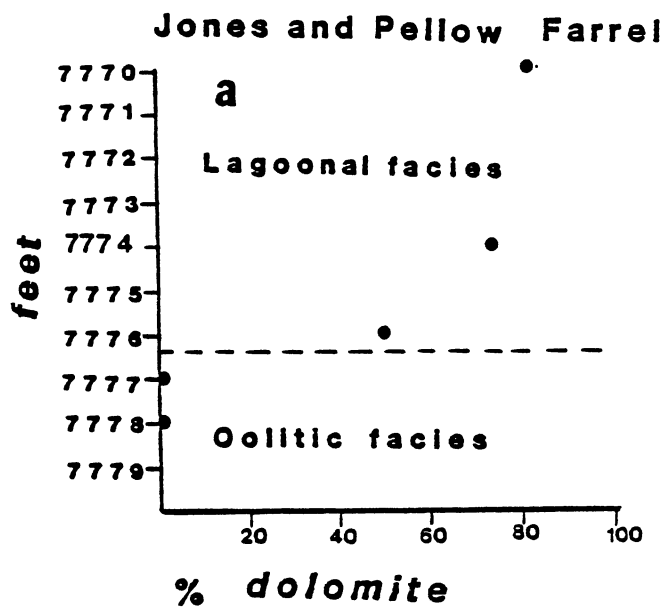


Figure 88(a,b). Decrease (a,b) in Dolomite in Southeast Lagoonal Facies Upon Approaching Oolite Contact. (data from x-ray diffraction)

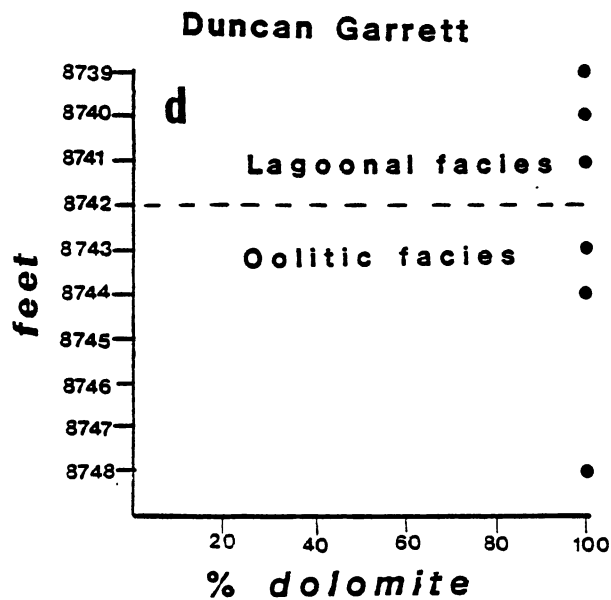
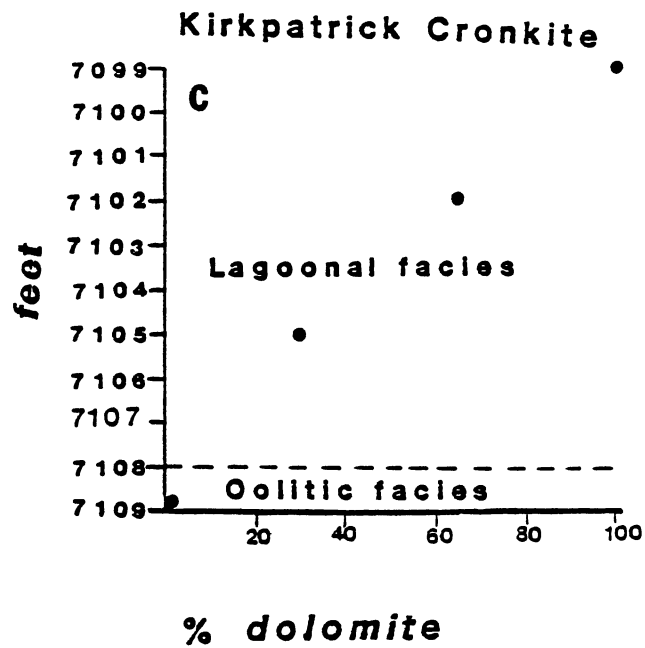


Figure 88(c,d). Decrease (c) in Dolomite in Southeast Lagoonal Facies Upon Approaching Oolite Contact, No Decrease (d) in Dolomite Upon Approaching Oolitic Facies in the Northwest. (data from x-ray diffraction)

No porosity appears in the southeast lagoonal facies, but to the northwest some sucrosic porosity (2-5%) developed.

Dolomitization of the Oolitic Facies

The oolitic facies was dolomitized in the northwestern part of the study area. The dolomite rhombs in the center of the ooliths are cloudy and anhedral (Figures 69 and 89), whereas, the rims of the ooliths contain clear, limpid dolomite as individual rhombs or overgrowths on pre-existing cloudy rhombs (Figures 69 and 89). Dolomite in the interoolitic pore space is idiotopic. The two different types of dolomite indicate two different dolomitization episodes. Hypersaline dolomitization is indicated by cloudy, anhedral rhombs, whereas freshwater/marine water mixing dolomitization is suggested by limpid, euhedral rhombs. Baroque dolomite also occurs in this facies.

The dolomitized oolites developed sucrosic, intracrystalline porosity in addition to the original interoolitic porosity (Figures 90-91). Dolomitization destroyed some interparticle pore space, but porosity in the dolomitized oolites is more abundant than in the calcitic oolites. The porosity in the calcitic oolites is interoolitic, but calcite cementation destroyed the primary porosity. Dissolution of cement and occasionally grains generated the porosity that has been reported in the calcitic oolites (Figure 92).

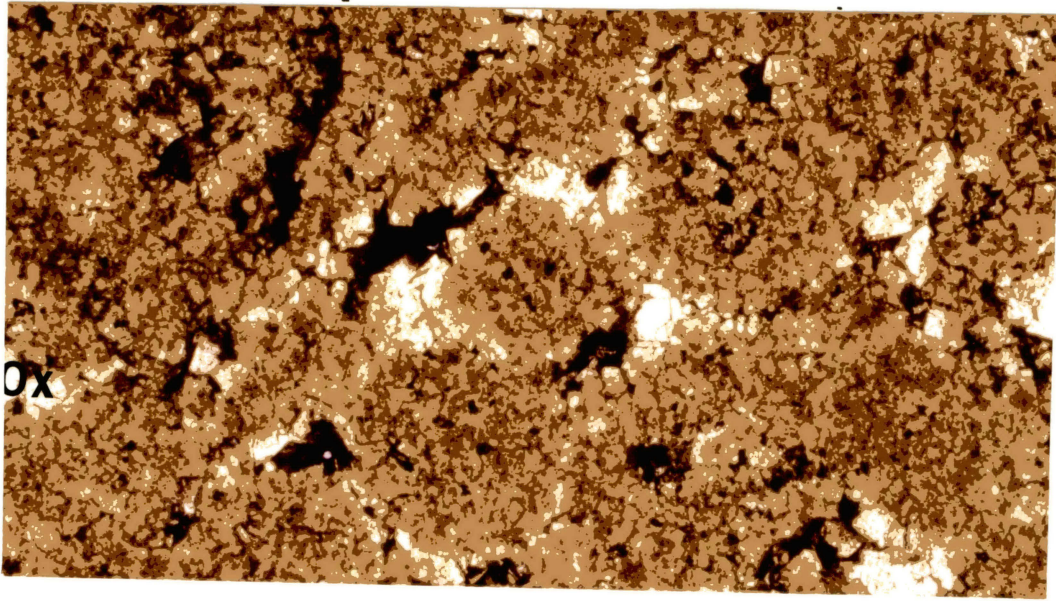


Figure 89. Photomicrograph Showing Cloudy, Hypersaline Dolomite in the Center of the Oolites and Clear, Mixed-Water Dolomite Around the Rims of the Oolites. (Duncan Garrett, 8751, 40 x ppl)

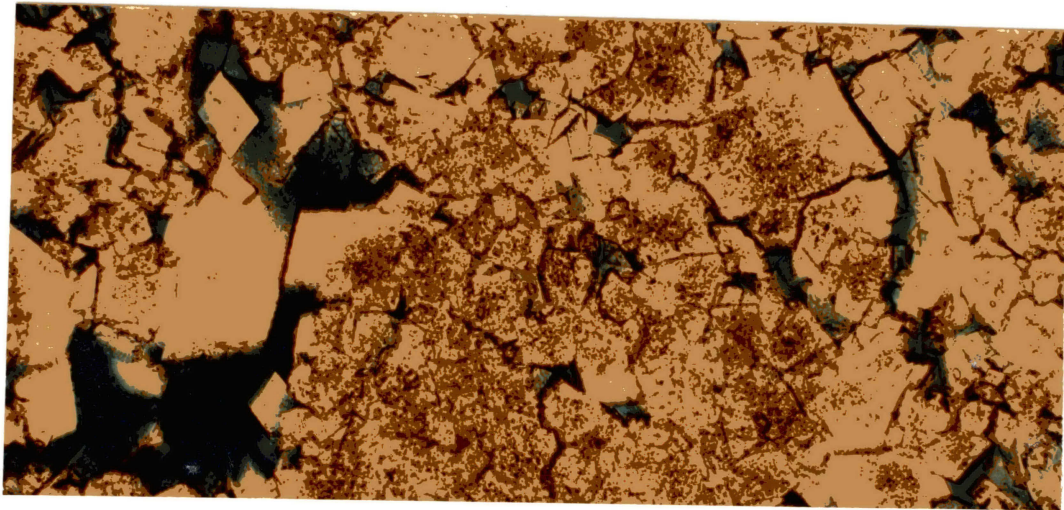


Figure 90. Photomicrograph Showing Inter- and Intra-oolitic Porosity. (Texaco Thompsen, 8868, 100 x ppl)

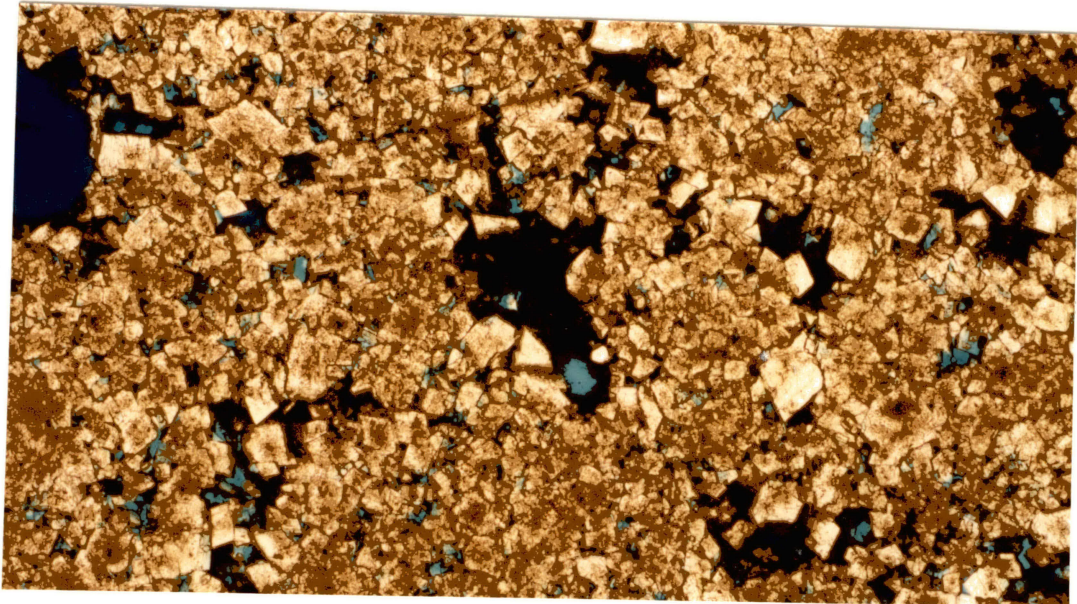


Figure 91. Photomicrograph Showing Inter- and Intra-oolitic Porosity. (Texaco Thompsen, 8868, 40 x ppl)

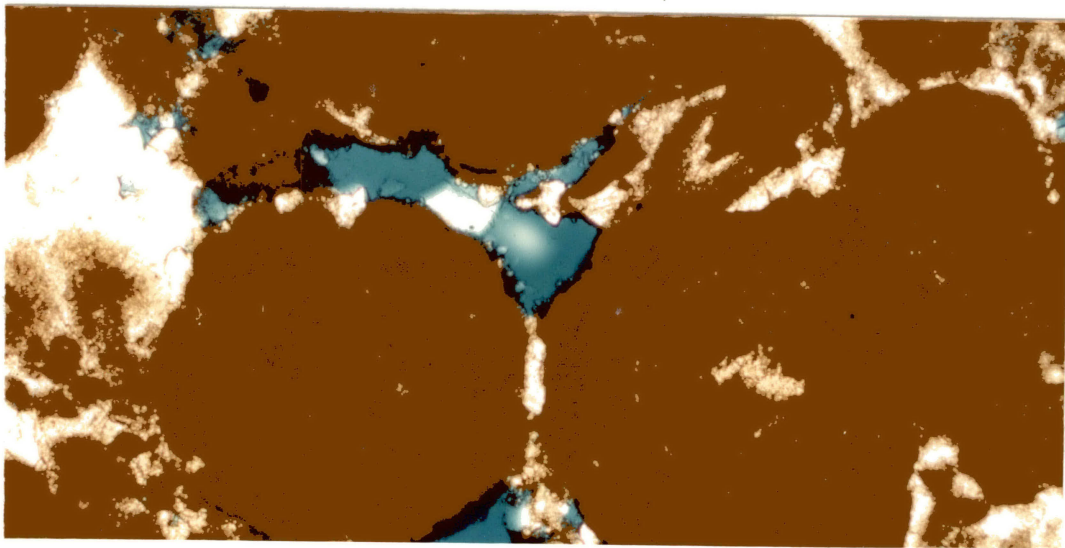


Figure 92. Photomicrograph Showing Interoolitic Porosity in Southeastern Oolitic Facies. (Gulf Streeter, 7053, 40 x)

Dolomitization of the Subtidal Facies

The subtidal facies was dolomitized near the oolitic contact with dolomite percentage decreasing downward (Figure 93). The dolomite rhombs in both the northwest and the southeast subtidal facies generally are limpid and euhedral; zoned rhombs appeared, only in the northwest. Baroque dolomite is commonly seen replacing fossil grains. Dolomitization did not develop any porosity in the subtidal facies.

Summary

The contrast between the dolomitized oolite to the northwest and the undolomitized calcitic oolite to the southeast is rather interesting. Perhaps the lack of permeability in the lagoonal facies, the early cementation of the calc-oolitic facies, and the type of dolomite formed suggest that the southeast oolitic facies "escaped" dolomitization.

Porosity has not been observed in the southeast lagoonal facies. The impermeability of this facies did not allow migration of dense hypersaline solutions into underlying sediments. As a result, decreasing dolomite percentages were observed near the oolitic contact (Figure 88). No decreases in dolomite percentages were observed in the northwest lagoonal facies. In this facies porosity is present. Dense hypersaline solutions were able to migrate through the northwest lagoonal facies, and dolomitized the

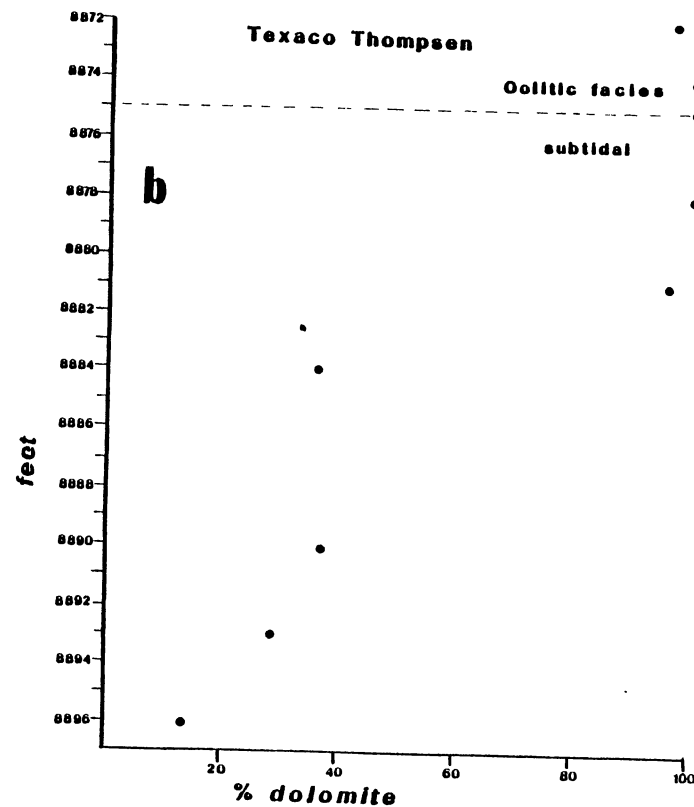
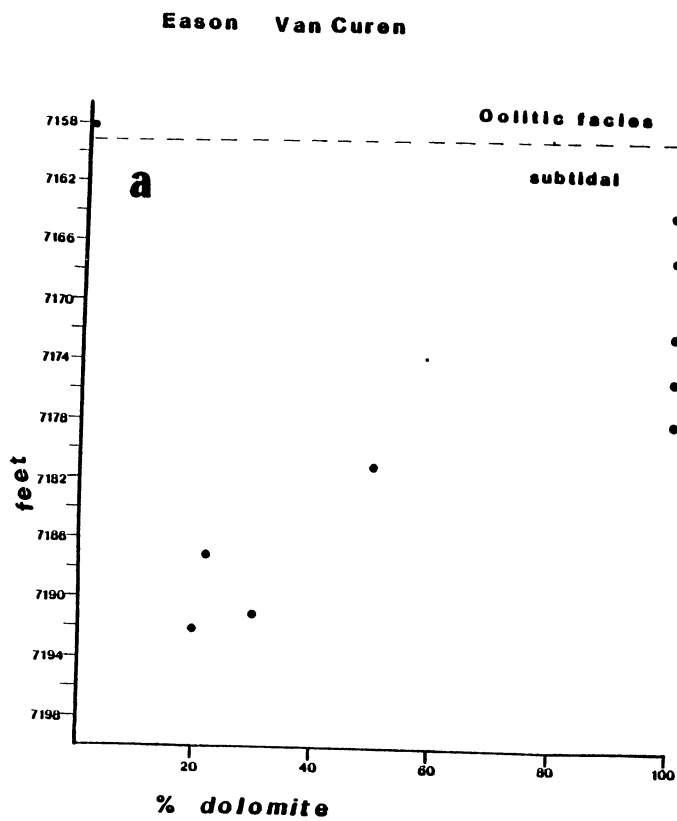


Figure 93(a,b). Graphs Showing Decrease in Dolomite in the Subtidal Facies in the Southeast(a) and Northeast(b). (Data from x-ray diffraction)

lagoonal, oolitic and part of the subtidal facies.

In absence of hypersaline dolomitizing fluids cementation occurred in the calcite oolite. Cementation prevented freshwater/marine water mixing solutions from entering this facies. Meniscus cement observed in several thin sections suggests emergence and early vadose cementation (Figure 95). The presence of a thin isopachous cement suggests marine phreatic cementation also an early cementation event. Both cements were followed by equant sparite that occluded porosity in the calcitic oolite. The porosity now present in this facies is secondary and related to dissolution of calcite.

The distribution of dolomite type was an important "clue" in the "non-dolomitization" processes. In the southeast lagoonal facies the majority of dolomite appears to have formed by hypersaline fluids (Figure 64); in the southeast subtidal facies the dolomite appears to have formed by freshwater/marine water mixing (Figure 82). In contrast, the northwest lagoonal, oolitic and subtidal facies zoned dolomite suggest two dolomitization processes (Figure 94).

It can be stated simply that the oolitic facies in the southeast was "missed" by the dolomitization processes (Figure 96). The impermeability of the lagoonal facies prevented hypersaline dolomitization. Early cementation of the oolitic facies also resulted in impermeability and prevented freshwater/marine water mixing dolomitization.

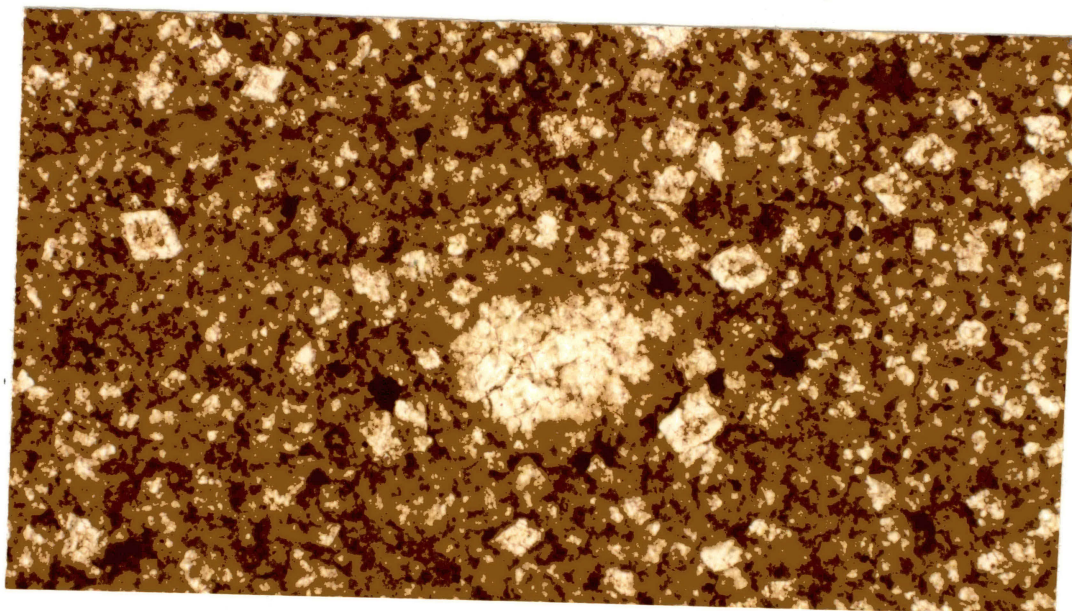


Figure 94. Photomicrograph Showing Zoned Dolomite in Northwest Subtidal Facies. (Texaco Thompsen, 8895, 100 x ppl)

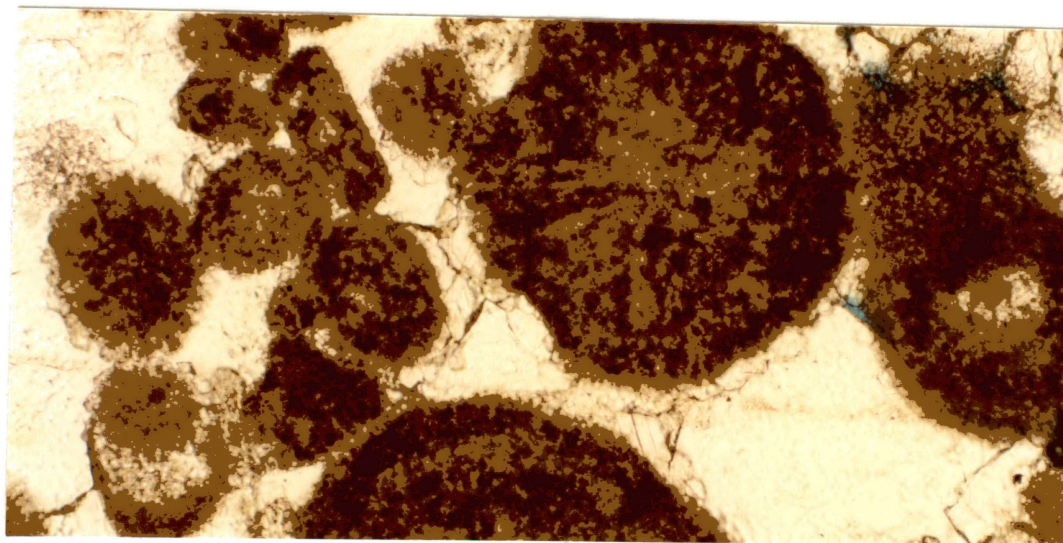


Figure 95. Photomicrograph Showing Meniscus Cement in Calcitic Oolitic Facies. (Gulf Streeter, 7053, 100 x ppl)

Dolomitization of Subtidal Facies in the Southeast

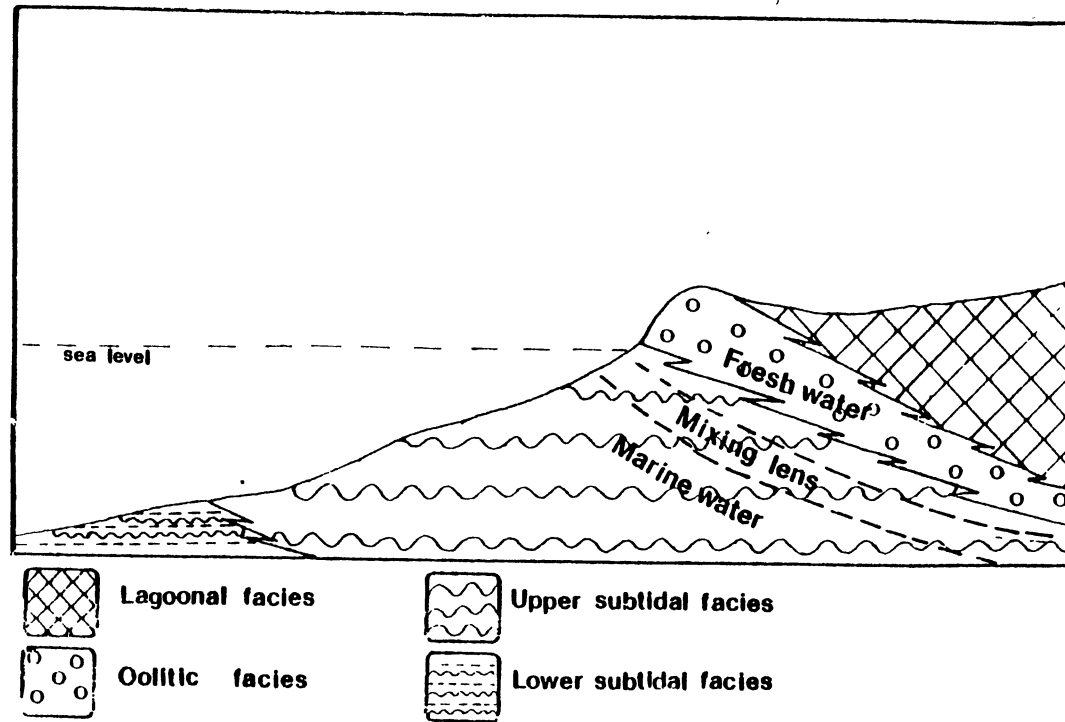


Figure 96. Dolomitization of the Subtidal Facies,
Mixing Lens Does Not Form in Impermeable
Oolitic Facies.

CHAPTER SIX

CONCLUSIONS

The conclusions derived from this study are:

Frisco Formation--

1. A crinoidal mound model has been proposed for the Frisco.
2. Facies in the Frisco are: a micritic-mound facies, a bioclastic intermound facies and a bioclastic capping facies.
3. The paleotopography and the paleoecology of crinoids were responsible for mound growth.
4. Porosity in the Frisco is related to facies, post-Frisco unconformity, and diagenetic effects.
5. Though all facies may develop porosity, a poorly winnowed intermound facies is the most likely facies to develop abundant porosity.
6. Effective porosity types are intraparticle porosity, enlarged intraparticle porosity and vuggy porosity.

Henryhouse Formation--

7. A carbonate ramp model is proposed for the deposition of Henryhouse Formation. The development of

oolites suggest a slope break in the Henryhouse paleotopography.

8. Three facies were identified: peloidal lagoonal facies, oolitic shoal facies, and packstone-wackestone-mudstone subtidal facies.

9. Dolomitization occurred by hypersaline replacement and freshwater/marine water mixing; deep burial dolomitization occurred in minor amounts.

10. The type of dolomite is related to facies; the lagoonal facies developed more hypersaline dolomite, the subtidal facies developed more freshwater/marine water mixed dolomite, when the oolitic facies is dolomitized it forms as a mixture of hypersaline dolomite and freshwater mixed dolomite.

11. Nondolomitization of the oolitic zone in the southeast was a result of low permeability in the lagoonal facies and early cementation of the oolitic facies.

12. Porosity is facies related. The dolomitic oolites developed interoolitic porosity and intraoolitic porosity; the calcitic oolites developed only interoolitic porosity.

SELECTED BIBLIOGRAPHY

- Adams, J. E., and Rhodes, M. L., 1960, Dolomitization by Seepage Reflux: Amer. Asso. Petro. Geol. Bull., Vol. 44, pp. 1912-1920.
- Adler, F. J., Future Petroleum Provinces of the Mid-Continent, In Future Petroleum Provinces of the United States, Their Geology and Potentials: Amer. Asso. Petro. Geol. Mem. No. 15, pp. 985-1120.
- Amsden, T. W., 1957, Introduction to Stratigraphy, pt. 1 of Stratigraphy and Paleontology of the Hunton Group in the Arbuckle Mtn. Regions: Okla: Geol. Sur. Circ., No. 44.
- Amsden, T. W., 1960, Hunton Stratigraphy, pt. 6 of Stratigraphy and Paleontology of the Hunton Group in the Arbuckle Mtn. Regions: Okla. Geol. Sur. Bull., No. 84.
- Amsden, T. W., 1961, Stratigraphy of the Frisco and Sallisaw Formations (Devonian) of Oklahoma: Okla. Geol. Sur. Bull., No. 90.
- Amsden, T. W., 1962, Silurian and Early Devonian Carbonate Rocks of Oklahoma: Amer. Asso. Petro. Geol. Bull., Vol. 46, pp. 1502-1519.
- Amsden, T. W., 1967, Silurian and Devonian Strata in Oklahoma: Tulsa Geol. Soc. Dig., Vol. 35, pp. 25-34.
- Amsden, T. W., 1975, Hunton Group (Late Ordovician, Silurian, and Early Devonian) in the Anadarko Basin of Oklahoma: Okla. Geol. Sur. Bull. 121.
- Amsden, T. W., 1980, Hunton Group (Late Ordovician, Silurian, and Early Devonian) in the Arkoma Basin of Oklahoma: Okla. Geol. Sur. Bull. 129.
- Amsden, T. W., and Rowland, T., 1967, Resume of Silurian and Devonian Strata in the Subsurface of Oklahoma: Tulsa Geol. Soc. Dig., Vol. 35, pp. 22-24.
- Amsden, T. W. and Rowland, R. L., 1971, Silurian and Devonian (Hunton) Oil and Gas Producing Formations: Amer. Assoc. Petro. Bull., Vol. 55, pp. 104-109.

- Amsden, T. W., and Ventress, W. P. S., 1963, Articulate Brachiopods of the Frisco Fm. (Devonian) pt. 1 of Early Devonian Brachiopods of Oklahoma: Okla. Geol. Sur., Bull. 94.
- Anderson, E. J., 1967, Paleoenvironments of the Coeymans Fm. (Lower Devonian) of New York State: Ph.D. dissertation, Brown University.
- Badiozamani, K., 1971, The Dorag Dolomitization Model-Association to the Middle Ordovician of Wisconsin: Jour. Sed. Pet., Vol. 43, pp. 965-984.
- Ball, M. M., 1967, Carbonate Sand Bodies of Florida and the Bahamas: Jour. Sed. Pet., Vol. 37, pp. 556-591.
- Banerjee, A., 1959, Petrology and Facies of Some Upper Visécan (Mississippian) Limestones in North Wales: Jour. Sed. Pet., Vol. 29, pp. 377-390.
- Bathurst, R. G. L., 1975, Developments in Sedimentology: Carbonate Sediments and Their Diagenesis: Elsevier Scientific Publishing Co.
- Bay, T. A., 1983, The Silurian of the Northern Michigan Basin, In Carbonate Buildups--A Core Workshop: Soc. Eco. Paleo. Min., Core Workshop No. 4, pp. 53-61.
- Beardall, G. B., 1983, Depositional Environment, Diagenesis and Dolomitization of the Henryhouse Fm., in the Western Anadarko Basin and Northern Shelf, Oklahoma: Okla. State Univer. Master's Thesis.
- Brand, U. and Veizer, J., 1981, Chemical Diagenesis of a Multi-Component Carbonate System-2: Stable Isotopes: Jour. Sed. Pet., Vol. 51, pp. 987-997.
- Boucot, A. J., 1962, Hunton Group (Silurian and Devonian) and Related Strata in Oklahoma: Discussion: Amer. Asso. Petro. Geol. Bull., Vol. 46, pp. 1528-1532.
- Cain, J. D. B., 1968, Aspects of the Depositional Environment and Paleoecology of Crinoidal Limestones: Scot. Jour. Geol., Vol. 4, pp. 191-208.
- Carozzi, A. V., and Soderman, J. G. W., 1962, Petrography of Mississippian (Borden) Crinoidal Limestones at Stobo, Indiana: Jour. Sed. Pet., Vol. 32, pp. 397-414.
- Choquette, P. W., 1968, Marine Diagenesis of Shallow Marine Lime-Mud Sediments: Insights from ^{18}O and ^{13}C Data: Science, Vol. 161, pp. 1130-1132.

- Choquette, P. W. and Steinen, R. P., 1980, Mississippian Non-Supratidal Dolomite, Ste. Genevieve Limestone, Illinois Basin: Evidence for Mixed-Water Dolomitization: In Concepts and Models of Dolomitization: Soc. Eco. Paleo. and Min. Spec. Publ., No. 28, pp. 163-196.
- Clark, A. H., 1915, Monograph of the Existing Crinoids, The Comatulids: Smithsonian Inst., U. S. N. M. Bull. 82, Vol. 1 (p.t 1), pp. 382.
- Clark, A. M., 1957, Crinoids: Geol. Soc. Amer. Mem. 67, Vol. 1, pp. 1183-1185.
- Clarkson, E. N. K., 1979, Invertebrate Paleontology and Evolution: Allen & Unwin, pp. 214-223.
- Clayton, R. N., Jones, B. F., and Verner, R. A., 1968, Oxygen and Carbon Isotope Studies of Dolomite Formation Under Sedimentary Conditions: Geochimica Cosmochimica Acta, Vol. 32, pp. 415-432.
- Croft, W. Y., Drackman, Y. C., and Moore, C. H., 1980, Jurassic Smackover Carbonate Grainstone Reservoir, North Haynesville Field, Claiborne Parish, Louisiana, In Carbonate Reservoir Rocks: Soc. Eco. Paleo. Min. Core Workshop, No. 1, pp. 120-136.
- Curtis, C. D., 1978, Possible Links in Sandstone Diagenesis and Depth Related Geochemical Reactions Occurring in Enclosing Mudstones: Geol. Soc. Lon. Jour., Vol. 135, pp. 107-117.
- Degens, E. and Epstein, S., 1964, Oxygen and Carbon Isotope Ratios in Coexisting Calcite and Dolomite: Geochimica et Cosmochimica Acta, Vol. 28, pp. 23-44.
- Dunham, J. B. and Olson, E. R., 1980, Shallow Subsurface Dolomitization of Subtidally Deposited Sediments in the Hanson Creek Formation (Ordovician-Silurian) of Central Nevada, In Concepts and Models of Dolomitization: Soc. Eco. Paleo. Min. Spec. Publ., No. 28, pp. 139-163.
- Evamg, B. D. and Shearman, D. J., 1965, The Development of Overgrowths from Echinoderm Fragments: Sedimentology, Vol. 5, pp. 211-233.
- Flügel, E., 1982, Microfacies Analysis of Limestones: Springer-Verlag.
- Folk, R. L., 1959, Practical Petrographic Classification of Limestones: Amer. Asso. Petro. Geol. Bull., Vol. 43, pp. 1-38.

- Folk, R. L. and Land, L. S., 1975, Mg/Ca Ratio and Salinity: Two Controls Over Crystallization of Dolomite: Amer. Asso. Petro. Geol. Bull., Vol. 59, pp. 60-68.
- Friedman, G. M., 1965, Terminology of Crystal Textures and Fabrics in Sedimentary Rocks: Jour. Sed. Pet., Vol. 35, pp. 643-655.
- Friedman, G. M., 1980, Dolomite is an Evaporite Mineral: Evidence from the Rock Record and from the Black Sea, In Concepts and Models of Dolomitization: Soc. Eco. Paleo. Min. Spec. Publ., No. 28, pp. 69-80.
- Grover, G., and Read, J., 1983a, Paleoaquifer and Deep Burial Related Cements Defined by Regional Cathodoluminescent Patterns, Middle Ordovician Carbonates, Virginia: Amer. Asso. Petro. Geol. Bull., Vol. 67, pp. 1275-1303.
- Grover, G., and Read, J., 1983b, Sedimentology and Diagenesis of Middle Ordovician Carbonate Buildups, Virginia, In Carbonate Buildups: Soc. Econ. Paleo. Min. Core Workshop, No. 4, pp. 2-25.
- Ham, W. E., Dennison, R. E., and Merritt, C. A., 1964, Basement Rocks and Structural Evolution of Southern Oklahoma: Okla. Geol. Sur. Bull., Vol. 95.
- Handshaw, B. B., Back, W., and Deike, R. G., 1971, A Geochemical Hypothesis for Dolomitization by Ground Water: Eco. Geol., Vol. 66, pp. 710-724.
- Harbaugh, J. W., 1957, Mississippian Bioherms in Northeast Oklahoma: Amer. Assoc. Petro. Geol. Bull., Vol. 41, pp. 2530-2544.
- Harvey, R., 1968, The West Cambell Field Key to Unlock the Hunton: Shale Shaker, Vol. 18, pp. 183-195.
- Hedgpeth, J. W., 1957, Classification of Marine Environments: Geol. Soc. Amer. Mem. 67, Vol. 1, pp. 17-27.
- Hollrah, T., 1978, Subsurface Lithostratigraphy of the Hunton Group, In parts of Payne, Lincoln and Logan Counties, Oklahoma: Shale Shaker, Vol. 28, pp. 150-156 and 168-175.
- Hsu, K. J., and Siegenthaler, 1969, Preliminary Experiments on Hydrodynamic Movement Induced by Evaporation and Their Bearing on the Dolomite Problem; Sedimentology, Vol. 12, pp. 11-25.

- Huffman, G., 1959, Pre-Desmoisian Isopachocus and Paleogeographic Studies in Central Mid-Continent Region: Amer. Asso. Petro. Geol. Bull., Vol. 43, pp. 2541-2573.
- Irwin, H. and Curtic, C., 1977, Isotopic Evidence for Source of Diagenetic Carbonates Formed During Burial of Organic-Rich Sediments: Nature, Vol. 269, pp. 209-213.
- Irwin, M. L., 1965, General Theory of Eperic Clearwater Sedimentation: Amer. Asso. Petro. Geol. Bull. Vol. 49, pp. 445-459.
- Isom, J. W., 1973, Subsurface Stratigraphic Analysis, Late Ordovician to Early Mississippian, Oakdale-Campbell Trend, Woods, Major, and Woodward Counties, Oklahoma: Shale Shaker, Vol. 24, pp. 32-42; 52-57.
- Keith, M. L. and Weber, J. N., 1963, Carbon and Oxygen Isotope Composition of Selected Limestones and Fossils: Geochimica et Cosmochimica Acta, Vol. 28, pp. 1787-1816.
- Krauskopf, K. B., 1979, Introduction to Geochemistry: McGraw-Hill.
- Land, L. S., 1967, Diagenesis of Skeletal Carbonates: Jour. Sed. Pet., Vol. 37, pp. 913-930.
- Land, L. S., 1980, The Isotopic and Trace Element Geochemistry of Dolomite: The State of the Art, In Concepts and Models of Dolomitization: Soc. Eco. Paleo. Min. Spec. Publ., No. 28, pp. 87-111.
- Laporte, L. F., 1969, Recognition of a Transgressive Carbonate Sequence Within an Epeiric Sea: Helderberg Group (Lower Devonian) of New York State, In Depositional Environments in Carbonate Rocks: Soc. Eco. Pet. Min. Spec. Publ., No. 14, pp. 98-114.
- Laudon, L. R., 1939, Stratigraphy of Osage Subseries of Northeastern Oklahoma: Amer. Asso. Petro. Geol. Bull., Vol. 23, pp. 325-338.
- Laudon, L. R., 1957, Crinoids: Geol. Soc. Amer. Mem., No. 47, pp. 961-972.
- Laudon, L. R. and Bowsher, A. L., 1941, Mississippian Formations of Sacramento Mountains, New Mexico: Amer. Assoc. Petro. Geol. Bull., Vol. 25, pp. 2107-2160.
- Leeder, M. R., 1982, Sedimentology: Allen and Unwin, pp. 211-226.

- London, W., 1973, A Geological and Engineering Study of the Mustang Pool, Canadian Co., Oklahoma: Shale Shaker, Vol. 23, pp. 4-12; 26-35; 50-55.
- Lucia, J. R., 1962, Diagenesis of a Crinoidal Sediment: Jour. Sed. Pet., Vol. 32, pp. 848-865.
- Marcher, M. V., 1962, Petrography of Mississippian Limestones and Cherts From the Northwestern Highland Rim, Tennessee: Jour. Sed. Pet., Vol. 32, pp. 819-832.
- Marr, J. W. S., 1963, Unstalked Crinoids of the Anartic Continental Shelf, Notes on Their Natural History and Distribution: Phil. Trans. Roy. Soc. B246, pp. 327-329.
- Mattes, B. W. and Mountjoy, E. W., 1980, Burial Dolomitization of the Upper Devonian Miette Buildup, Jasper National Park, Alberta, In Concepts and Models of Dolomitization: Soc. Eco. Paleo. Min. Spec. Publ., No. 28, pp. 259-297.
- Maxwell, R., 1959, Post-Hunton Pre-Woodford Unconformity in Southern Oklahoma, In Petroleum Geology of Southern Oklahoma: Ardmore Geol. Soc., Vol. 2, pp. 101-126.
- McCrea, J. M., 1950, On the Isotopic Chemistry of Carbonates and a Paleotemperature Scale: Jour. of Chem. and Physics, Vol. 18, pp. 849-857.
- McGee, D. and Jenkins, H., 1946, West Edmond Oil Field, Central Oklahoma: Amer. Asso. Petro. Geol. Bull., Vol. 30, pp. 1797-1829.
- McKenzie, J. A., Hsu, and Schnieder, J. F., 1980, Movement of Subsurface Waters Under the Sabkha, Abu Dhabi, UAE, and Its Relationship to Evaporite Dolomite Genesis, In Concepts and Models of Dolomitization: Soc. Eco. Paleo. Min. Spec. Pub., No. 28, pp. 11-30.
- Meyers, W. J., 1980, Compaction in Mississippian Skeletal Limestones, Southwestern New Mexico: Jour. Sed. Pet., Vol. 50, pp. 457-474.
- Moore, R. C., 1957, Mississippian Carbonate Deposit of the Ozark Region, In Regional Aspects of Carbonate Deposition--a Symposium: Soc. Eco. Paleo. Min. Spec. Pub., No. 5, pp. 101-124.
- Morgan, W., 1983, Productive Upward Shoaling Sequences Within the Hunton Group (Silurian): Mt. Everette and Southwest Reeding Fields, Kingfisher County,

- Oklahoma, In Carbonate Reservoirs Casebook:
Springer-Verlag.
- Morgan, W., Schneider, R., and Copley J., 1982, Identification of Subtle Porosity and Traps Within Frisco Fm., Canadian Co., Oklahoma: A Geologic Seismic-Waveform Approach, In the Deliberate Search for the Subtle Trap: Amer. Asso. Petro. Mem. pp. 93-114.
- Murray, R. C., 1960, The Origin of Porosity in Carbonate Rocks: Jour. Sed. Pet., Vo. 30, pp. 59-84.
- Reeckmann, A and Friedman, G., 1982, Exploration for Carbonate Petroleum Reservoirs, John Wiley and Sons, pp. 65-79.
- Reeds, C. A., 1911, The Hunton Formation of Oklahoma: Amer. Jour. Sci., Vol. 182, pp. 256-268.
- Reeds, C. A., 1926, The Arbuckle Mountains: Okla. Geol. Sur. Circ. 14.
- Sears, S. O. and Lucia, F. J., Dolomitization of Northern Michigan Niagara Reefs by Brine Refluxion and Fresh-water/Seawater Mixing, In Concepts and Models of Dolomitization: Soc. Eco. Paleo. Min. Spec. Publ. No. 28, pp. 215-237.
- Shannon, P., 1962, Hunton Group (Silurian-Devonian) and Related Strata in Oklahoma: Amer. Asso. Petro. Geol. Bull., Vol. 46, pp. 1-29.
- Smosna, R. A., 1984, Sedimentary Facies and Early Diagenesis of an Oolite Complex from the Silurian of West Virginia, In Carbonate Sands--A Core Workshop: Soc. Eco. Paleo. Min. Core Workshop, No. 5, pp. 20-57.
- Sokolova, M. N., 1959, On the Distribution of Deep-Water Bottom Animals in Relation to Their Feeding Habits and the Character of Sedimentation: Deep Sea Research, Vol. 6, pp. 1-4.
- Sternbach, L. R. and Friedman, G. M., 1984, Deposition of Ooid Shoals Marginal to the Late Cambrian Proto-Atlantic (Iapetus) Ocean in New York and Alabama; Influence on the Interior Shelf, In Carbonate Sands--A Core Workshop: Soc. Eco. Paleo. Min. Core Workshop, No. 5, pp. 2-19.
- Strimple, H. L., 1963, Crinoids of the Hunton Group (Devonian-Silurian) of Oklahoma: Okla. Geol. Sur. Bull., Vol. 100.

- Swesnik, R. M., 1948, Geology of the West Edmond Oil Field, Logan, Canadian and Kingfisher Counties, Oklahoma, In Structure of Typical American Oil Fields: Amer. Assoc. Petro. Geol., Vol. 3, pp. 359-398.
- Taff, J. A., 1902, Description of the Atokan Quadrangle (Indian Territory): U.S. Geol. Sur. Geologic Atlas, Folio 79.
- Tarr, R., 1955, Paleogeologic Map at the Base of the Woodford, and Hunton Isopach of Oklahoma: Amer. Asso. Petro. Geol. Bull., Vol. 39, pp. 1851-1858.
- Tasch, P., 1973, Patterns of Five: Creatures with Tube Feet, In Paleobiology of the Invertebrates (Data Retrieval from the Fossil Record) pp. 741-774.
- Todd, D. K., 1980, Groundwater Hydrology, John Wiley and Sons, pp. 494-502.
- Tucker, M. E., 1969, Crinoidal Turbidites from the Devonian of Cornwall and Their Paleogeographic Significance: Sedimentology, Vol. 13, pp. 281-290.
- Tucker, M. E., 1981, Sedimentary Petrology An Introduction: Wiley and Sons, pp. 140-157.
- Weber, J. and Raup, D., 1966, Fractionation of the Stable Isotopes of Carbon and Oxygen in Marine Calcareous Organisms--the Echinoidea, Part I and II: Geochimica et Cosmochimica Acta, Vol. 30, pp. 681-736.
- Weber, J. and Raup, D., 1968, Comparison of $^{13}\text{C}/^{12}\text{C}$ and $^{18}\text{O}/^{16}\text{O}$ in the Skeletal Calcite of Recent and Fossil Echinoids: Jour. Sed. Pet., Vol. 42, pp. 37-50.
- Wilson, J. L., 1974, Characteristics of Carbonate Platform Margins: Amer. Asso. Petro. Geol. Bull., Vol. 58, pp. 810-824.
- Wilson, J. L., 1975, Carbonate Facies in Geologic History: Springer-Verlag.
- Zenger, D. H., 1972, Significance of Supratidal Dolomitization in the Geologic Record: Geol. Soc. Amer. Bull., Vol. 83, pp. 1-11.
- Zenger, D. H. and Dunham, J. B., 1980, Concepts and Models of Dolomitization, In Concepts and Models of Dolomitization: Soc. Eco. Paleo. Min. Spec. Publ., No. 28, pp. 1-11.

APPENDIX I

Stable Oxygen and Carbon Isotopes
of the Henryhouse

Sample	Mineralogy	$^{13}\text{C}^*$	$^{18}\text{O}^*$
Cleary Kramp Cobb#1	Dolomite	+3.4	-6.8
Shell Dill#1	Dolomite	+4.2	-5.9
Texaco Theo Thompson#1	Dolomite	+2.2	-6.0
Duncan Garrett#2	Dolomite	+3.1	-6.1
Kirkpatrick Cronkite#1	Calcite	+4.9	-4.3
Eason Van Curen#1	Calcite	+3.4	-4.6
Jones and Pellow Farrel#1	Calcite	+2.2	-5.7
Gulf Streeter#1	Calcite	+3.6	-5.0

*PDB Scale

APPENDIX II

STABLE OXYGEN AND CARBON ISOTOPES
OF THE FRISCO

Type and Sample	Mineralogy	$^{13}\text{C}^*$	$^{18}\text{O}^*$
<u>Micrite</u>			
Jones and Pellow Leeper 3-1	Calcite	+1.0	-5.8
Gulf Streeter #1	Calcite	-0.1	-3.9
Apexco Curtis #2	Calcite	+1.8	-4.0
Midwest McManus #1	Calcite	+1.5	-4.5
<u>Sparry Calcite</u>			
Jones and Pellow Leeper 3-1	Calcite	-0.1	-4.9
Gulf Streeter #1	Calcite	+0.5	-6.4
Apexco Curtis #2	Calcite	+4.0	-7.7
Midwest McManus #1	Calcite	+2.6	-3.7
<u>Crinoids</u>			
Jones and Pellow Leeper 3-1	Calcite	+2.0	-3.0
Gulf Streeter #1	Calcite	+1.9	-3.2
Apexco Curtis #2 (8544)	Calcite	+2.4	-2.8
Apexco Curtis #2 (8553)	Calcite	+2.0	-3.1
Midwest McManus #1	Calcite	+2.6	-3.7
<u>Brachiopod</u>			
Midwest McManus	Calcite	+2.6	-3.5

*PDB Scale

APPENDIX III
CORE SUMMARIES

Name: Apexco Curtis
Location: Sec. 27 T11N R5W

There is 70 ft. of the Frisco (8522-8592) present in the Curtis core. The overlying contact is not present; the underlying contact is assigned to the Bois D'Arc.

The Frisco is grey to black depending on the amount of mud present. The chief constituent of the Frisco is skeletal grains. Pelmatozoans are the most abundant grain (30-59%). Other important grains are: bryozoans (1-22%), brachiopods (2-5%), trilobites (1%) and coral (0-3%). Horizontal and inclined oriented grains are seen in the capping facies; massive bedding predominates the mound facies.

Abundant dissolution features are seen as: calcite filled, micrite filled and open vugs. The open vugs enhance the porosity. Intraparticle and enlarged intraparticle porosity are present in zooecia.

Micrite and sparite are cements in the Curtis core. The dominant cement is dependent on the facies.

There appears to be at least two phases of dissolution in the Curtis core; an initial dissolution phase after early cementation and a second phase after more extensive cementation. Compaction occurred after most of the cementation had been completed.

The lowest portion (8592-8553) of the Curtis was deposited near the mound facies, some areas contain some oriented grains but poor sorting and massive bedding are

present. The rock is a packstone. The mixing of sedimentary features indicates close proximity to a mound. Eventually the mound facies predominates (8538-8553). The rock is a wacke/mudstone. The mound facies is overlain by a capping facies (8538-8522) with oriented grains and sparry calcite cement. The rock here is a grainstone.

Name: Gulf Shaddix
Location: Sec. 29 T6N R3W

Forty-five feet of Frisco is present in the Shaddix (9205-9245) core. Upper and lower contacts are not contained in this core.

The Shaddix is a light brown fossiliferous lime wacke/packstone. Skeletal fragments include abundant crinoids (10-58%), bryozoans (1-27%), brachiopods (1-5%), trilobites (0-5%) and coral (0-5%). The core is massively bedded. Sorting is poor in this core. Micrite is the major cement, though, minor overgrowths of sparry calcite occur.

The porosity developed is intraparticle, enlarged intraparticle, and vuggy. Some hydrocarbons were observed.

The abundant micrite, poor sorting, massiveness and the lack of current structures leads to a mound facies for the area of deposition.

Name: Jones and Pellow Boyd
Location: Sec. 28 T12N R2W

There is 47 ft. of the Frisco present in the Boyd core. There is an abrupt contact with the overlying Woodford shale; the underlying contact is not present.

Skeletal grains make up the bulk of this core. Grains which are present are: pelmatozoans (33-62%), bryozoans (1-20%), brachiopods (3-10%), trilobites (1-5%), corals (0-1%) and gastropods (0-1%). The grains are oriented horizontally or inclined. The rock is a pack/grainstone.

The major cement is sparry calcite formed as overgrowths around crinoids. Micrite is present in several thin sections but in very minor amounts. Some of the micrite is secondary as a result of disaggregation of overlying material by solutions. Minor glauconite is present as a plugger of intraparticle pore spaces.

Solutions undersaturated with calcium carbonate are responsible for the majority of the porosity in the Boyd core. Vugs are filled with sparry calcite and secondary micrite or they can be open. Some intraparticle porosity is present, but it is rare and not effective.

Low mud content and grain orientations are indicative of an intermound environment.

Name: Midwest McManus
Location: Sec. 13 T13N R6W

The McManus core contains 39 ft. of Frisco (8072-8111). The upper contact is not present while the lower contact is sharp with the Henryhouse. The Bois D'Arc/Haragan sequence was removed by pre-Frisco erosion.

Skeletal fragments are the major grain present. The skeletal constituents are: crinoids (22-44%), bryozoans, (22-44%), brachiopods (0-8%), trilobites (0-6%), and corals (0-5%). The major sedimentary structures are horizontal and inclined grain orientations. The rock is pack/grainstone. The major cement is sparite.

Porosity in the McManus is negligible and restricted to intraparticle and minor vuggy porosity. Dissolution features are abundant, but vugs are filled with sparite or secondary micrite.

The environment of deposition was in the intermound area. This interpretation is based on: winnowed grains, oriented grains and fragmented grains.

Name: Duncan Garrett
Location: Sec. 22 T17N-R8W

Thirty-five feet of the Henryhouse is contained in this core. The overlying contact is sharp with the Woodford shale; the underlying contact is not present in this core. Three facies are present in this core: lagoonal, oolitic, and subtidal.

Dolomitization has obliterated most of the textures of the lagoonal facies (8738-8742). Poorly preserved peloids are present in the mudstone. Rare pelmatozoans and brachiopods are also present. The dolomite is mostly xenotopic and cloudy, but zoned dolomite is also present.

The oolitic facies (8742-8752) has been completely dolomitized which also destroyed most of the textures in this facies. The rock is a grainstone with abundant dolo-ooliths; fossil fragments are rare. The center of the ooliths contains cloudy xenotopic dolomite while the rims contain limpid idiotopic dolomite. Porosity in this facies is inter- and intraoolitic.

A subtidal facies (8752-8773) lies below the oolitic facies. The subtidal facies is a dolo-mud/wackestone with crinoid, brachiopod, and trilobite fragments. Dolomite percentage decreases downward in this facies.

Name: Eason Van Curen
Location: Sec. 3 T15N-R5W

There is 56 ft. of the Henryhouse present in the Eason core. The overlying and underlying units are not present in this core. Three facies are present in the Eason core.

A peloid dolo-mudstone (7136-7143) represents the lagoonal facies. Dolomite percentage decreases toward the contact with the underlying unit; the dolomite is cloudy and xenotopic. Dolomitization obliterated many sedimentary structures, but faint burrows are present. Rare fossils included pelmatozoans and brachiopods.

Below the lagoonal facies is an oolitic facies (7143-7159). The oolitic facies is pure calcite. The rock is a grainstone with abundant ooliths and rare fossil debris. Cross and horizontal stratification is present. Drusy spar occludes most of the porosity.

Below the oolitic facies is a subtidal facies (7159-7192). This facies is a dolo-mudstone at the top of the facies and a lime-mudstone at the bottom. Hummocky bedding is present. Fossil fragments include crinoids, brachiopods, bryozoans, trilobites and corals.

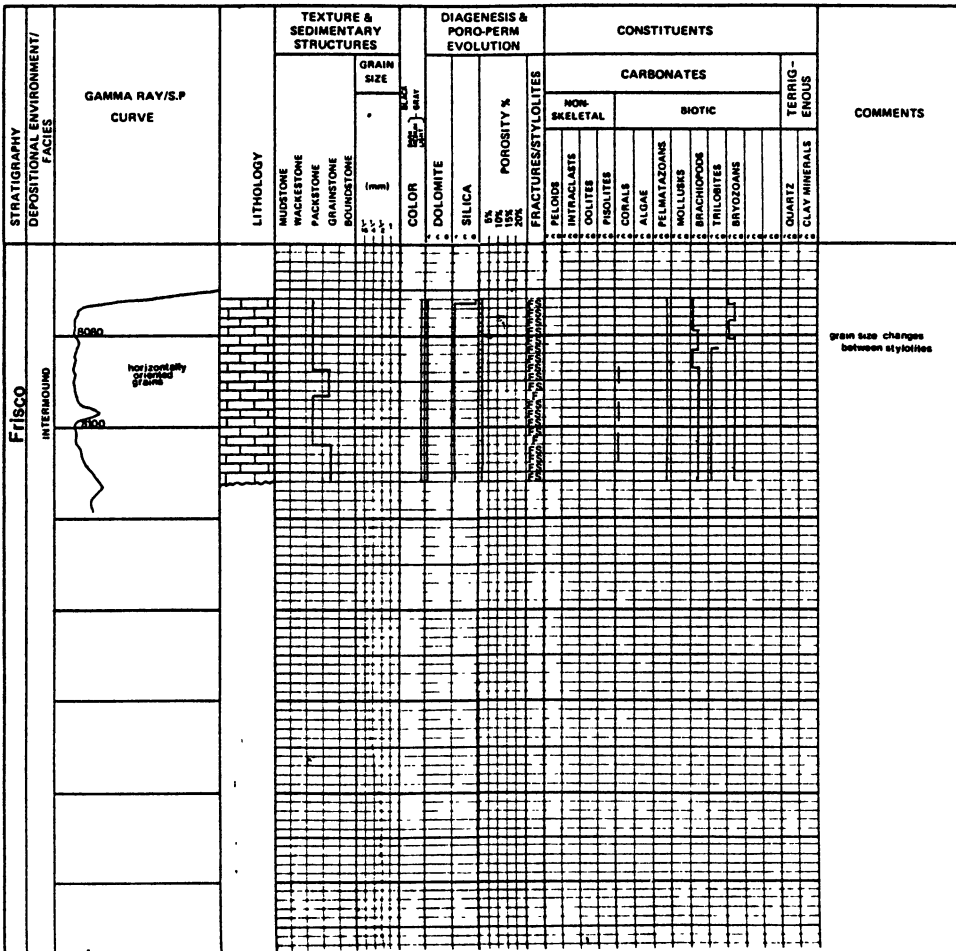
APPENDIX IV

PETROLOGS

HUNTON GROUP PETROLOG

Well Midwest McManus
 Location Sec.13 T. 13 N. R. 6 W.
Canadian Co., OKLAHOMA

Lithology	Sedimentary Structures	Fracture	Stylolites	Miscellaneous
<ul style="list-style-type: none"> CLAY CLAYSTONE SILTY CLAYSTONE/MUDSTONE SILTY SHALE SAND/SANDSTONE INTERBEDDED SANDSTONE/MUDSTONE MUDDY SANDSTONE CONGLOMERATE BRECCIA COAL/LIGNITE LIMESTONE DOLOMITE GYPSUM/ANHYDRITE HALITE CHERT MARL DOLOMITIC ROCKS CHERTY ROCKS GYPSIFEROUS/ANHYDRITIC ROCKS 	<ul style="list-style-type: none"> HORIZONTAL BEDDING HORIZONTAL LAMINATION TROUGH CROSSBEDDING TABULAR CROSSBEDDING DISTURBED BEDDING GRADED BEDDING MODULAR OR SLIGHTLY HUMMOCKY BEDDING MASSIVE BEDDING RIPPLE CROSS LAMINAR FLASER LAMINAR ALGAL LAMINATION LAMINATION CURRENT SOLE MARKS LOW-ANGLE INCLINED STRATIFICATION BURROWS LOADCASTS MUDCRACKS BURROW-BOTTLED ROOTLETS CONCRETIONS 	<ul style="list-style-type: none"> OPEN CLOSED FILLED 	<ul style="list-style-type: none"> COARSE FINE 	<ul style="list-style-type: none"> ○ DOMINANT GRAIN OR RHOMB SIZE ◊ SECONDARY MODE FOR GRAIN OR RHOMB SIZE ◄ THIN SECTION ■ X-RAY DIFFRACTION SAMPLE * GLAUCONITE P PYRITE C CARBONACEOUS DETRITUS F RARE C COMMON A ABUNDANT

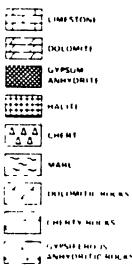
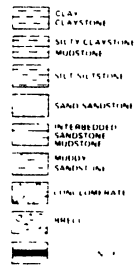


HUNTON GROUP

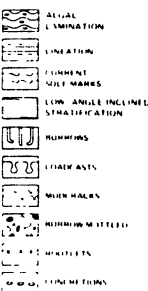
PETROLOG

Well Jones and Pellow Boyd
 Location Sec. 28 T. 12 N., R. 2 W.
 Oklahoma Co. OKLAHOMA

Lithology



Sedimentary Structures



Fracture

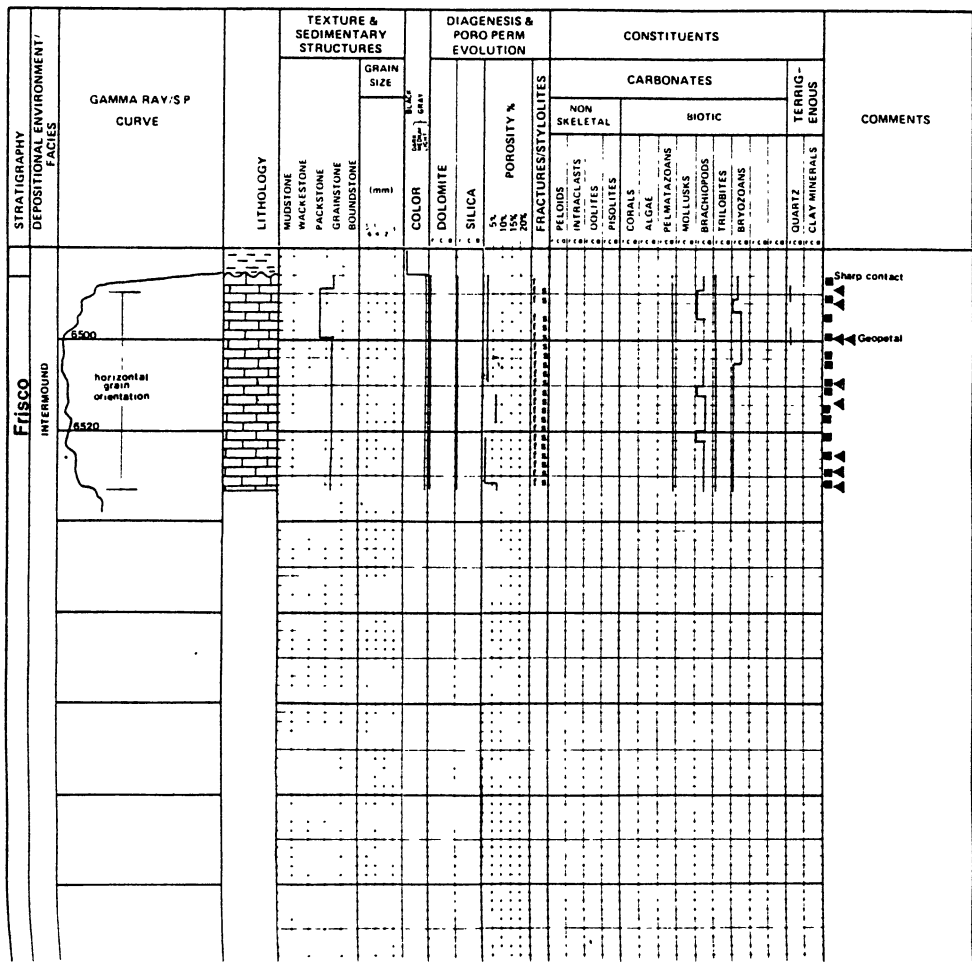


Stylolites



Miscellaneous

- DOMINANT GRAIN OR MINERAL SIZE
- SECONDARY MODE FOR GRAIN OR MINERAL SIZE
- ◀ THIN SECTION
- X-RAY DIFFRACTION SAMPLE
- CLASH POINT
- ◇ PYRITE
- FERMINGITE OR TRITON
- F RARE C COMMON A ABUNDANT



HUNTON GROUP

PETROLOG

Well Gulf Shaddix
 Location Sec. 29 T.6 N., R. 3 W
 McClain Co., OKLAHOMA

<p>Lithology</p> <ul style="list-style-type: none"> CLAY CLAYSTONE SILTY CLAYSTONE MUDSTONE SILT SILTSTONE SAND SANDSTONE INTERBEDDED SANDSTONE MUDSTONE MUDDY SANDSTONE CONGLOMERATE BRECCIA TALUS LIGNITE LIMESTONE DOLOMITE GYPSEUM ANHYDRITE MALITE CHERT MARL DOLOMITIC MUDS CHERTY MUDS GYPSEIFEROUS ANHYDRITIC ROCKS 	<p>Sedimentary Structures</p> <ul style="list-style-type: none"> HORIZONTAL BEDDING HORIZONTAL LAMINATION TROUGH CROSSBEDS TABULAR CROSSBEDS DISTURBED BEDDING GRADED BEDDING MODULAR OR KNOBBY HUMMOCKY BEDDING MASSIVE BEDDING HIPPED MISSILE LAMINAE FLASH LAMINAE ALGAL LAMINATION LINATION CURRENT SILE MARKS LOW ANGLE INCLINED STRATIFICATION BURNINGS LOADCASTS MUDCRACKS BURROW MOTTLED MARTELES INCH THINS 	<p>Fracture</p> <ul style="list-style-type: none"> OPEN CLOSED FILLED 	<p>Stylolites</p> <ul style="list-style-type: none"> COARSE FINE 	<p>Miscellaneous</p> <ul style="list-style-type: none"> DOMINANT GRAIN OR RHOMB SIZE SECONDARY MODE FOR GRAIN OR RHOMB SIZE THIN SECTION RAY DIFFRACTION SAMPLE LIGNITE PMITE SHRIMP ETLIN OR T. T. RARE COMMON RHOMB ANT
--	---	---	---	--

STRATIGRAPHY DEPOSITIONAL ENVIRONMENT/ FACIES	GAMMA RAY/S P CURVE	LITHOLOGY	TEXTURE & SEDIMENTARY STRUCTURES		DIAGENESIS & PORO PERM EVOLUTION			CONSTITUENTS							COMMENTS									
			MUDSTONE PACKSTONE GRAINSTONE BOUNDSTONE	GRAIN SIZE (mm)	COLOR	DOLOMITE	SILICA	POROSITY %	CARBONATES															
									PELOIDS	INTRACLASTS	OOOLITES	PISSOLITES	NON SKELETAL	BIOTIC				TERRIG- ENDOUS						
Frisco Mound	massive	[Lithology symbols]	[Texture symbols]	[Grain size symbols]	[Color symbols]	[Dolomite symbols]	[Silica symbols]	[Porosity symbols]	[Fractures]	[Stylolites]	[Peloids]	[Intraclasts]	[Oolites]	[Pissolites]	[Non skeletal]	[Algae]	[Foliated]	[Mollusks]	[Brachiopods]	[Trilobites]	[Bryozoans]	[Quartz]	[Clay minerals]	poorly sorted

VITA²

Patrick Lee Medlock

Candidate for the Degree of
Master of Science

Thesis: DEPOSITIONAL ENVIRONMENT AND DIAGENETIC HISTORY OF
THE FRISCO AND HENRYHOUSE FORMATIONS IN CENTRAL
OKLAHOMA

Major Field: Geology

Biographical:

Personal Data: Born in Lawrence, Kansas, October 30,
1959, son of Charles and Mary Beth Medlock.

Education: Received Bachelor of Science degree in
Geology, May, 1982, from the University of
Kansas, Lawrence, Kansas; completed requirements
for the Master of Science degree at Oklahoma State
University in December, 1984.